

https://dspace.org/

Power quality assessment of when a microgrid containing a diesel generator and/or solar PV is islanded

Allessing, Chaniel Precious

2021

https://hdl.handle.net/10539/31884

Downloaded from a DSpace repository. https://dspace.org/



Power quality assessment of when a microgrid containing a diesel generator and/or solar PV is islanded

Full Name: Chaniel Precious Allessing

University of Witwatersrand, Johannesburg, 2019

A dissertation submitted to the Faculty of Engineering and the Built Environment, University of Witwatersrand, Johannesburg, in fulfilment of the requirements for the degree of Master of Science in Engineering.

Declaration

I declare that this dissertation is my own unaided work. It is being submitted for the degree of Master of Science in Engineering to the University of the Witwatersrand, Johannesburg. It has not been submitted before for any degree or examination to any other University.

.....Blessing.....

(Signature of Candidate)

15 day of February year 2021

Abstract

Distributed Generation (DG) plays a significant role in improving the reliability of a power supply. However, connecting DGs into the network also introduces a possibility of islanding that could create power quality issues in the network. A 400 V microgrid connected to a 22 kV rural network was simulated using DIgSILENT PowerFactory software. The microgrid contained a Synchronous Generator (SG) with a diesel engine as a prime mover or Solar PhotoVoltaic (SPV) or a SG in parallel with SPV. The frequency and voltage disturbances after islanding were investigated. The diesel engine was modelled with a governor (Degov) and the SG had an Automatic Voltage Regulator (AVR)(AC5A). The SPV was modelled using the WECC distributed PV plant generic model (PVD1). Three different cases concerning the types of load were analysed: static pure resistance, static series RL and composite (both a dynamic load (induction motor) and a static load). Various SG active power and SPV active power percentage contributions to the load demand during the grid-connected condition were also studied. The voltage and frequency behaviour after the islanding varied with both the SPV and the DG active power percentage contributions prior to the islanding. The voltage and frequency behaviour of the different types of DGs differed based on the cause of the islanding: sectionalisation (disconnection without a fault) or clearance of an upstream three-phase fault (disconnection with a fault). For a DG of a diesel generator and/or SPV, the purely resistive load and the series RL load showed similar trends of voltage disturbance (decrease in voltage) and frequency disturbance (decrease in frequency) during islanding. It was also observed that the voltage disturbance of the network is affected by the location of the three-phase short-circuit fault. Power quality issues are mostly observed for DG with a lower percentage active power contribution prior to the islanding and for islanding following a three-phase short-circuit fault.

Dedication

The author would like to dedicate this to friends and family.

Acknowledgements

The author would like to thank the ESKOM Power Plant Engineering Institute (EPPEI)-HVAC and the School of Electrical and Information Engineering, University of the Witwatersrand, Johannesburg, for the financial support and for providing the computational facilities.

Contents

Declaration ..... **i**

Abstract ..... **ii**

Dedication ..... **iii**

Acknowledgements ..... **iv**

List of Figures ..... **viii**

List of Tables ..... **xv**

Glossary of Terms and Abbreviations ..... **xvi**

Publications ..... **xvii**

Chapter 1 – Introduction **1**

1.1 Islanding 1

1.2 Anti-islanding techniques 2

1.3 Power quality issues 2

Chapter 2 – Research Issues **6**

2.1 General issues of islanding 6

2.2 Problem statement 7

2.3 Objectives 8

2.4 Research scope 9

2.5 Limitation of the research 9

Chapter 3 – Literature review **10**

3.1 Governors and AVRs 10

3.1.1 Different types of governors 12

3.1.2 Different types of AVRs 14

3.2 SPV 15

3.3 The probability of continued islanding occurring 15
3.4 History of specifying the maximum islanding time 16
3.5 Different load models in power system studies 17
3.5.1 Static load 18
3.5.2 Dynamic loads 21
Chapter 4 – Methodology 25
4.1 SG Only 25
4.1.1 Purely resistive load 27
4.1.2 Series RL load 28
4.1.3 Composite load 28
4.1.4 Governor model 29
4.1.5 AVR model 30
4.1.6 Assumption 33
4.2 SPV only 33
4.2.1 SPV GFW inverter Model 36
4.2.2 Purely resistive load 39
4.2.3 Series RL load 40
4.2.4 Composite load 40
4.3 SG and SPV in parallel 41
Chapter 5 – Simulation results 42
5.1 SG simulations results 42
5.1.1 Purely resistive load 42
5.1.2 Series RL load 47
5.1.3 Induction motor 52
5.1.4 Induction motor driving a pump 56
5.2 Solar PV Generation simulations results 59

5.2.1 Purely resistive load 59

5.2.2 Series RL load 63

5.2.3 Induction motor 66

5.3 SG in parallel with SPV simulations 72

5.3.1 Islanding due to sectionalisation 72

5.3.2 Islanding due to an upstream three-phase short-circuit fault. 73

Chapter 6 – Discussion 76

6.1 RMS voltage and frequency compatibility levels 76

6.2 SG discussion 77

6.2.1 RMS voltage and frequency behaviour analysis 77

6.2.2 RMS voltage and frequency percentage reduction (normal condition versus islanding condition) 80

6.3 SPV discussion 83

6.3.1 RMS voltage and frequency behaviour analysis 83

6.3.2 RMS voltage and frequency percentage reduction (normal versus islanding condition) 86

Chapter 7 – Power quality versus IDM reliability 89

Chapter 8 – Conclusion 95

Chapter 9 – Recommendations 97

9.1 Reducing the RMS voltage and frequency fluctuations after islanding 98

References 99

List of Figures

Figure 1.1: Intentional or unintentional islanding (the DG may not have the capability of continuously supplying the load when the microgrid is islanded) 1

Figure 1.2: Classification of IDMs [2] 2

Figure 1.3: Undervoltage and underfrequency after islanding (load MW > DG MW) 4

Figure 1.4: Overvoltage and overfrequency after islanding (load MW < DG MW) 5

Figure 3.1: Three-level control hierarchy of a microgrid [14] 11

Figure 3.2: Behaviour of a governor having speed droop [16] 12

Figure 3.3: Typical dynamic response of a governor to a step change in reference speed 14

Figure 3.4: Probability of islanding occurring versus the relationship between the load MW and DG MW [5] 16

Figure 3.5: History of the two-second maximum islanding time requirement 17

Figure 3.6: Classification of load models 18

Figure 3.7: Equivalent circuit of a three-phase induction motor 22

Figure 3.8: Typical current-speed curve of an induction motor 23

Figure 3.9: Typical torque-speed curve of an induction motor 23

Figure 4.1: Synchronous Generator scenarios studied 26

Figure 4.2: Diesel Generator simulated network diagram 27

Figure 4.3: Network diagram illustrating the purely resistive load 28

Figure 4.4: Composite network diagram for the static and dynamic load 29

Figure 4.5: Torque-speed curve of a pump mechanical load 29

Figure 4.6: Degov diesel engine governor model 30

Figure 4.7: AC5A AVR model 31

Figure 4.8: Step response of the AC5A AVR model (equation (4.1)) 32

Figure 4.9: (a) active power versus frequency droop characteristic for grid-following units with dead-band and (b) active power versus frequency droop characteristic for grid-forming units without dead-band 34

Figure 4.10: SPV scenarios 34

Figure 4.11: SPV system simulated network diagram 35

Figure 4.12: Block diagram of the WECC distributed PV (PVD1) model [28]. 36

Figure 4.13: Distributed inverter PV model including FW function 38

Figure 4.14: Network overview of SPV supplying a purely resistive load during islanding 40

Figure 4.15: Diesel generator in parallel with SPV system network diagram 41

Figure 5.1: (a) shows the RMS voltage at the SG prior to and during islanding due to sectionalisation, (b) shows the speed of the diesel engine prior to and during islanding due to sectionalisation, (c) shows the mechanical power versus the electrical power prior to and during islanding due to sectionalisation with an SG MW percentage contribution of 10%. 44

Figure 5.2: Illustration of the effect of the integral-term gain on the oscillation of the signal 45

Figure 5.3: Illustration of the effect of the controller gain (Ka) 46

Figure 5.4: Purely resistive load: (a) shows the RMS voltage of the SG prior to and during islanding due to an upstream three-phase short-circuit fault, (b) shows the speed of the diesel engine prior to and during islanding due to an upstream three-phase short-circuit fault. 47

Figure 5.5: Series RL load (pf=0.996): (a) shows the RMS voltage of the SG prior to and during islanding due to sectionalisation, (b) shows the speed of the diesel engine prior to and during islanding due to sectionalisation. 48

Figure 5.6: Series RL load (pf=0.95): (a) shows the RMS voltage of the SG prior to and during islanding due to sectionalisation, (b) shows the speed of the diesel engine prior to and during islanding due to sectionalisation 49

Figure 5.7: Series RL load (pf=0.9): (a) shows the RMS voltage at the SG prior to and during islanding due to sectionalisation, (b) shows the speed of the diesel generator prior to and during islanding due to sectionalisation. 50

Figure 5.8: Series RL load (pf=0.9) (a) shows the RMS voltage of the SG prior to and during islanding due to an upstream three-phase short-circuit fault, (b) shows the speed of the diesel engine prior to and during islanding due to an upstream three-phase short-circuit fault. 52

Figure 5.9: Unloaded induction motor (a) shows the RMS voltage at the SG and the RMS voltage at the induction motor prior to and during islanding due to sectionalisation, (b) shows the speed of the diesel engine and of the induction motor prior to and during islanding due to sectionalisation. 53

Figure 5.10:Unloaded induction motor (a) shows the RMS voltage at the SG and the voltage at the induction motor prior to and during islanding due to an upstream three-phase short-circuit fault, (b) shows the speed of the diesel engine and the speed of the induction motor prior to and during islanding following an upstream three-phase short-circuit fault. 54

Figure 5.11:Unloaded induction motor versus series RL load (pf=0.9) (a) shows the RMS output current from the SG prior to and during islanding due to a three-phase

short-circuit current fault, (b) shows the RMS voltage at the SG prior to and during islanding due to an upstream three-phase short-circuit fault. 55

Figure 5.12: Induction motor driving a pump in parallel with a series RL load (pf=0.9) versus series RL load (pf=0.9) only (a) shows the RMS voltage behaviour of the SG prior to and during islanding due to sectionalisation. (b) shows the speed behaviour of the diesel engine prior to and during islanding due to sectionalisation. 57

Figure 5.13: Induction motor driving a pump in parallel with a series RL load (pf=0.9) versus series RL load (pf=0.9) only. (a) shows the RMS current behaviour of the SG prior to and during islanding due to an upstream three-phase short-circuit fault, (b) shows the RMS voltage behaviour of the SG prior to and during islanding due to an upstream three-phase short-circuit fault. 58

Figure 5.14: Induction motor driving a pump. Illustrates the speed behaviour of the SG prior to and during islanding due to an upstream three-phase short-circuit fault versus sectionalisation. 59

Figure 5.15: Purely resistive load (a) shows the RMS voltage of the SPV prior to and during islanding due to sectionalisation, (b) shows the frequency behaviour of the SPV prior to and during islanding due to sectionalisation. 60

Figure 5.16: Purely resistive load (a) shows the RMS voltage behaviour of the SPV capable of supplying the load, (b) shows the frequency behaviour of the SPV capable of supplying the load, (c) shows the RMS voltage behaviour of the SPV not capable of supplying the load, (d) shows the frequency behaviour of the SPV not capable of supplying the load. 61

Figure 5.17: Purely resistive load (a) shows the frequency behaviour of the SPV prior to and during islanding due to an upstream three-phase short-circuit fault, (b) shows the voltage of the SPV prior to and during islanding due to an upstream three-phase short-circuit fault. 62

Figure 5.18: Series RL load (pf=0.9) (a) shows the RMS voltage of the SPV prior to and during islanding due to sectionalisation, (b) shows the frequency behaviour of the SPV prior to and during islanding due to sectionalisation. 63

Figure 5.19: PVD1 volt-var control (VCC) curve 64

Figure 5.20: (a) shows the RMS voltage behaviour in pu of the SPV, (b) shows the RMS reactive current behaviour in pu of the SPV based on different reactive load demand, (c) shows the reactive load demand in pu. 64

Figure 5.21: Series RL load (pf=0.9) (a) shows the RMS voltage of the SPV prior to and during islanding due to an upstream three-phase short circuit fault, (b) shows the frequency behaviour of the SPV prior to and during islanding due to an upstream three-phase short circuit fault. 65

Figure 5.22: SPV supplying both series RL load and an induction motor 67

Figure 5.23: (a) shows the speed of the induction motor prior to and during islanding due to sectionalisation, (b) shows the RMS voltage behaviour prior to and during islanding due to sectionalisation. 68

Figure 5.24: (a) shows the RMS voltage behaviour of the SPV prior to and during islanding due to sectionalisation, (b) shows the reactive current injected by the SPV prior to and during islanding due to sectionalisation. 69

Figure 5.25: Modified volt-var controller for the PVD1 system 70

Figure 5.26: (a) shows the speed behaviour of the induction motor prior to and during islanding due to an upstream three-phase short-circuit fault, (b) shows the RMS voltage behaviour of the SPV prior to and during islanding due to an upstream three-phase short-circuit fault. 71

Figure 5.27: Series RL in parallel with induction motor (a) shows the RMS voltage behaviour of the network at the PC prior to and during islanding. (b) Illustrates the frequency behaviour of the network at the CP prior to and during islanding. 73

Figure 5.28: Series RL in parallel with induction motor (a) shows the RMS voltage behaviour of the network at the CP prior to and during islanding due to an upstream three-phase short-circuit fault, (b) shows the frequency behaviour of the network at the CP prior to and during islanding due an upstream three-phase short-circuit fault. 74

Figure 5.29: Series RL load in parallel with an induction motor (a) shows the RMS voltage behaviour of the network with the fault at different distances, (b) shows the RMS current behaviour of the SG with the fault at different distances. 75

Figure 6.1: Frequency versus active power droop relationship 78

Figure 6.2: Reactive power versus voltage droop relationship 79

Figure 6.3: Frequency versus series RL load power factor, supplied by different SG initial percentage MW contributions (10%, 50%, and 90%), at 0.5 seconds after islanding 80

Figure 6.4: RMS voltage versus series RL load power factor on an islanded network, supplied by different SG initial percentage MW contributions (10%, 50%, and 90%) at 0.5 seconds after islanding 80

Figure 6.5: RMS voltage percentage reduction for different SG initial percentage MW contributions (10%, 50%, and 90%) for sectionalisation that leads to islanding for a series RL load (pf=0.9) 82

Figure 6.6: Frequency percentage reduction of different SG initial percentage MW contributions (10%, 50%, and 90%) for sectionalisation that leads to islanding for a series RL load (pf=0.9) 83

Figure 6.7: SPV power versus voltage curve 84

Figure 6.8: RMS voltage behaviour for a series RL load (pf=0.9), supplied by different PV initial percentage MW contributions (10%, 50%, and 90%) at 0.5 seconds after islanding due to sectionalisation or a three-phase short-circuit fault 84

Figure 6.9: Frequency behaviour for a series RL load (pf=0.9), supplied by different solar PV initial percentage MW contributions (10%, 50%, and 90%) at 0.5 seconds after islanding due to either sectionalisation or a three-phase short-circuit fault 85

Figure 6.10: Percentage reduction of RMS voltage at 0.5 seconds after islanding of an RL load (pf=0.9) supplied by different PV initial percentage MW contributions. 87

Figure 6.11: Percentage reduction of frequency at 0.5 seconds after islanding with RL load (pf=0.9) supplied by different SPV initial percentage MW contributions and following sectionalisation or a three-phase short circuit fault. 88

Figure 7.1: Geographical area of Estancia/Estancia North 22 kV 89

Figure 7.2: Research approach to simulated network 90

Figure 7.3: SG network diagram 90

Figure 7.4: The frequency behaviour of the SG during islanding 91

Figure 7.5: Frequency derivative behaviour 92

List of Tables

Table 1.1: The differences between the local and remote IDMs [5] 2

Table 3.1: Load model summary [20]. 18

Table 3.2: Ideal circuit element versus real-world circuit element 21

Table 4.1: Degov recommended parameter values [26] 30

Table 4.2: Typical values for type AC5A excitation systems [19] 32

Table 4.3: Grid following versus grid forming 33

Table 4.4: PVD1 IEEE/WECC recommended values 37

Table 5.1: Simulation scenarios 42

Table 5.2: Simulated parameters 66

Table 5.3: Simulation parameters (SG and PV system in parallel) 72

Table 6.1: Deviation from standard or declared voltage [8], [35] 76

Table 6.2: Deviation from nominal frequency [35] 77

Table 7.1: ROCOF value of a load of 0.6 MVA, nominal frequency of 50 Hz and rotor inertia constant of 5 93

Glossary of Terms and Abbreviations

Abbreviation/Term	Description
DG	Distributed Generation
IDM	Islanding Detection Method
NDZ	Non-Detection Zone
NREL	National Renewable Energy Laboratory
C	Capacitance
L	Inductance
R	Resistance
SG	Synchronous Generator
SPV	Solar Photovoltaic
SPVG	Solar Photovoltaic Generation
WECC	Western Electricity Coordinating Council
DPV	Distributed PV
GFW	Grid-following
GFM	Grid-Forming
FW	Frequency-Watt
RMS	Root Mean Square
UL	Underwriters Laboratories
VVC	Volt-Var Controller

Publications

Peer-reviewed conference papers related to this dissertation

Chapter

[5.1,8]	C. P. Allessing, H. Kruger and J. Van Coller , "Simulation-based analysis of the anti-islanding requirement specified within the grid connection code for renewable power plant (gccrpp)," *2019 Southern African Universities Power Engineering Conference/Robotics and Mechatronics/Pattern Recognition Association of South Africa (SAUPEC/RobMech/PRASA),* pp. 406-411, Jan 2019

Chapter 1 – Introduction

1.1 Islanding

Distributed Generation (DG) (often renewable sources such as wind and solar) are becoming more common for environmental and economic reasons. DG is small-scale generation located at or near the load [1]. DG comes with the disadvantage that islanding becomes a possibility.

Islanding occurs when the DG continues to supply the local load when the utility supply becomes intentionally or unintentionally disconnected [2][3] as illustrated in Figure 1.1. The utility supply will not be available, for example, when there is a scheduled outage, operation of circuit breakers in response to a fault or human error, sectionalisation or an act of nature. In most cases, unintentional islanding should be detected and terminated immediately [4].

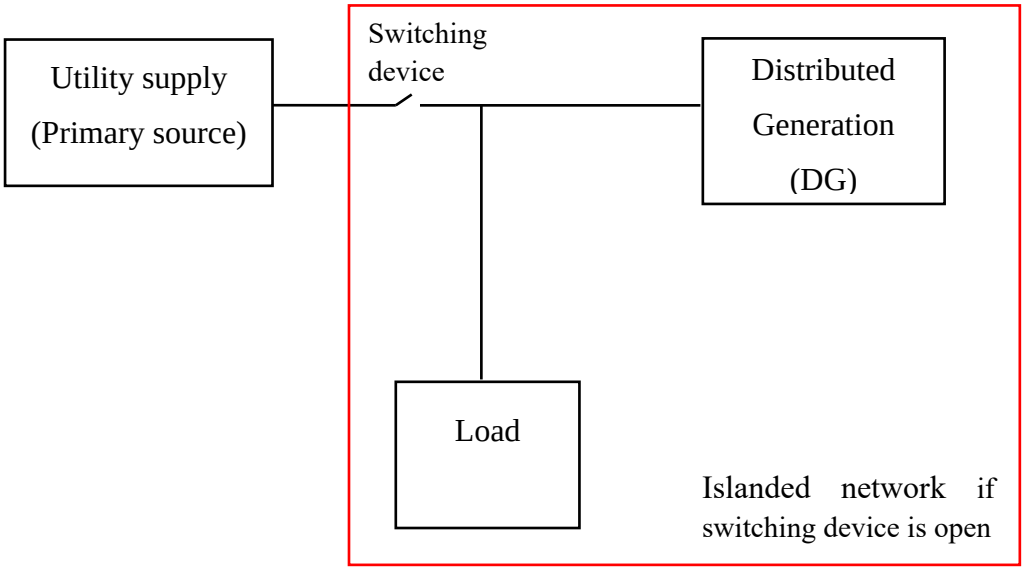


Figure 1.1: Intentional or unintentional islanding (the DG may not have the capability of continuously supplying the load when the microgrid is islanded)

1.2 Anti-islanding techniques

There are two types of Islanding Detection Methods (IDMs): local islanding detection and remote islanding detection. Local islanding detection is further divided into three groups: active, passive and hybrid [2]. Figure 1.2 illustrates the two types with their differences given in Table 1.1. The IDM depends on the type of DG unit (inverter-based or non-inverter-based).

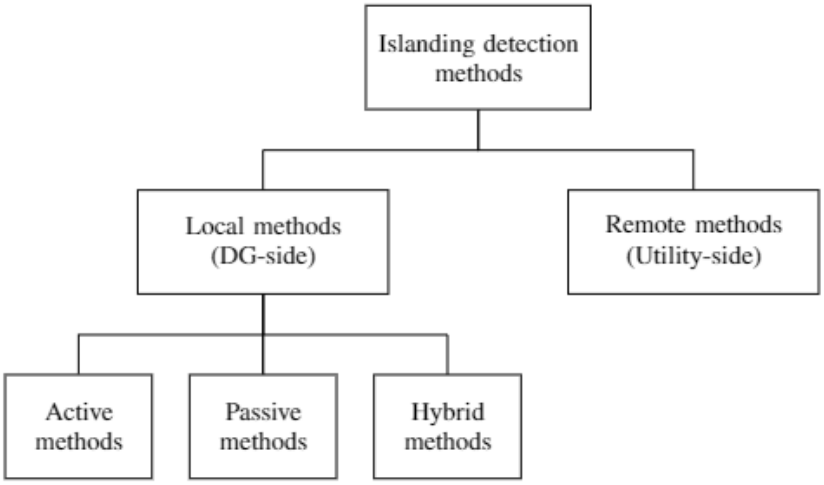


Figure 1.2: Classification of IDMs [2]

Table 1.1: The differences between the local and remote IDMs [5]

Local IDMs	**Remote IDMs**
Monitored on the DG side	Monitored on the utility side
Allows the disconnection decision to be made by the DG	Allows the disconnection decision to be made by the utility
Restricted by the non-detection zone	Reliable
Cost-effective	Expensive

1.3 Power quality issues

Any power system must be able to meet the continually changing load demand for active and reactive power. The quality of the power supply must meet specific minimum standards with regards to the following factors:

- Constant frequency
- Constant voltage
- Level of reliability

The utility is responsible for controlling the voltage and frequency supplied to its customers. The utility does not, however, have control of the voltage and frequency of the islanded network. Uncontrolled voltage and frequency worsen the power quality experienced by the customer. Islanding also carries the risk of damaging utility and customer equipment if the voltage and frequency are not adequately controlled. Islanding may interfere with the restoration of normal service by the utility - reclosing onto an islanded network may result in re-tripping of the line or damage to the DG or other equipment due to out-of-phase reclosing [6], [7].

Power quality is a measure of network parameters such as voltage and frequency with reference to established specifications. The IEEE definition of power quality is the powering and grounding of sensitive equipment in a manner that is suitable for the operation of that equipment. Poor power quality can cause malfunction of or damage to utility and customer equipment. Customer equipment has become more sensitive to voltage disturbances. Voltage sags and frequency deviations reduce the power quality experienced by the customer. According to IEEE 1159 and NRS 048-2, any voltage that is below 0.9 pu is defined as a voltage sag (also defined as a voltage dip) and any voltage that is above 1.1 pu is defined as a voltage swell [8].

Sensitive customer loads include equipment such as Process Controllers (PCs), Programmable Logic Controllers (PLCs), Adjustable Speed Drives (ASDs), robotics and motors. The customer loads have different sensitivity thresholds. For example, in automation facilities, PLCs are sensitive to continuous voltages of less than 0.9 pu and motors are sensitive to continuous voltages of less than 0.7 pu.

An islanding event can be illustrated by voltage versus time and frequency versus time graphs, as shown in Figures 1.3 and 1.4. Figure 1.3 demonstrates that when the demand for active and reactive power is greater than the output of the DG after islanding, undervoltage and underfrequency will result. The voltage and frequency

first decrease when islanding is initiated. If there is an Automatic Voltage Regulator (AVR) within the islanded network, the AVR will respond to the voltage drop and boost the voltage to a level at which the reactive power is balanced (in an AC circuit increasing the voltage out of a generator generates capacitive reactive power). The active power (frequency) controller (governor for a diesel generator) will also respond to the frequency drop. Even though the islanded network has reached its steady-state after the active power (frequency) controller and the AVR have responded to the frequency and voltage drops, respectively, the frequency can be below its set-point. This will trigger the underfrequency relay to trip a preselected portion of the load before a typical time of 500 ms if there are underfrequency load shedding relays in that particular portion of the network [9].

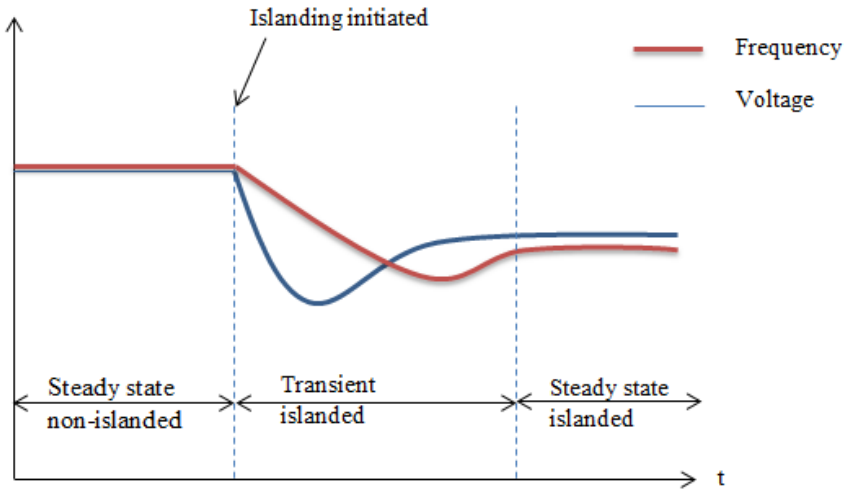


Figure 1.3: Undervoltage and underfrequency after islanding (load MW > DG MW)

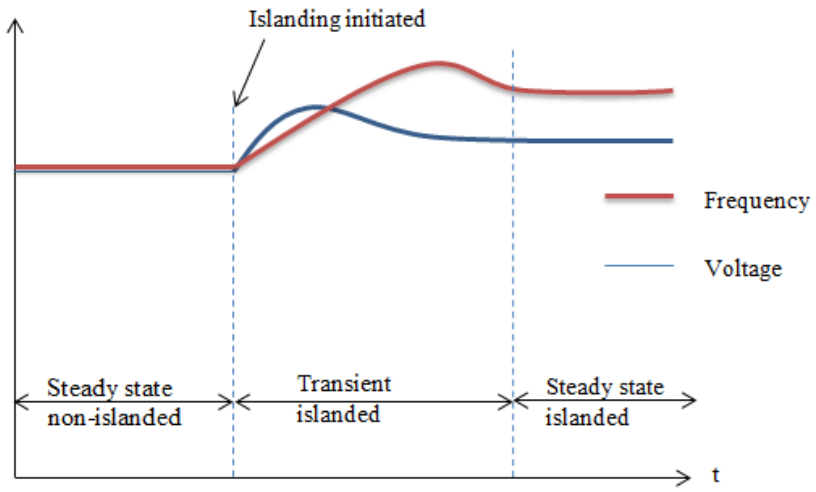


Figure 1.4: Overvoltage and overfrequency after islanding (load MW < DG MW)

If the frequency is below the nominal value, motors will generally slow down and thus consume less active power. If the voltage is significantly below the nominal value, this can result in motors stalling, potentially resulting in damage to equipment and/or customer complaints.

Figure 1.4 illustrates when the demand for active and reactive power is less than the output of the DG after islanding. The frequency and the voltage first increase when islanding is initiated [9]. The frequency controller and AVR will then react to the overfrequency and overvoltage, respectively, to return the network to its new steady-state condition.

If the frequency is above the nominal value, motors will run faster and thus consume more active power. If the voltage is significantly above the nominal value, this could result in equipment damage on the utility and/or customer networks.

Chapter 2 – Research Issues

2.1 General issues of islanding

Some risks associated with islanding are:

1) Power Quality

The utility is responsible for maintaining the desired power quality to its customers. To maintain the network and manage the availability of the supply to the load, the voltage and frequency must be monitored and controlled. The utility has no control of the voltage and frequency of an islanded network. Uncontrolled frequencies and voltages on the islanded network can damage utility and customer equipment.

2) Out-of-synchronism reclose

The problem regarding the utility switching onto an islanded network is synchronization. That is, the voltage amplitude, phase angle, phase sequence and frequency of the DG and the utility grid must be the same. Out-of-synchronism reclosing is also called out-of-phase reclosing. Such an event can potentially cause damage to utility and customer equipment, as well as to the DG.

Out-of-phase re-closing is discussed in [10]. Different types of equipment typically found in networks and the potential damage to each type of equipment due to out-of-phase re-closing are discussed. Islanding and subsequent re-synchronising also affects one of the common Reliability Indices, the System Average Interruption Duration Index (SAIDI), due to the delay in the restoration of the normal service beyond the three second threshold of the SAIDI.

3) Personnel safety

Islanding also creates an unsafe condition for utility workers who are unaware that the islanded system is energised.

2.2 Problem statement

Many international and national standards, such as the South African Grid Code of Renewable Power Plant (SAGCRPP) [11] stipulate that islanding must be detected and terminated within two seconds for DGs with rated power greater than 1 MVA (categories B and C) and within 0.2 seconds for DG with rated power up to 1 MVA (category A). The SAGCRPP anti-islanding requirement is adopted from the IEEE 1547-2018 standard [3], which requires islanding to be detected and the DG disconnected within two seconds.

The longer the islanding is allowed to continue, the longer the utility and customer equipment will experience the RMS voltage and frequency fluctuations. The power quality of an islanded network within the specified islanding detection time is becoming a growing concern in the backdrop of increasing susceptibility of customer equipment to degraded power quality. The voltage and frequency compatibility levels specified in standards are discussed in section 6.1.

There is, however, no literature that exclusively studies the voltage and frequency behaviour after islanding of networks with SG or SPV or SG in parallel with SPV of different active power contribution percentages (prior to islanding), supplying various types of loads (after islanding) with varying power factors. This dissertation investigates the voltage and frequency behaviour after islanding of a power network with SG and/or SPV. This dissertation also examines, in terms of power quality, the maximum islanding time stipulated by IEEE 1547-2018 and the SACGRPP document and proposes ways of reducing the RMS voltage and frequency fluctuations after islanding. The voltage and frequency behaviour in a network after islanding were studied using the DIgSILENT PowerFactory software.

The research problem statement includes:

1. There is a lack of information on the power quality, especially the voltage and frequency behaviour, after the initiation of islanding of a network supplied by SG and/or SPV with different types of loads

2. A smaller maximum islanding time is preferable to a customer. At present, there are no attempts made to reduce the time stipulated in the standards (IEEE 1547-2018)

2.3 Objectives

The issues that come with islanding triggered research into ways to detect and terminate islanding. [17] and [18] comprehensively evaluate the types of IDMs, including which method is able to detect and terminate islanding almost instantaneously, which is a remote (utility) IDM.

Studies of the impacts and ways to prevent the negative effects of islanding in the network have been studied. This dissertation investigates the voltage and frequency behaviour following islanding due to sectionalisation (without a fault) or due to fault clearance (clearance of an upstream three-phase short-circuit).

There are four objectives:

1. To analyse the voltage and frequency behaviour at the customer after islanding due to sectionalisation and due to the clearance of an upstream three-phase short-circuit, when a diesel generator supplies the islanded network.
2. To analyse the voltage and frequency behaviour at the customer after islanding due to sectionalisation and due to the clearance of an upstream three-phase short-circuit, when SPV (PVD1 model) supplies the islanded network.
3. To analyse the voltage and frequency behaviour at the customer after islanding due to sectionalisation and due to the clearance of an upstream three-phase short-circuit, when SPV in parallel with a diesel generator supplies the islanded network.
4. To propose/recommend ways of reducing the RMS voltage and frequency fluctuations after islanding.

2.4 Research scope

This dissertation focuses on studying the voltage and frequency behaviour (power quality issues) of an SG or SPV or SG in parallel with SPV after islanding for different types of loads.

A 400 V microgrid connected to a 22 kV rural network was simulated using the DIgSILENT PowerFactory software. Two different causes of islanding were investigated: islanding due to sectionalisation (no fault present) and islanding due to fault clearance (an upstream three-phase short-circuit) where the utility feeder protection opens the utility breaker thereby islanding the microgrid.

Different types of load (static loads, dynamic loads and the combination of the two) and different active power percentage contributions of SG and SPV (prior to islanding) were also considered. Ways to avoid power quality issues after islanding, such as changing the maximum islanding termination time, as well as a controller that can be used to regulate the RMS voltage and frequency of the network, are also discussed.

2.5 Limitation of the research

The limitation of this research includes the absence of measurements to validate the simulated results. The simulated network is not an existing network. Hence there is no historical data available to validate the simulated results. The simulated network represents a standard network topology (in terms of arrangements of nodes and equipment used). Studying different MW contribution of the SPV system and diesel generator, account for different network sizes within existing networks. There are different types of loads within networks, hence studying the network behaviour with different types of load is crucial.

Chapter 3 – Literature review

Islanding has been of increasing concern due to the rapidly growing penetration of DG into the grid. There have been many studies that have focused on the effect of islanding [9]. Islanding carries risks such as damaging the utility and the customer equipment. One of the most significant risks of islanding is that it creates an unsafe condition for utility workers who may unknowingly try to work on a system that is energised during islanding. Standards such as IEEE 1547-2018 [3] are now in place to control the maximum time allowed for islanding to occur in a network.

There are different types of DGs such as traditional synchronous generators (driven by combustion engines) and non-traditional sources (such as renewable, storage, and electrochemical devices). Different DGs may respond in terms of voltage and frequency differently after islanding. Some DG may favour islanding with the help of governors and other types of controllers and some may not. Depending on the type of DG, the response to islanding (maintaining the state of equilibrium or stability) may be different [12], [13].

3.1 Governors and AVRs

In [14] and [15] the authors describe the three-level control hierarchy for voltage and frequency stabilization and regulation. During grid-connected conditions where the DG is a Synchronous Generator (SG), the functions of the governor and Automatic Voltage Regulator (AVR) are to control the active power and reactive power flow between the SG and the network. The SG should also be able to synchronise with the external grid which is operating at the same frequency and phase angle. When the external grid is disconnected, then the whole demand from the consumer must be supplied by the DG (SG).

The SG, in this case, must be able to supply the demand sufficiently during islanding. The speed of the SG will be affected in such a case according to the

governor behaviour. The three-level control hierarchy is shown in Figure 3.1 [14] and [15]. Only primary control (to stabilise the voltage and frequency after islanding) is examined in this dissertation with no secondary control to return the parameters to their nominal values.

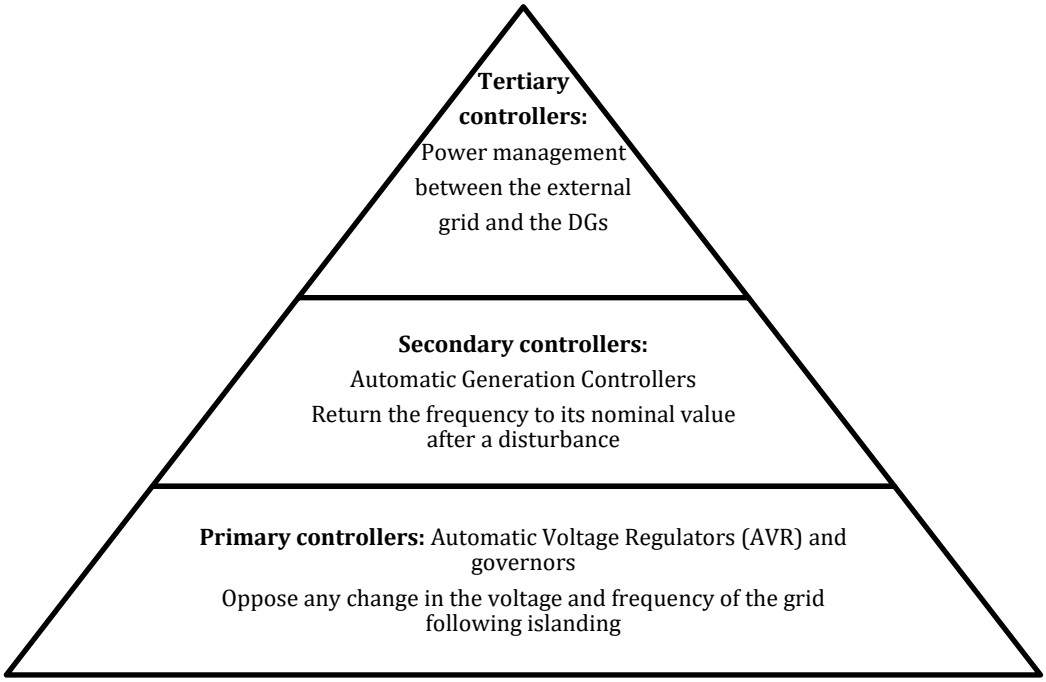
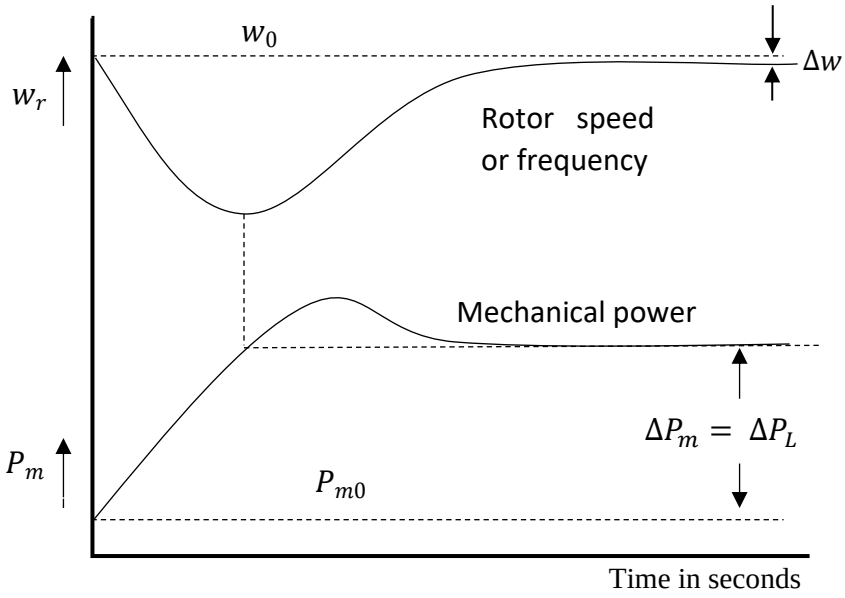


Figure 3.1: Three-level control hierarchy of a microgrid [14]

Traditionally, the speed of a diesel-generator set has been regulated using a fixed droop mechanism.

A constant frequency ensures a constant speed of induction motors and synchronous motors. In a network, a significant drop in frequency could result in a high magnetizing current in induction motors and transformers. The frequency of a system is dependent on the active power balance. A change in active power demand is reflected throughout the system by a change of frequency.

A governor provides the diesel engine with the feedback mechanism to change the speed as needed and maintain the speed/frequency once reached, as illustrated by Figure 3.2.



P_m = Mechanical power

P_{m0}= Initial mechanical power

P_L = Load power

w_r = Rotor speed

w_0 = Initial rotor speed

Δw = Change in rotor speed

Figure 3.2: Behaviour of a governor having speed droop [16]

3.1.1 **Different types of governors**

Governors are classified into four types:

i. Constant speed: the engine runs at a constant speed regardless of the load
ii. Speed limiting: the engine runs between some minimum and maximum speed
iii. Load limiting: the fuel-flow rate is limited to ensure that the engine is not loaded above some specified value regardless of the speed
iv. Variable speed: the engine runs at a variable speed

There are different types of governors for each of the four types listed above:

i. Mechanical centrifugal: droop not adjustable
ii. Hydraulic: can include temporal droop (compensation)
iii. Mechanical: hydraulic amplification
iv. Electronic: droop easily adjustable

Governors often use Proportional Integral Derivative (PID) controllers [17]

i. Proportional (P) term: produces an output value that is proportional to the speed error.
ii. Integral (I) term: provides an output value that varies with the integral of the speed error. This will eventually drive any residual speed error to zero.
iii. Derivative (D) term: produces an output value that varies with the rate of change of speed error. This provides damping of any speed oscillation.

There are four characteristics of the controller response (Figure 3.3)

- Rise time
- Overshoot
- Settling time
- Steady-state error

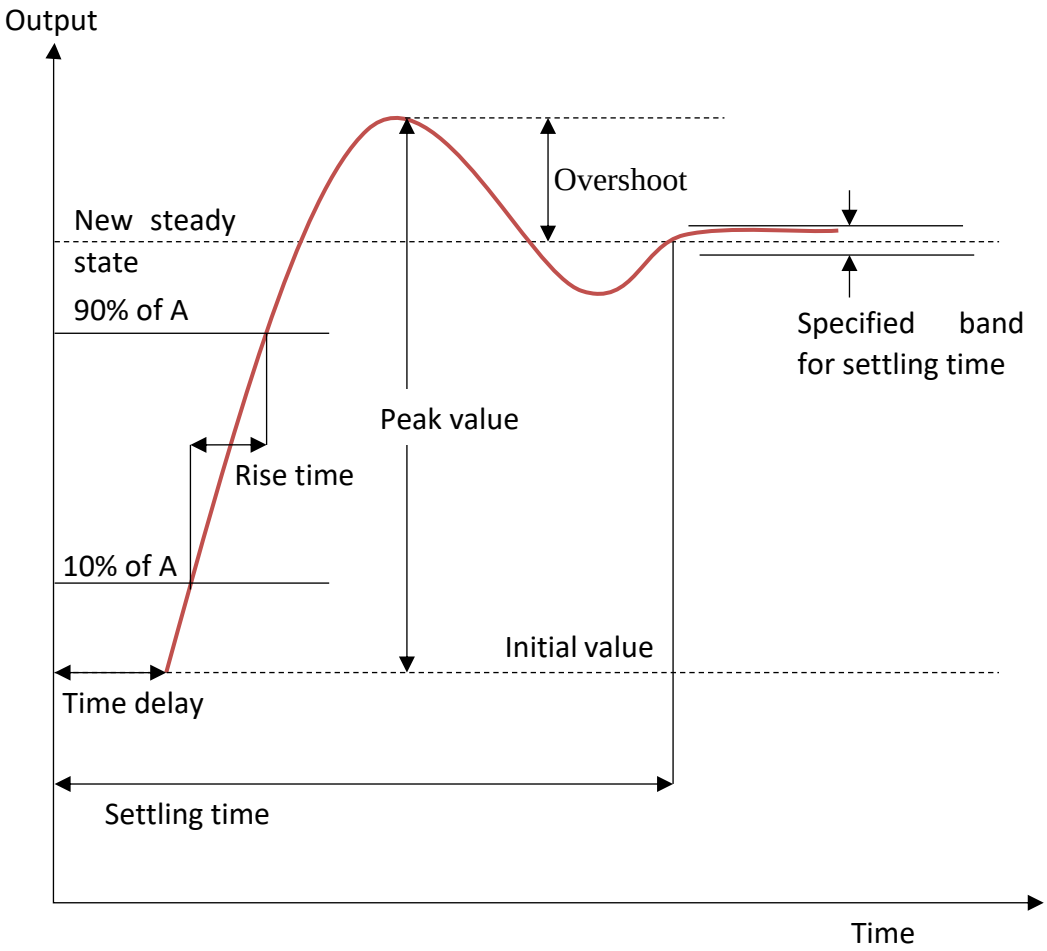


Figure 3.3: Typical dynamic response of a governor to a step change in reference speed

3.1.2 **Different types of AVRs**

A SG has a rotor field winding supplied with a DC current. The DC current is generated via an excitation system. The excitation system together with the AVR attempts to maintain steady-state voltage stability and improve dynamic voltage stability during a disturbance. Automatic Voltage Regulators (AVRs) use feedback to maintain a constant generator terminal voltage whenever RMS voltage fluctuations occur due to varying load [18].

The main types of excitation systems are:

i. Direct current (DC) commutator rotating exciter

ii. Alternating current (AC) alternator that uses either stationary or rotating rectifiers to produce the DC field current [19].
iii. Static excitation system (ST) that uses rectifiers, either controlled or uncontrolled, to produce the DC field current [19]. The most commonly used types of static excitation systems are the STA1 and STA2.

3.2 SPV

Solar PhotoVoltaic (SPV) uses solar energy as a renewable source. SPV is inverter-based distributed generation (DG).

The SPV synchronises with the utility voltage in terms of the frequency and voltage phase angle. Therefore, during the interconnection of the SPV system and the utility grid, the SPV system will be operating at the same frequency and voltage phase angle as the utility voltage.

The primary function of an inverter is to convert DC to AC. However, its role is expanding to help improve grid stability and efficiency. Some inverters come with an anti-islanding functionality. There are two types of inverters, grid-following inverters and grid-forming inverters (discussed in section 4.2).

3.3 The probability of continued islanding occurring

[5] addresses an important concept of islanding, that is the probability of continued islanding. The probability of continued islanding is dependent on the relationship between the load MW and the DG MW. In cases where the minimum load MW is much greater than the maximum DG MW the probability of continued islanding is small [5]. In cases where the DG MW is greater than the load MW, the DG will be able to continue to supply the load; hence the probability of continued islanding is high (the probability is one).

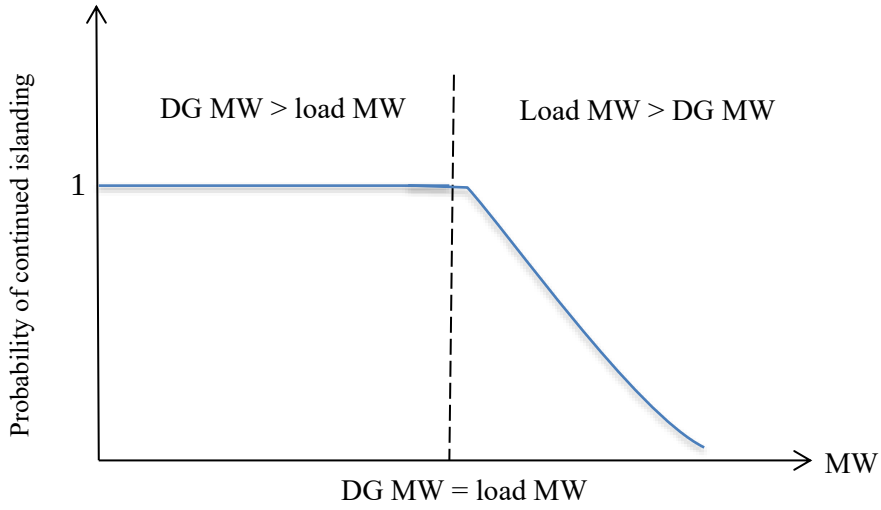


Figure 3.4: Probability of islanding occurring versus the relationship between the load MW and DG MW [5]

3.4 History of specifying the maximum islanding time

Ideally unintentional islanding should be detected and terminated immediately. However, during the development of the IEEE 1574-2003 standard, a short islanding time of two seconds was allowed. The problems associated with islanding were taken into consideration during the choice of the maximum islanding time. The open-time settings of the grid auto-reclosers played a major role in determining a maximum allowed islanding time, due to the hazards of out-of-phase reclosing.

The grid auto-recloser open-time setting was assumed to be two seconds which differs from that used by utilities, which is ten seconds. When the utility recloser opens in response to a fault, the recloser was assumed to wait two seconds (auto-reclosing open-time setting) and then reclose to restore power. If the recloser closes (auto-recloses) more quickly onto an islanded network, it might cause out-of-phase reclosing and damage equipment. The two seconds was originally introduced in the IEEE 929-1999 standard for PV with ratings of 10 kW and below [10]. The DG manufacturers were then required to meet the two seconds maximum islanding time requirement. The history of the two seconds maximum islanding requirement is shown in Figure 3.5.

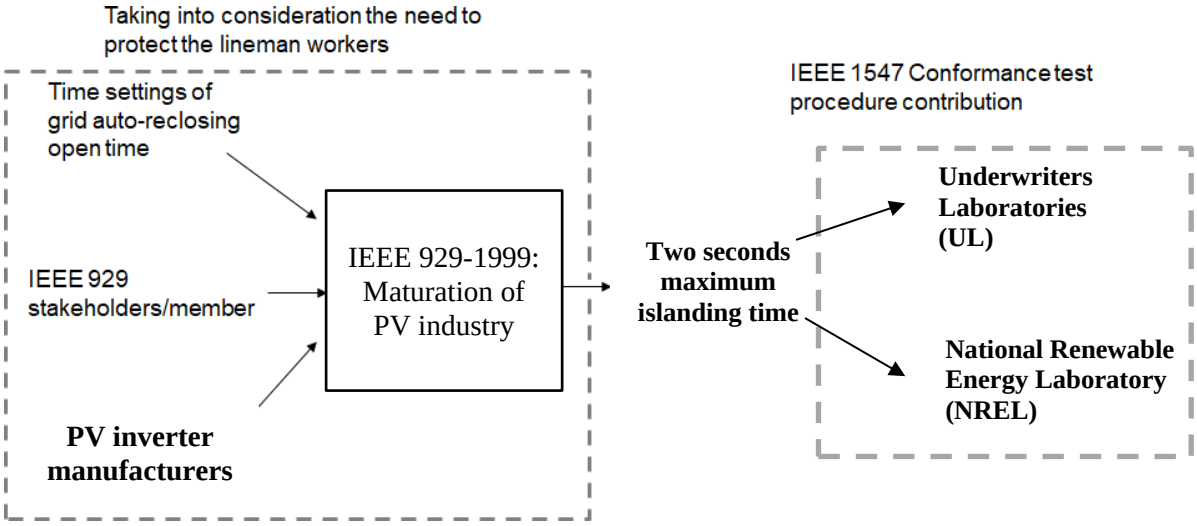


Figure 3.5: History of the two-second maximum islanding time requirement

3.5 Different load models in power system studies

For dynamic power system studies, the transient and steady-state variation of the load active power and reactive power with changes in RMS voltage and frequency must be modelled. The load characteristics are among the key factors influencing the voltage and frequency stability. Stable operation of the power system depends on its ability to continuously match the electrical output of generating units to the electrical load on the system [16].

Loads are traditionally classified as either static or dynamic as illustrated in Figure 3.6 with the advantages and disadvantages listed in Table 3.1. Static loads represent the active and reactive power as a function of RMS voltage and frequency. Whereas dynamic loads represent active and reactive powers as a function of RMS voltage, frequency and time [20] and [21].

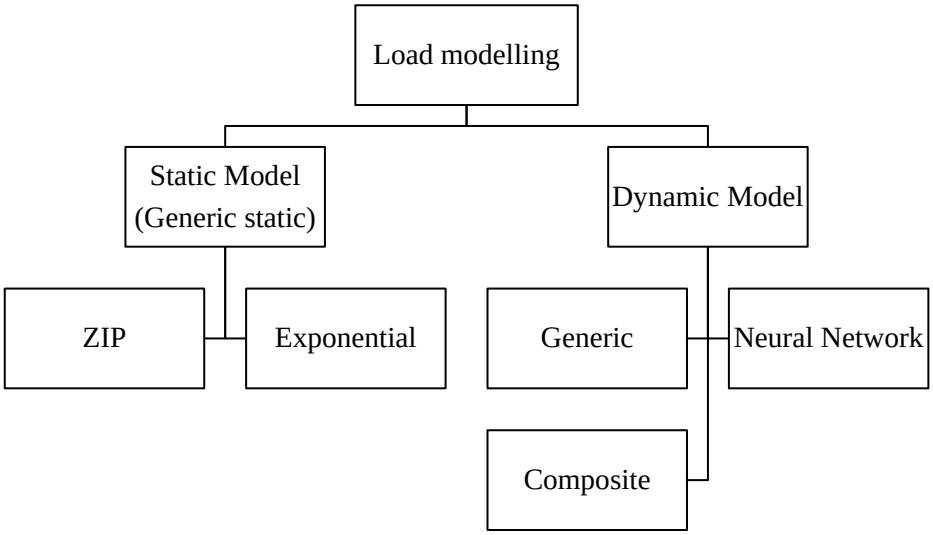


Figure 3.6: Classification of load models

Table 3.1: Load model summary [20].

Load model	Advantage	Disadvantage
Generic Static	Less complex and can be applied to a large number of loads	Does not represent dynamic load behaviour
Generic Dynamic	Can be applied to a large number of load models	Model is based on the response to a RMS voltage disturbance. Will change for different conditions
Composite Dynamic	Combines generic static and generic dynamic loads	Dynamic behaviour of many loads usually too complicated to express in a simple analytic form
Neural Network Dynamic	Can map any complex relationship between load parameters. Ability to learn and adapt	Does not directly model the physical load attributes

3.5.1 Static load

Static load models are used for static load components such as resistive loads and as an approximation for dynamic loads. Static load models include the exponential model and the ZIP model, illustrated in Figure 3.6.

A. Exponential load model

Static load models can be expressed in an exponential form to relate the power (reactive and active) and the RMS voltage at a load bus. The load is modelled as a voltage dependent load using equation (3.1) and equation (3.2) for the active power and the reactive power respectively. The most commonly accepted static load model is to represent the active and reactive powers as [22]:

Constant active power:	$p = p_0$	(3.1)
Constant current (active power proportional to RMS voltage only):	$p = p_0(\frac{u}{u_o})$	
Constant impedance (active power proportional to the square of the RMS voltage only) :	$p = p_0(\frac{u}{u_o})^2$	
Constant reactive power:	$q = q_0$	(3.2)
Constant current (active power proportional to RMS voltage only):	$q = q_0(\frac{u}{u_o})$	
Constant impedance (active power proportional to the square of the RMS voltage only) :	$q = q_0(\frac{u}{u_o})^2$	

Where

u_o = Reference busbar RMS voltage (V)

u = Actual busbar RMS voltage (V)

p_o = Active power at the reference busbar RMS voltage (W)

q_o = Reactive power at the reference busbar RMS voltage (Var)

B. ZIP/ Polynomial load model

The ZIP model is commonly used in both steady-state and dynamic studies [2]. This model represents the relationship between the RMS voltage magnitude and power as a polynomial equation. It combines constant impedance (Z), constant current (I) and constant power (P) components, using the exponential parameters described as equation (3.3) and (3.4). For composite loads, their value depends on the aggregate characteristic of the load.

$$p = p_0\left(a + b\left(\frac{u}{u_o}\right) + c\left(\frac{u}{u_o}\right)^2\right) \tag{3.3}$$

$$q = q_0\left(d + e\left(\frac{u}{u_o}\right) + f\left(\frac{u}{u_o}\right)^2\right) \tag{3.4}$$

Where; $a, b, c, d, e\ and\ f$ are the constants of proportionality of the static parts of the load.

u_o = Reference busbar RMS voltage (V)

u = Actual busbar voltage (V)

p_o = Active power at the reference busbar voltage (W)

q_o = Reactive power at the reference busbar voltage (Var)

C. Frequency dependency

The frequency dependency of the load is presented by multiplying the exponential or ZIP model by a factor that depends on the frequency of the RMS voltage applied [22]. The factor can be represented using equation (3.5).

$$\mathrm{f_{factor}} = [1 + a_f(\mathrm{f} - f_0)] \tag{3.5}$$

a_f = Frequency coefficient

f = Frequency of the busbar RMS voltage (Hz)

f_0 = Nominal frequency (50 Hz)

[22] recommends that if nothing is known about the load characteristics, then a constant current model can be used for the active power and a constant impedance model can be used for the reactive power. All modelled loads within this document are modelled based on equations (3.3), (3.4) and (3.5).

Table 3.2 summarizes the ideal circuit element versus the real-world circuit element, to justify the implemented load models.

Table 3.2: Ideal circuit element versus real-world circuit element

Load type	**Description**	**V and I relationship**	**Real-world examples**
Pure resistance	Loads consisting of heating elements are classified as resistive loads	$V_R = I_R \times \mathrm{R}$	Electric heaters Cookers Incandescent lamps Irons Geysers
Series RL	An inductive load is a load that requires a magnetic field to operate.	$V = V_R + V_L$ $V_R = I_R \times \mathrm{R}$ $V_L = I \times 2\pi fL$	Fans Air conditioners Dishwashers Electric motors
Parallel RL		$V = V_R = V_L$ $V_R = I_R \times R$ $V_L = I_L \times 2\pi fL$	
Parallel RC	Shunt capacitors are used in distribution systems for power factor correction and feeder voltage control.	$V = V_R = V_C$ $V_R = I_R \times \mathrm{R}$ $V_C = I_C \times \frac{1}{2\pi fC}$	Resistive loads with shunt capacitors

3.5.2 **Dynamic loads**

For loads that are subjected to large fluctuations in RMS voltage and/or frequency, dynamic load modelling becomes important [22], [23]. The equivalent circuit of the induction motor, shown in Figure 3.7 is one type of dynamic load model.

Rs and Rr’ are the stator and (referred) rotor winding resistances respectively Xs, Xr’ and Xm are the stator leakage, (referred) rotor leakage and magnetizing reactances, respectively and s is the rotor slip.

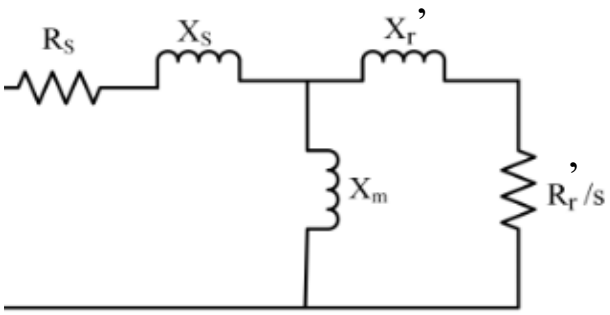


Figure 3.7: Equivalent circuit of a three-phase induction motor

An induction motor is the most commonly used motor for industrial drives [24]. Its dynamic behaviour has a significant influence on the transient behaviour of the power system [25]. During start-up and other disturbances, the induction motor draws large current, produces voltage dips, oscillatory torques and current harmonics.

There are two important curves describing the induction motor steady-state behaviour: the current-speed curve and the torque-speed curve.

A. Current-speed curve of the induction motor

The current-speed curve is obtained from the equivalent circuit of the induction motor by substituting different values of slip. The typical current-speed curve of the induction motor is shown in Figure 3.8.

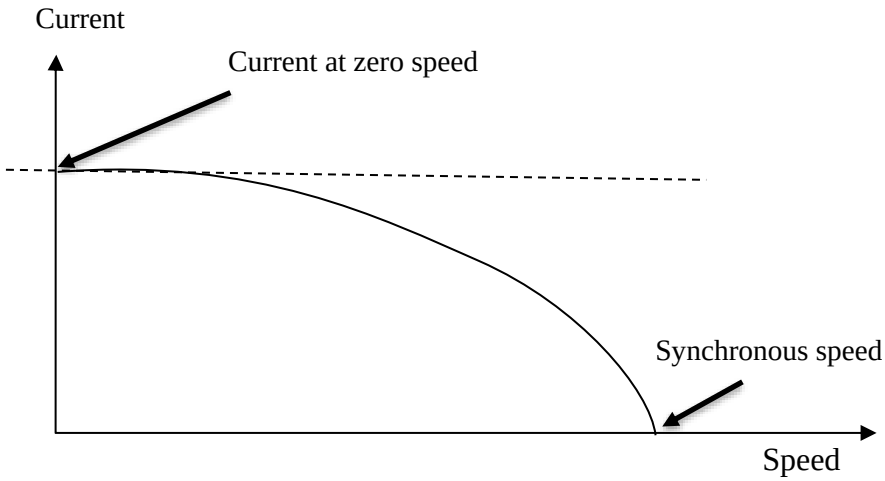


Figure 3.8: Typical current-speed curve of an induction motor

B. The torque-speed curve of the induction motor

The typical torque-speed curve of the induction motor is shown in Figure 3.9 and is also obtained from the equivalent circuit. The pull-out torque is the maximum possible torque that the motor can produce.

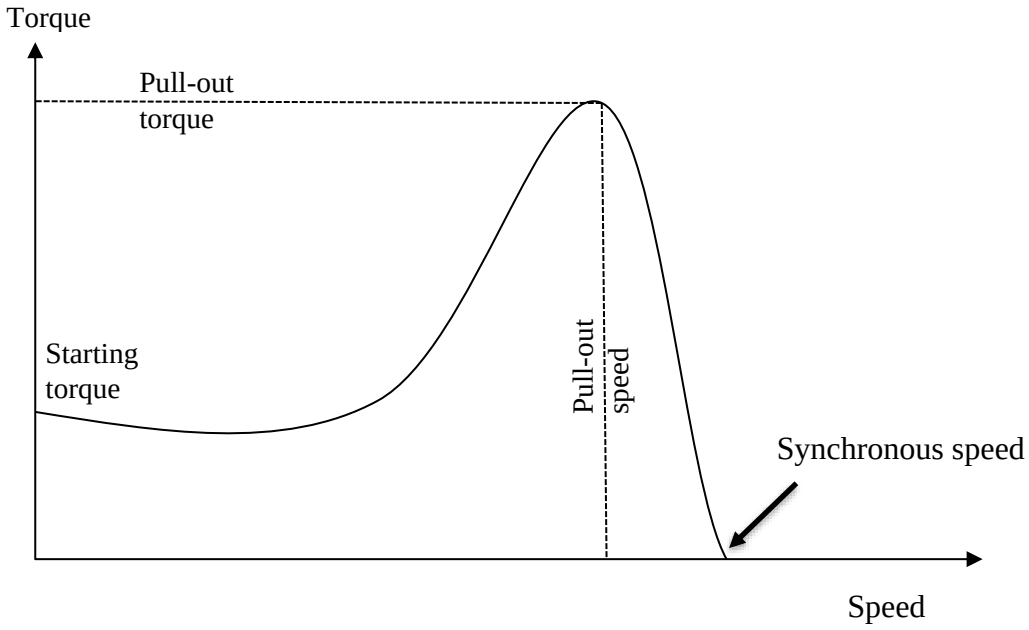


Figure 3.9: Typical torque-speed curve of an induction motor

C. The mechanical load connected to the induction motor

The type of mechanical load of interest in this dissertation was the centrifugal pump. The centrifugal pump has a torque-speed curve where the torque is proportional to the square of the speed and the mechanical power is proportional to the cube of the speed. The rating of the pump at synchronous speed is set equal to the power rating of the motor.

Chapter 4 – Methodology

This chapter describes the methodology used to investigate the RMS voltage and frequency behaviour of a 400 V microgrid containing SG and/or SPV after islanding.

4.1 SG Only

The RMS voltage and frequency behaviour after islanding of a 400 V microgrid previously connected to a 22 kV rural network was simulated. The load types (purely resistive, series RL, or series RL plus induction motor) and SG active power percentage contribution were modelled as variables in the islanded network. Figure 4.1 illustrates the scenarios studied in diagrammatic form. The simulated network diagram is shown in Figure 4.2.

The power quality assessment was performed using the DIgSILENT PowerFactory software. To model the equivalent source or the external grid, the following was required: pre-fault voltage, short-circuit current and the source impedance of the utility grid at the point of supply.

The Root Mean Square (RMS) simulation tool within DIgSILENT PowerFactory was used to analyse the RMS voltage and frequency behaviour after islanding.

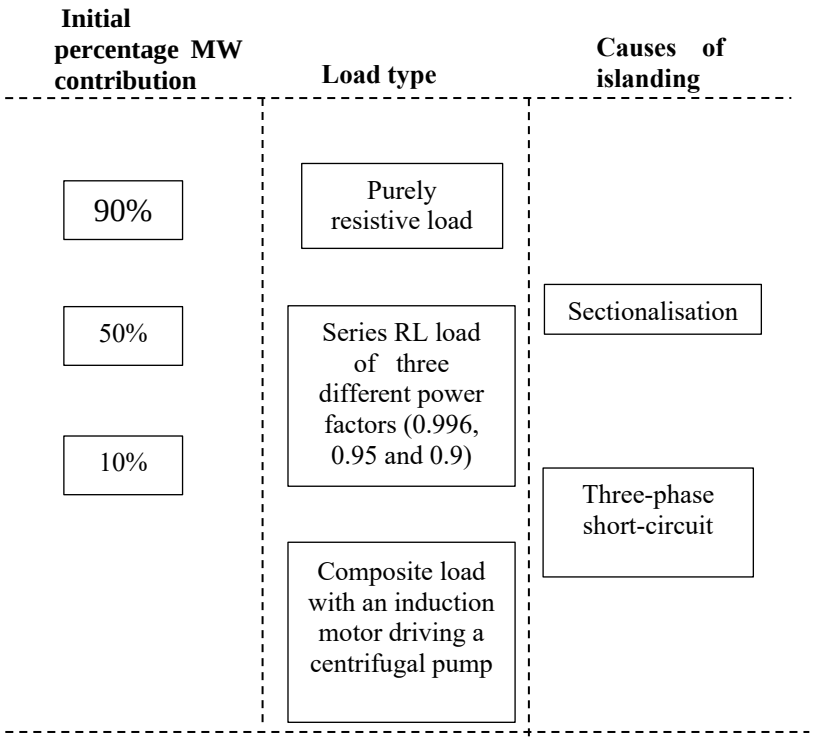


Figure 4.1: Synchronous Generator scenarios studied

The governor responds to the underfrequencies associated with the low SG initial percentage MW contributions and raises the MW contribution up to 100% so that no load needs to be shed.

In South Africa, power factors between 0.95 and 1.0 lagging are regarded as good. The utility (Eskom) charges an additional reactive power fee where a facility's power factor is less than 0.95. A lower inductive power factor causes higher current flow for a given active power load, reduces the distribution network voltage and increases the network losses.

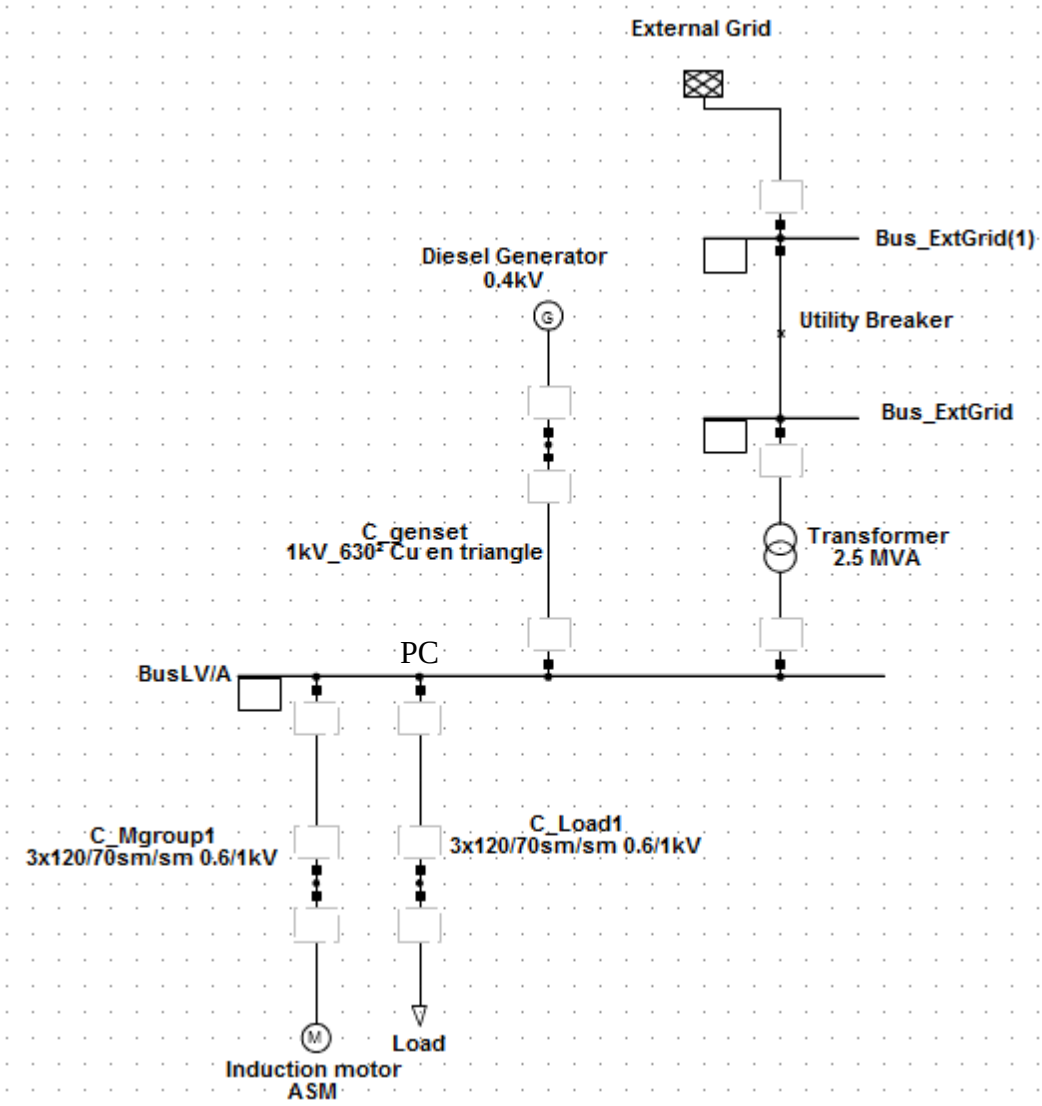


Figure 4.2: Diesel Generator simulated network diagram

4.1.1 **Purely resistive load**

A purely resistive load was kept constant and the SG initial (prior to islanding) percentage MW contributions were 10%, 50% and 90%, as illustrated by 50% in Figure 4.3.

Islanding was initiated at 10s of the simulation run by creating an event that opened the utility breaker. The event was either a fault on the incoming 22 kV feeder, which causes the feeder protection to operate, which causes islanding, or it was due to

sectionalisation (no fault present). The RMS voltage and frequency behaviours were measured at the Point of Connection (PC).

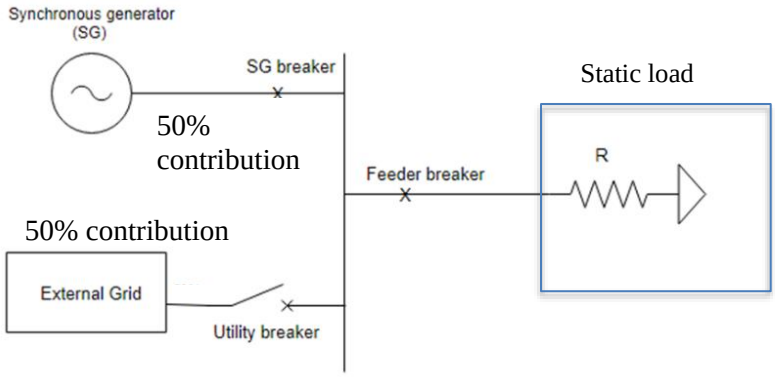


Figure 4.3: Network diagram illustrating the purely resistive load

4.1.2 **Series RL load**

In this case, the resistance was kept constant while the SG initial percentage MW contribution and the power factor of the series RL load were varied. The SG initial percentage MW contributions were 10%, 50%, and 90% and the power factors were 0.996, 0.95 and 0.9.

4.1.3 **Composite load**

In this analysis, the frequency, RMS voltage and RMS current as a function of time during islanding were of interest. The SG initial percentage MW contributions were 10%, 50% and 90%. The speed and mechanical load of the induction motor were also studied. The network diagram is shown in Figure 4.4 and shows the combination of the static load model and the induction motor model.

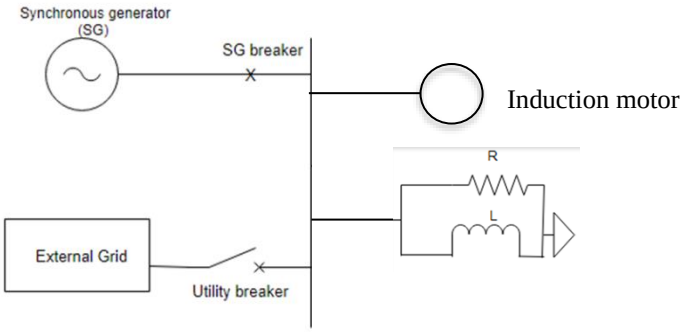


Figure 4.4: Composite network diagram for the static and dynamic load

The mechanical load was modelled as a centrifugal pump rated at 200 kW, with the torque-speed curve shown in Figure 4.5. The torque-speed curve shape is similar for all centrifugal pumps (the pump torque varies as the square of its speed).

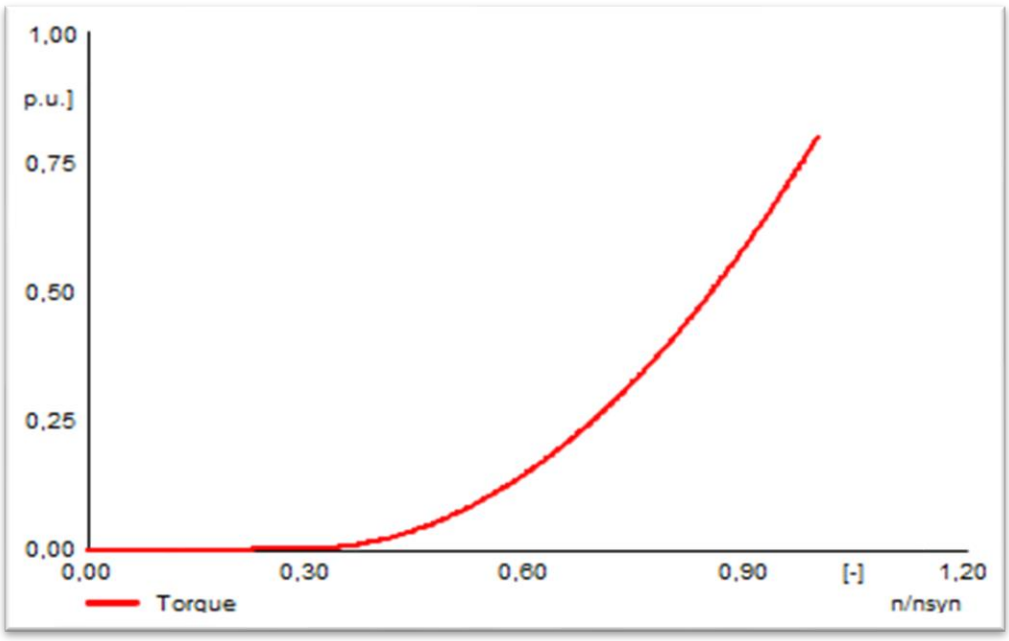


Figure 4.5: Torque-speed curve of a pump mechanical load

4.1.4 **Governor model**

The governor model used was the Degov (diesel governor) model, shown in Figure 4.6, with the recommended parameter values [26] tabulated in Table 4.1.

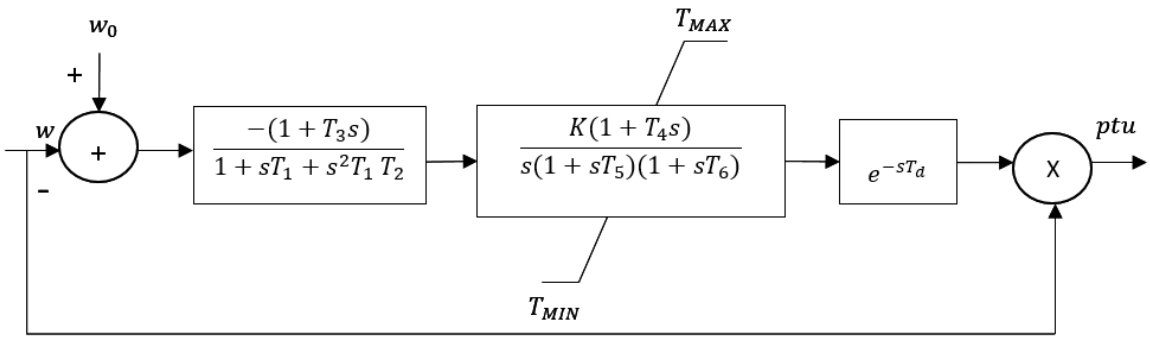


Figure 4.6: Degov diesel engine governor model

Table 4.1: Degov recommended parameter values [26]

Degov			
Name	**Value**	**Unit**	**Description**
T_1	0,01	[s]	Controller time constant
T_2	0,02	[s]	Controller time constant
T_3	0,2	[s]	Controller time constant
K	20	[pu]	Actuator gain
T_4	0,025	[s]	Actuator time constant
T_5	0,009	[s]	Actuator time constant
T_6	0,0384	[s]	Actuator time constant
T_d	0,0208	[s]	Engine delay
T_{MIN}	0	[pu]	Actuator min output
T_{MAX}	1,1	[pu]	Actuator max output

4.1.5 AVR model

The AVR excitation system model used was the AC5A. The AC5A model is an IEEE standard simplified brushless excitation control system model with a rotating rectifier, described in IEEE standard 421.5. This model is widely used in industry.

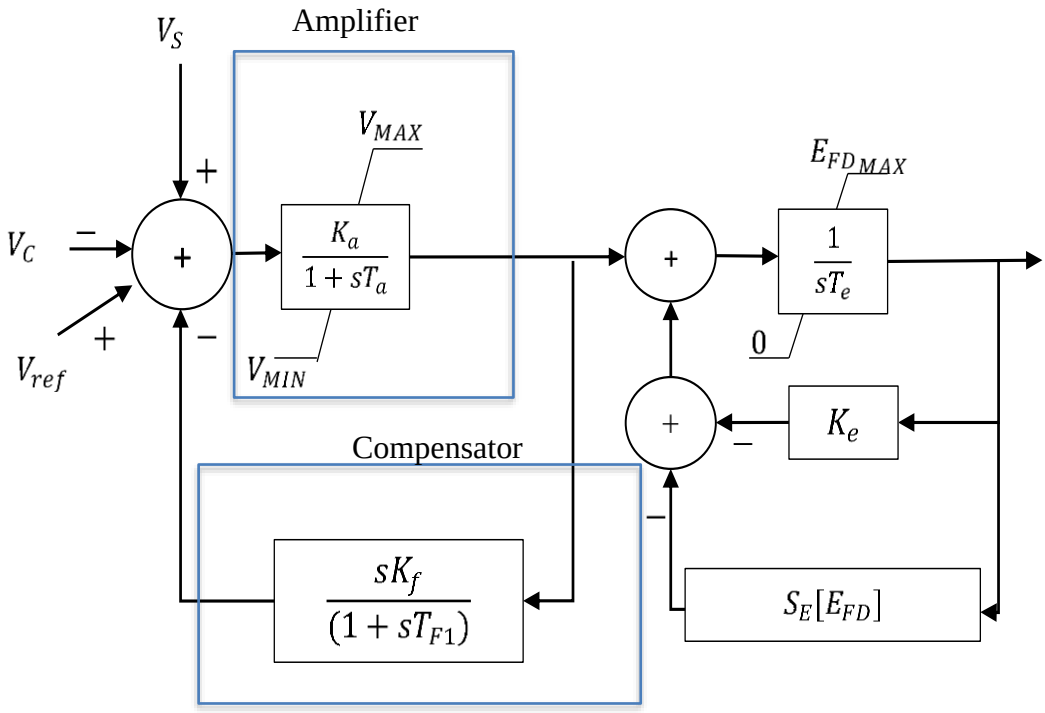


Figure 4.7: AC5A AVR model

The AC5A AVR model is shown in Figure 4.7 and the parameter values are tabulated in Table 4.2.

The output of the amplifier model highlighted in Figure 4.7 includes the saturation characteristic of the controller. The transfer function of the compensator is also highlighted in the model. The compensator allows the process variable output to be measured such that the input variable can be manipulated as needed to drive the process variable towards the reference value. The controller adds integral and derivative terms to improve the damping, steady-state error, overshoot and settling time.

The closed-loop AVR model transfer function (assuming no saturation) is described in equation (4.1). The simulated step response of the controller is illustrated in Figure 4.8, which shows the response from the initial value of 0, to the desired value (approximately 1 pu).

$$\text{Closed loop Tf} = \frac{k_a(sT_{f1}+1)}{T_aT_{f1}s^2 + (T_a + T_{f1} + k_ak_f)s + 1} \qquad (4.1)$$

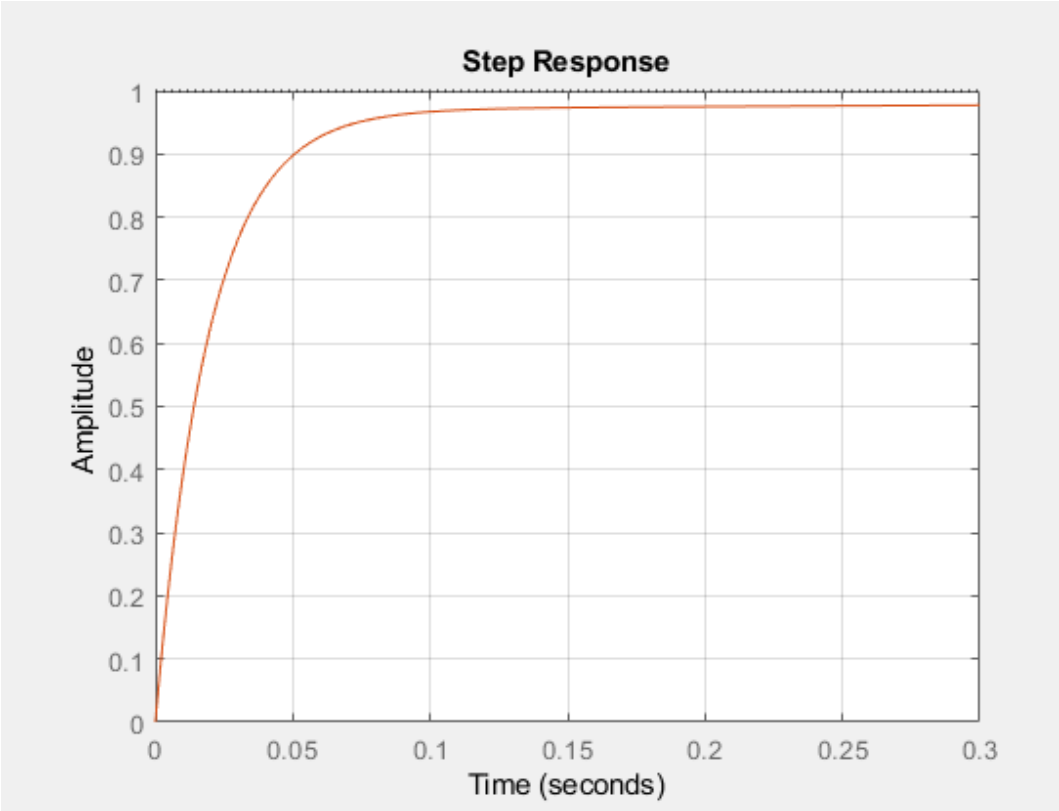


Figure 4.8: Step response of the AC5A AVR model (equation (4.1))

Table 4.2: Typical values for type AC5A excitation systems [19]

Name	Value	Unit	Description
K_a	400	[pu]	Controller Gain
T_a	0,02	[s]	Controller Time Constant
K_e	1	[pu]	Excitor Constant
T_e	0,25	[s]	Excitor Time Constant
K_f	0,03	[pu]	Compensator Gain
T_{f1}	1	[s]	Compensator Time Constant
E_{FD}	5,6	[pu]	Saturation Factor 1
$S_E[E_{FD}]]$	0,86	[pu]	Saturation Factor 2
E_{FD2}	4,2	[pu]	Saturation Factor 3
$S_E[E_{FD2}]$	0,5	[pu]	Saturation Factor 4
V_{MIN}	-7,3	[pu]	Controller Minimum Output
V_{MAX}	7,3	[pu]	Controller Maximum Output

The above typical values were adjusted to improve the step response during the simulation (Figure 5.2 and 5.3).

4.1.6 Assumption

The generator output power can ramp up to supply the full load demand during islanding.

The simulation results are in section 5.1.

4.2 SPV only

There are two types of PV inverters namely [27];

- Grid-forming (GFM)
- Grid-following (GFW)

The grid-forming (GFM) inverter maintains a constant microgrid frequency and voltage. The grid-following (GFW) inverter dispatches active and/or reactive power into an existing grid. Typical active power versus frequency droop curves of the GFM and GFW inverters are shown in Figure 4.9 and their differences are tabulated in Table 4.3. Grid-forming inverters are used to improve the transient stability of autonomous microgrids and active distribution systems [27].

Table 4.3: Grid following versus grid forming

Grid-following (GFW)	**Grid-forming (GFM)**
Modelled as a current source	Modelled as a voltage source
Current Control (active and reactive)	Voltage and frequency control
Cannot work in islanded mode	Can work in islanded mode

The majority of grid-tied inverters operate as GFW inverters that track the phase angle of the grid voltage to control their output current.

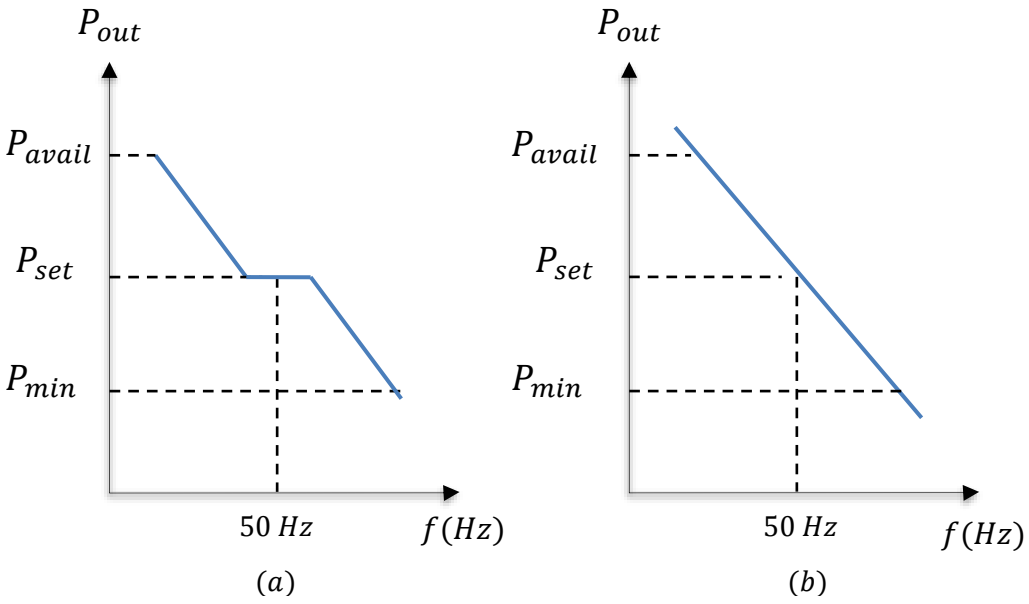


Figure 4.9: (a) active power versus frequency droop characteristic for grid-following units with dead-band and (b) active power versus frequency droop characteristic for grid-forming units without dead-band

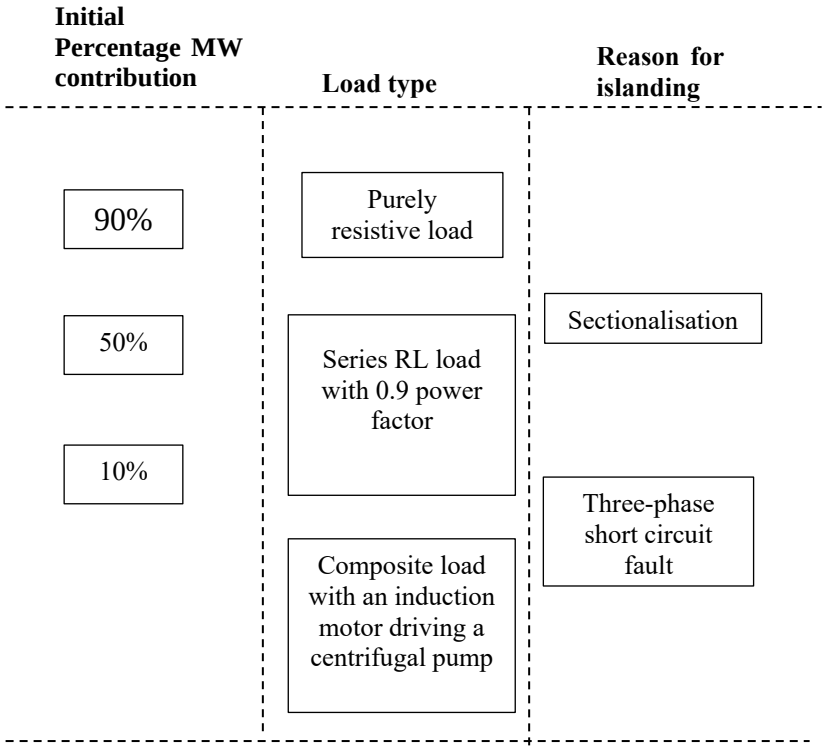


Figure 4.10: SPV scenarios

To understand how the SPV responds to islanding in terms of RMS voltage and frequency, three load conditions were considered (purely resistive load, series RL load and the combination of an induction motor and a series RL load). The scenarios studied are shown in Figure 4.10. The simulated network is shown in Figure 4.11.

The SPV was simulated for an initial percentage MW contribution of 90% of the load demand (SPV initially curtailed by 10%). When the microgrid was islanded the SPV was able to ramp up to the full 100% load demand. For an initial percentage MW contribution of 10% (SPV also initially curtailed by 10%) the SPV was able to ramp up to only 11% of the load demand and the balance of the load had to be shed. For an initial contribution of 50% (SPV also initially curtailed by 10%) the SPV was able to ramp up to only 55% of the load demand and the balance of the load was shed.

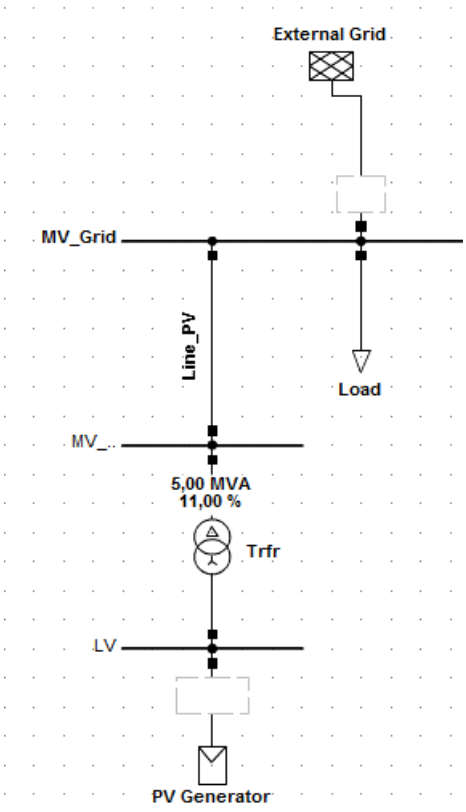


Figure 4.11: SPV system simulated network diagram

4.2.1 SPV GFW inverter Model

The WECC SPV GFW model (PVD1) was employed for the following conditions.

i. The undervoltage and underfrequency ramp-down functionalities were disabled [28] [29].
ii. The zero-voltage ride-through capability was enabled

The PVD1 model shown in Figure 4.12 represents small-scale distributed PV aggregated at the distribution level. The PVD1 model includes both active and reactive power control. The IEEE/WECC recommended parameter values are tabulated in Table 4.4.

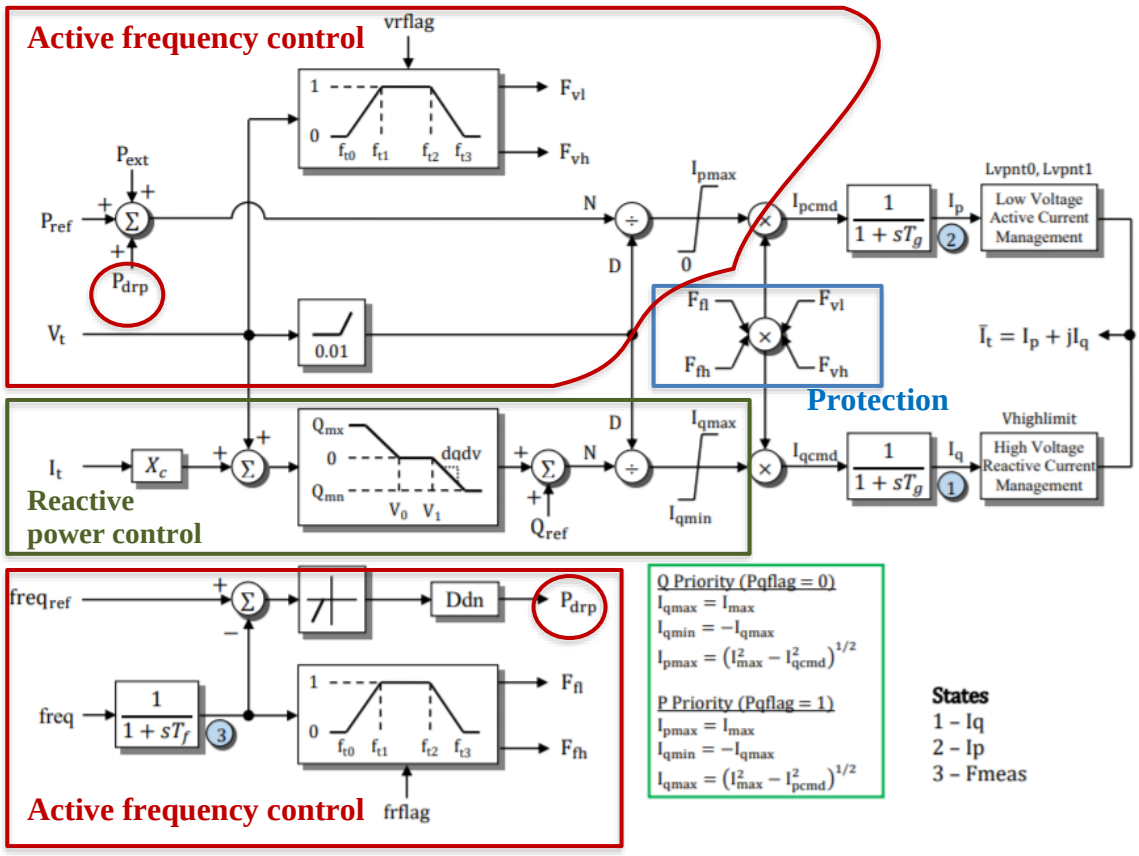


Figure 4.12: Block diagram of the WECC distributed PV (PVD1) model [28].

Table 4.4: PVD1 IEEE/WECC recommended values

Name	Value	Unit	Description
Pqflag	1		Priority on current limit flag: 1=P priority.; 0=Q priority
I_{max}	10	[pu]	Maximum allowable total converter current
T_g	0,02	[s]	Inverter current regulator time constant
X_c	0	[pu]	Line drop compensation reactance
Q_{mx}	10	[pu]	Maximum reactive power
Q_{mn}	-10	[pu]	Minimum reactive power
V_0	0,3	[pu]	Low voltage threshold for Volt/Var Control
V_1	1,9	[pu]	High voltage threshold for Volt/Var Control
Dqdv	0	[pu]	Voltage/Var droop compensation
Fdbd	-99	[pu]	Frequency deadband over-frequency response
Ddn	0		Down regulation droop [pu Power/pu Frequency]

4.2.1.1 Active power-frequency (P-f) control and Voltage-var control (VCC)

The majority of SPV grid-connected inverters operate in the GFW mode. This type of current control (active and reactive) is unable to control the voltage and frequency of the islanded microgrid without another voltage source it can synchronise with.

Active power-frequency (P-f) control allows the SPV to participate in frequency control when the microgrid is grid-connected by adjusting the output active power according to a droop curve (also known as Frequency-Watt (FW) control). Voltage-var control (VVC) allows the SPV to control its voltage when the microgrid is grid-connected by adjusting the output reactive power according to the droop curve.

A. Principle of FW control

FW control measures the variation of the grid frequency and subsequently changes the power output, as shown in Figures 4.9 and 4.13. The disadvantage of using the GFW inverter with FW is that it introduces unwanted oscillation in the frequency response due to the time delay between the measured frequency and the change of the output power [30].

One of the fundamental concepts of using the GFW with FW is the dynamic, curtailed output power of the source, in this case, the SPV. The curtailed power enables the SPV to regulate the frequency. Without the curtailed power, the system would not be able to participate in frequency regulation (this behaviour is later simulated).

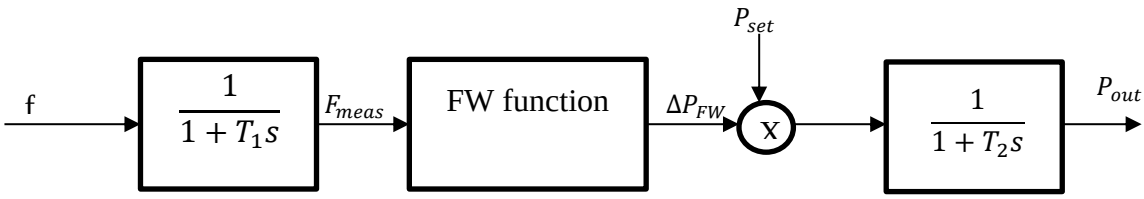


Figure 4.13: Distributed inverter PV model including FW function

B. Principle of Volt-Var control (VCC)

Generally, the problem with SPV is the voltage rise due to reverse power flow and volt-var control is typically used to maintain the voltage within acceptable ranges [31]. Similar to FW, the VVC measures the variation of the grid voltage and subsequently changes the reactive power output.

4.2.1.2 PVD1 model

The PVD1 model models the current source behaviour of the GFW inverter.

The inputs of the PVD1 are P_{req} (the required power), $Freq_{req}$ (the required frequency) and V_t (terminal voltage) to determine the required output current.

The two control modes are:

A. Active power control

The active power control determines the active current that is injected by the SPV, it is shown in Figure 4.12.

The difference between the $\mathrm{Freq}_{\mathrm{ref}}$ and the Freq gives the frequency deviation. This error signal passes through a dead-band block, so only negative results

(overfrequency) will take effect in the control as per the dead-band (Figure 4.12). The output signal passes through a gain block (Ddn), providing the adjustment that is applied to the reference power in order to eliminate the overfrequency. The result is divided by the terminal voltage, giving the active current to be injected into the network [32].

B. Reactive power control

The reactive power control determines the reactive current that is injected by the SPV. The control logic is shown in Figure 4.12. The terminal voltage (V_t) is added to the line drop compensation ($I_t \times X_c$) to produce the internal voltage. The result is used to determine the reactive power droop that is added to the reactive power reference (Q_{ref}). In this way, the reactive current to be injected into the system is computed by dividing the reference reactive power (Q_{ref}) by the terminal voltage.

The two parameters that are relevant for modelling the partial loss of SPV due to voltage sags are Vt_1 and Vt_0. Between the voltage levels bound by Vt_1 and Vt_0 a linear function is implemented so that an increasing amount of DPV is disconnected as the voltage decreases. This functionality was disabled in this study.

Voltage stability is usually expressed in terms of a stability margin. It is defined as the difference between the loadability limit and the current operating load level. The reserved loadability limit in the simulations is 10% of the initial operating load level.

4.2.2 **Purely resistive load**

The SPV initial percentage MW contributions were 10%, 50%, and 90%. The SPV supplying a purely resistive load is shown in Figure 4.14. Islanding was initiated by creating an event to open the utility breaker after 10 seconds into the simulation. The voltage and frequency behaviour were measured at the point of connection (PC).

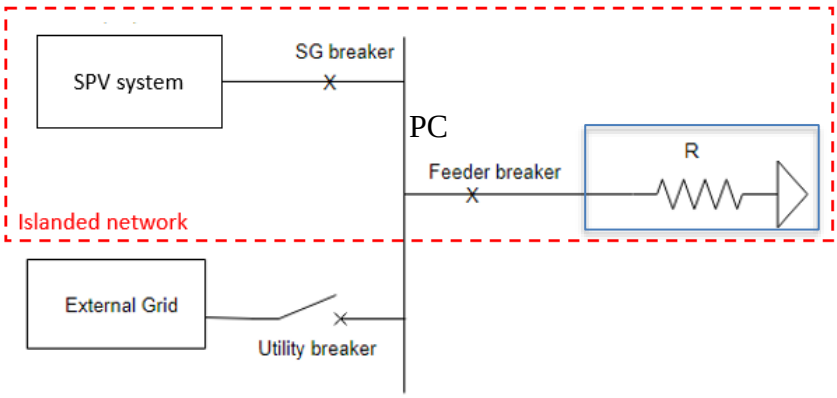


Figure 4.14: Network overview of SPV supplying a purely resistive load during islanding

4.2.3 **Series RL load**

In this case, the resistance and reactance were kept constant while the MW contribution of the PV was varied. The SPV MW contributions were 10%, 50%, and 90% and the power factor of the load was set at 0.9.

4.2.4 **Composite load**

As described in section 4.1.3, the same simulation model was used. The simulation results are in section 5.2

4.3 SG and SPV in parallel

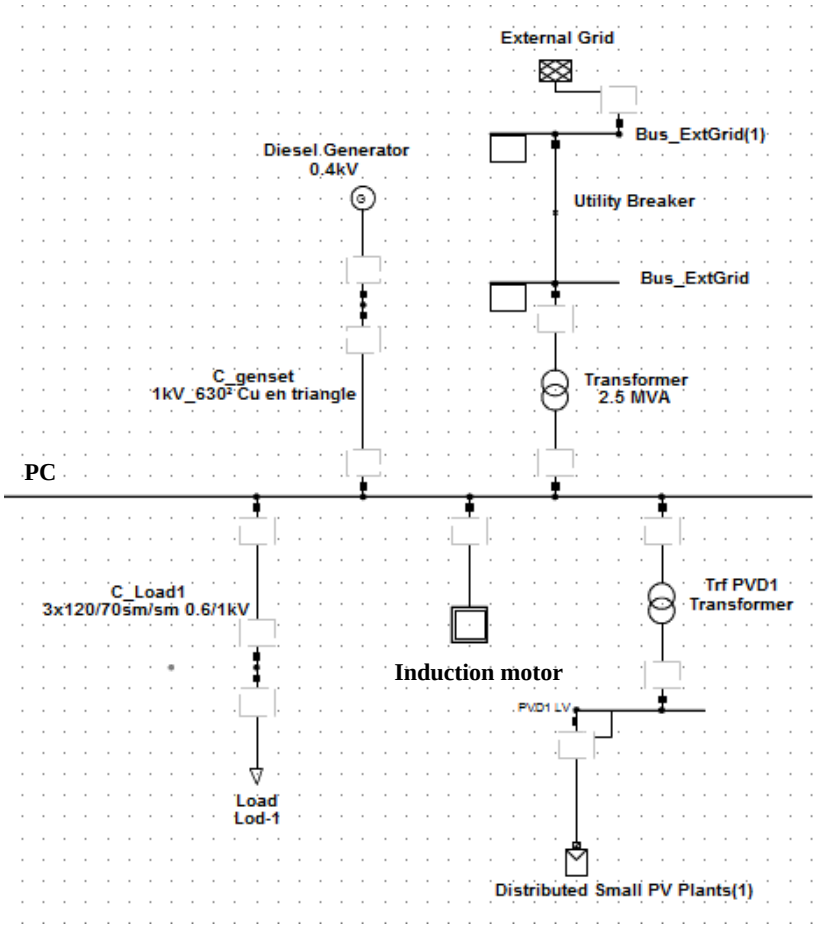


Figure 4.15: Diesel generator in parallel with SPV system network diagram

The voltage and frequency behaviour following islanding of a 400 V microgrid previously connected to a 22 kV rural network was investigated. The load types (purely resistive, series RL, or series RL plus induction motor) and SG and SPV initial percentage MW contributions were modelled as variables in the islanded network. The simulated network diagram is shown in Figure 4.15. The simulation results are shown in section 5.3.

Chapter 5 – Simulation results

The RMS voltage and frequency behaviour of a 400 V microgrid containing SG (diesel generator) and/or SPV after islanding due to sectionalisation or due to an upstream three-phase short-circuit fault was investigated. The simulation scenarios are tabulated in Table 5.1.

Table 5.1: Simulation scenarios

Parameter	**Value**
SG/SPV MW set value	50 kW (10% initial contribution), 250 kW (50% initial contribution) and, 450 kW (90% initial contribution)
Purely resistive load	0.5 MW
Series RL load	0.5 MW (with pf=0.9, 0.95 and 0.996)
Induction motor	0.1 MW and 0.05 Mvar

5.1 SG simulations results

5.1.1 Purely resistive load

The RMS voltage and frequency behaviour of an SG supplying a purely resistive load after islanding due to sectionalisation or due to an upstream three-phase short-circuit fault were studied.

5.1.1.1 Islanding due to sectionalisation

At ten seconds, sectionalisation was initiated (by opening the utility breaker), which can either be intentional or unintentional. The SG was then forced to operate as a standalone supply (islanded mode). Given a SG with an initial contribution of 0.25 MW at nominal frequency of 50 Hz, the active power of the SG increased due to the change in load demand from 0.25 MW to 0.5 MW from the SG.

Based on equation (5.1) and as illustrated by Figure 5.1 (c), an increase in speed is expected when $P_{Mechanical} > P_{Electrical}$ and when $P_{Mechanical} < P_{Electrical}$ a decrease in speed is expected to compensate for the load change. When

$P_{Mechanical} = P_{Electrical}$ constant speed is expected from the diesel engine as shown in Figure 5.1. The load increase caused the diesel engine to slow down. The Degov responds by increasing the control valve position until the reference speed was attained.

$$P_{Mechanical} - P_{Electrical} = Jw\frac{dw}{dt} \quad (5.1)$$

Where;

$P_{Mechanical}$	=	Generator mechanical power [MW]
$P_{Electrical}$	=	Generator electrical power [MW]
J	=	Generator inertia
W	=	Angular speed

The speed/frequency of the network should be maintained at 1 pu. The proportional term reduces the speed error but does not prevent overshoot. The derivative term reduces the overshoot. The integral term reduces any long-term speed error.

It is observed that the RMS output voltage and speed of the SG during islanding is affected by the SG initial percentage MW contribution. For a 10% SG initial percentage MW contribution, a nadir RMS voltage and frequency of 0.955 pu and 0.953 pu are observed, respectively.

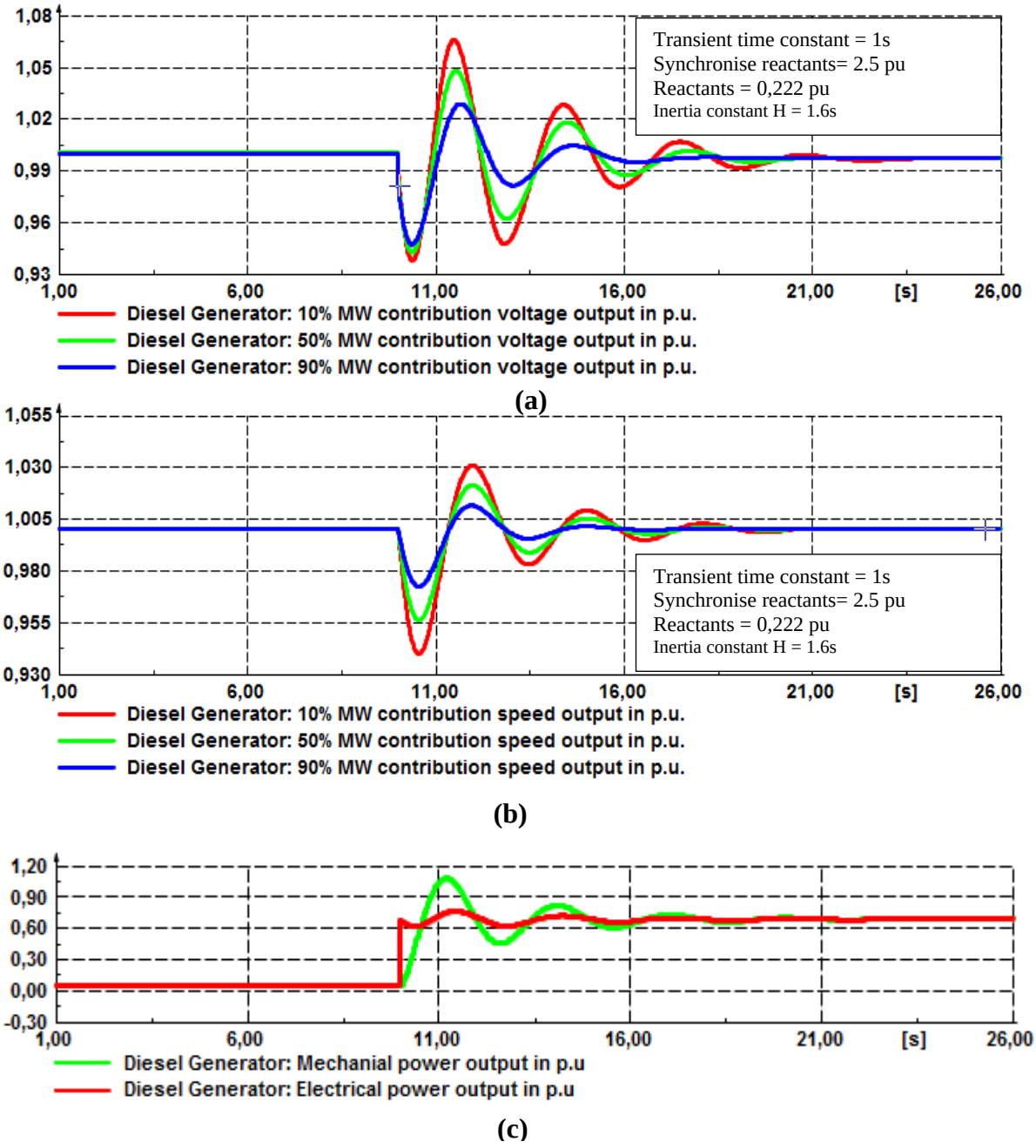


Figure 5.1: (a) shows the RMS voltage at the SG prior to and during islanding due to sectionalisation, (b) shows the speed of the diesel engine prior to and during islanding due to sectionalisation, (c) shows the mechanical power versus the electrical power prior to and during islanding due to sectionalisation with an SG MW percentage contribution of 10%.

An integral term was used to drive the process towards the set-point but can cause an oscillation. The smaller the integral-term gain, the more the response is prone to

oscillation. However, the critical factor in this analysis was the RMS voltage and frequency nadir (the minimum RMS voltage and frequency of the system and not necessarily the transient settling time of the signal), which is not significantly affected by the integral term of the controller as illustrated by Figure 5.2. Hence the recommended parameters from IEEE 421.5 were used in the simulations.

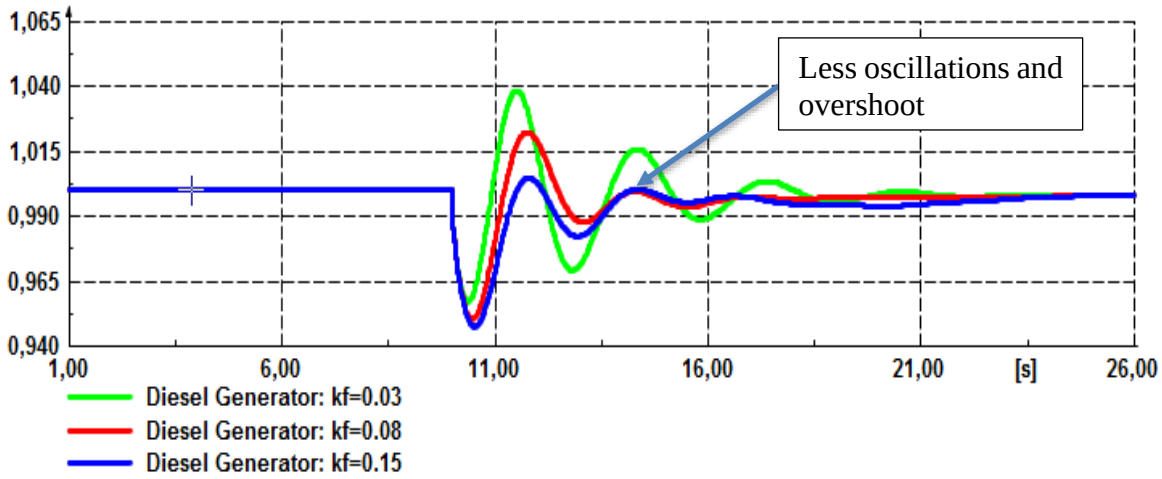


Figure 5.2: Illustration of the effect of the integral-term gain on the oscillation of the signal

Figure 5.3 illustrates the influence of the controller gain K_a It is shown that higher values of K_a shifted the stabilised value closer to unity. [33] recommends K_a>100 to be used for the AC5A AVR.

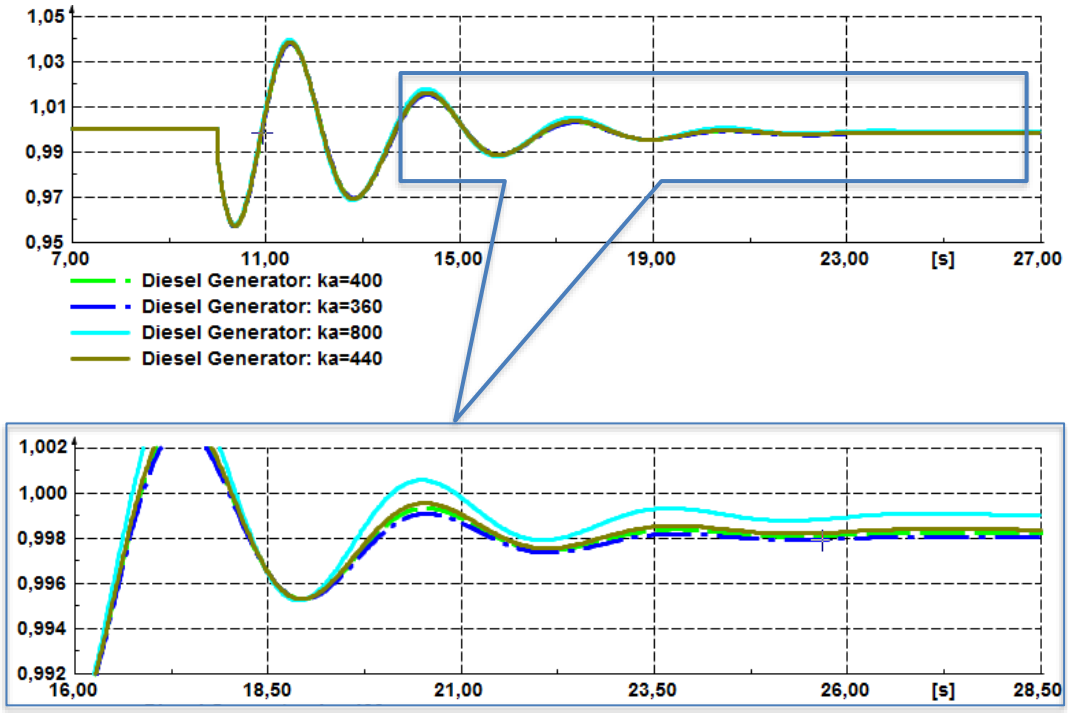


Figure 5.3: Illustration of the effect of the controller gain (Ka)

5.1.1.2 Islanding due to an upstream three-phase short-circuit fault

An upstream three-phase short-circuit fault was introduced at nine seconds at the incoming feeder of the external grid (utility). A three-phase short-circuit fault is considered to be the most severe condition that an SG can experience. The protection setting of the utility breaker were set to operate after one second of the initiated three-phase short-circuit fault. Thus, at ten seconds the utility breaker opened to clear the three-phase short-circuit fault, which establishes islanding.

The RMS voltage of the network collapses during the three-phase short-circuit, as shown in Figure 5.4 (a). After the fault is cleared, the governor and the AVR operate to try and bring the frequency and RMS voltage back to the nominal values and maintain those parameters, respectively, as shown in Figure 5.4. During the three-phase short-circuit fault, the SG electrical power output dropped due to the low fault voltage. Hence, this causes the speed of the diesel engine to increase as shown in Figure 5.4 (b).

Figure 5.4 (a) shows that for all SG MW percentage contributions, when an upstream three-phase short-circuit fault is introduced into the network, the RMS voltage drops to 0.2 pu.

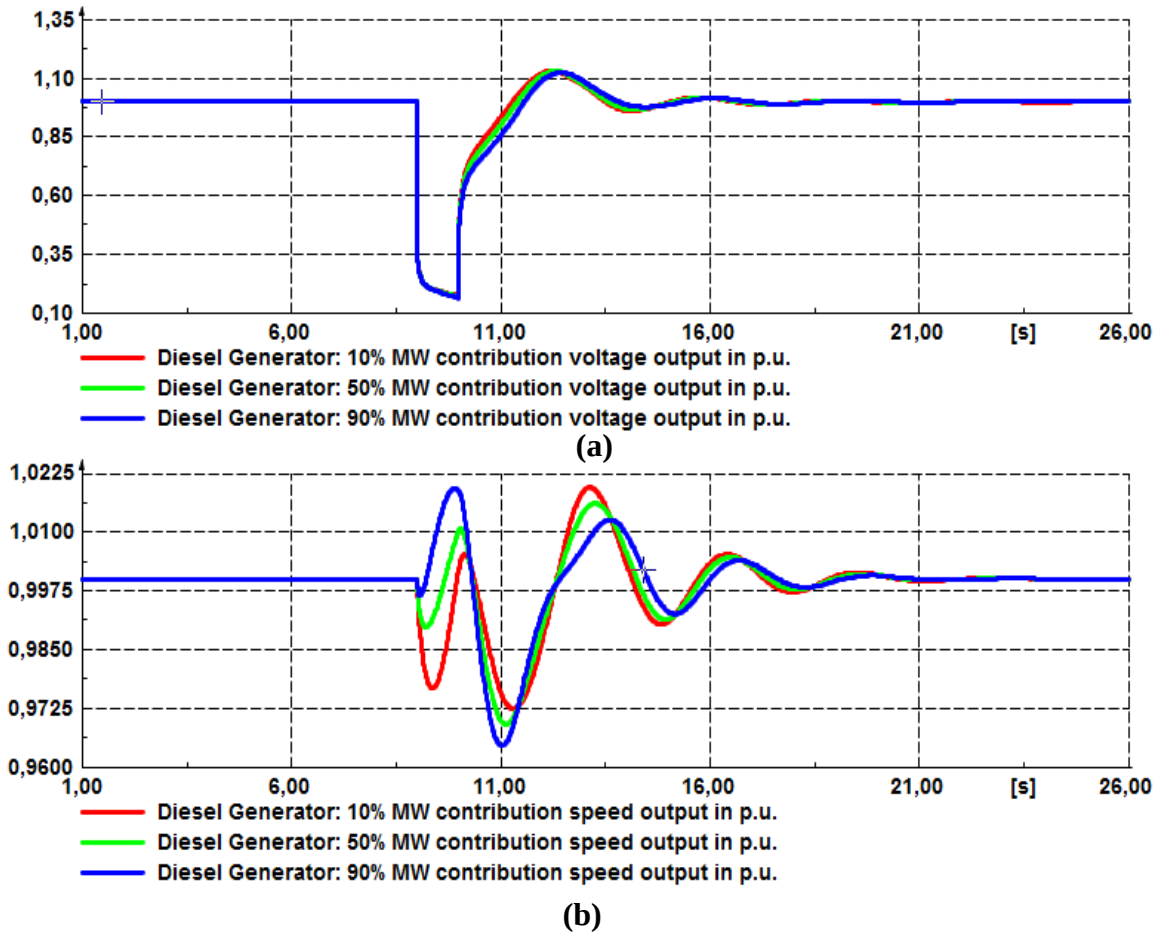


Figure 5.4: Purely resistive load: (a) shows the RMS voltage of the SG prior to and during islanding due to an upstream three-phase short-circuit fault, (b) shows the speed of the diesel engine prior to and during islanding due to an upstream three-phase short-circuit fault.

5.1.2 **Series RL load**

The RMS voltage and frequency behaviour of an SG supplying a series RL load (of different power factors: 0.9, 0.95 and 0.996) during islanding due to sectionalisation and an upstream three-phase short-circuit fault were studied.

5.1.2.1 Sectionalisation

The RMS voltage and frequency behaviour of the SG supplying a series RL load during islanding due to sectionalisation were studied. Islanding is initiated at ten seconds by opening the utility breaker (sectionalisation).

A. RL load with a power factor of 0.996

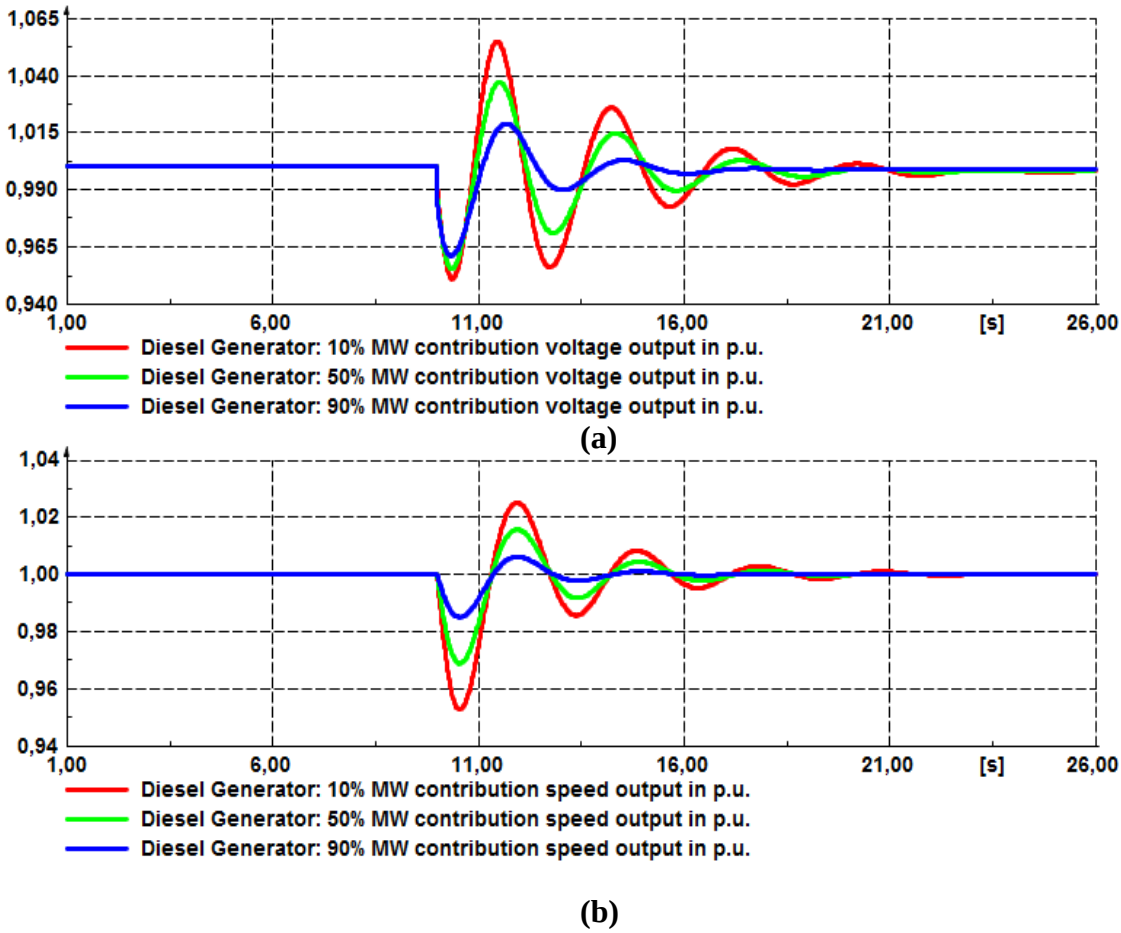


Figure 5.5: Series RL load (pf=0.996): (a) shows the RMS voltage of the SG prior to and during islanding due to sectionalisation, (b) shows the speed of the diesel engine prior to and during islanding due to sectionalisation.

Figure 5.5 shows the RMS voltage and speed/frequency behaviour of the SG supplying a series RL load with a power factor of 0.996, prior to and during islanding due to sectionalisation. It is observed that the RMS voltage and speed of the diesel engine during islanding are affected by the SG initial percentage MW

contribution. For a 10% SG initial percentage MW contribution, a nadir RMS voltage and frequency of 0.951 pu and 0.953 pu were observed, respectively.

B. Series RL load with 0.95 power factor

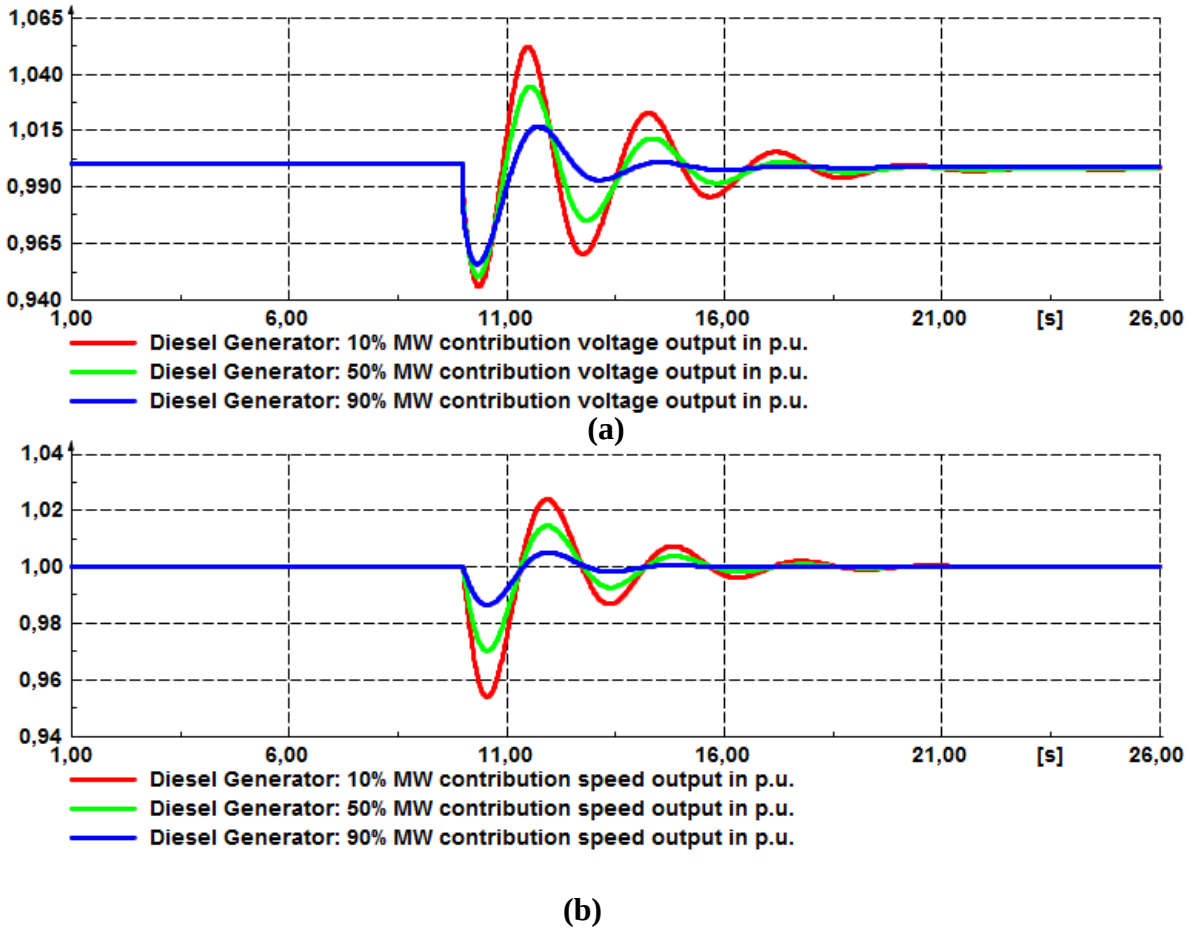


Figure 5.6: Series RL load (pf=0.95): (a) shows the RMS voltage of the SG prior to and during islanding due to sectionalisation, (b) shows the speed of the diesel engine prior to and during islanding due to sectionalisation

Figure 5.6 shows the RMS voltage and speed/frequency behaviour of the SG supplying a series RL load with a power factor of 0.950, prior to and during islanding due to sectionalisation. It is observed that the output RMS voltage and speed of the diesel engine during islanding are affected by the SG initial percentage MW contribution. For a 10% SG initial percentage MW contribution, a nadir RMS voltage and frequency of 0.946 pu and 0.955 pu were observed, respectively. The

network RMS voltage is less affected when the SG initial MW contribution is closer to the load MW demand as compared to when the SG initial MW contribution is less than the load MW demand.

C. Series RL load with power factor of 0.9

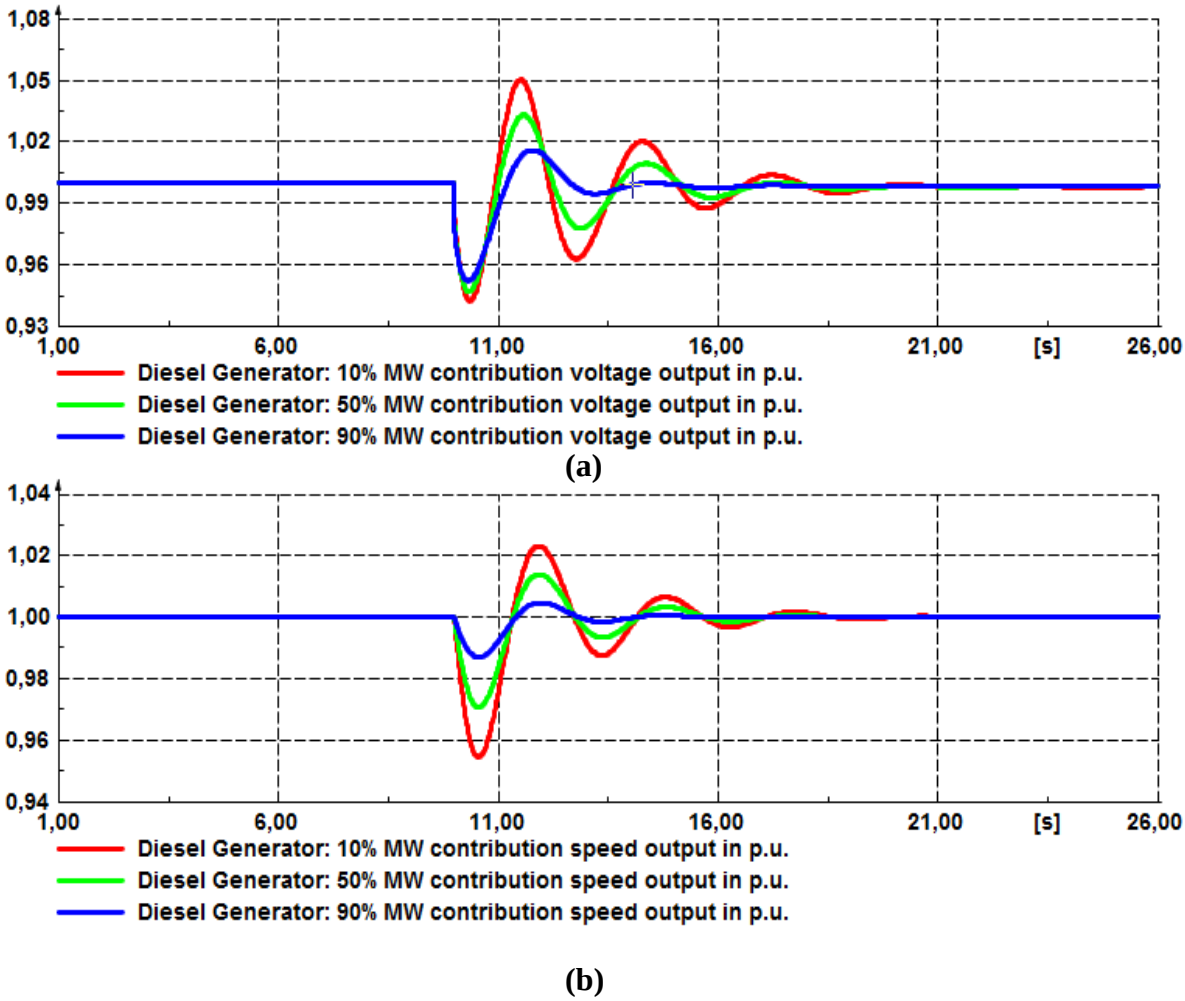


Figure 5.7: Series RL load (pf=0.9): (a) shows the RMS voltage at the SG prior to and during islanding due to sectionalisation, (b) shows the speed of the diesel generator prior to and during islanding due to sectionalisation.

Figure 5.7 shows the RMS voltage and speed/frequency behaviour of the SG supplying a series RL load with a power factor of 0.9, prior to and during islanding due to sectionalisation. It is observed that the output RMS voltage and speed of the SG during islanding are affected by the SG initial percentage MW contribution. For

a 10% SG initial percentage MW contribution, a nadir RMS voltage and frequency of 0.942 pu and 0.955 pu were observed, respectively.

5.1.2.2 Upstream three-phase short-circuit fault

The RMS voltage and frequency behaviour of the SG supplying a series RL load (of different power factors) prior to and during islanding due to an upstream three-phase short-circuit fault were studied.

The upstream three-phase short-circuit fault was introduced at nine seconds at the upstream feeder of the external grid. The protection settings of the utility breaker were set to operate one second after the initiation of the three-phase short-circuit fault. Thus, at ten seconds, the utility breaker opens, which establishes islanding. The RMS voltage of the network collapsed to 0.2 pu during the three-phase short-circuit fault, as expected and as shown in Figure 5.8 (a). After the fault was cleared, the governor and the AVR operated to bring the frequency and RMS voltage back to the nominal values and maintain those parameters, respectively, as shown in Figure 5.8. During the three-phase short-circuit fault, the SG electrical power output dropped due to the low fault voltage. An upstream three-phase short-circuit analysis was performed on the simulated network and a short-circuit current value of 7.795 kA was expected at the load bus bar.

As shown in Figure 5.8 (a), for all SG initial percentage MW contributions, when an upstream three-phase short-circuit fault is introduced into the network, the output voltage collapses to the same value. The output RMS voltage behaviour of the SG prior to the termination of islanding was the same for all series RL loads with different power factors.

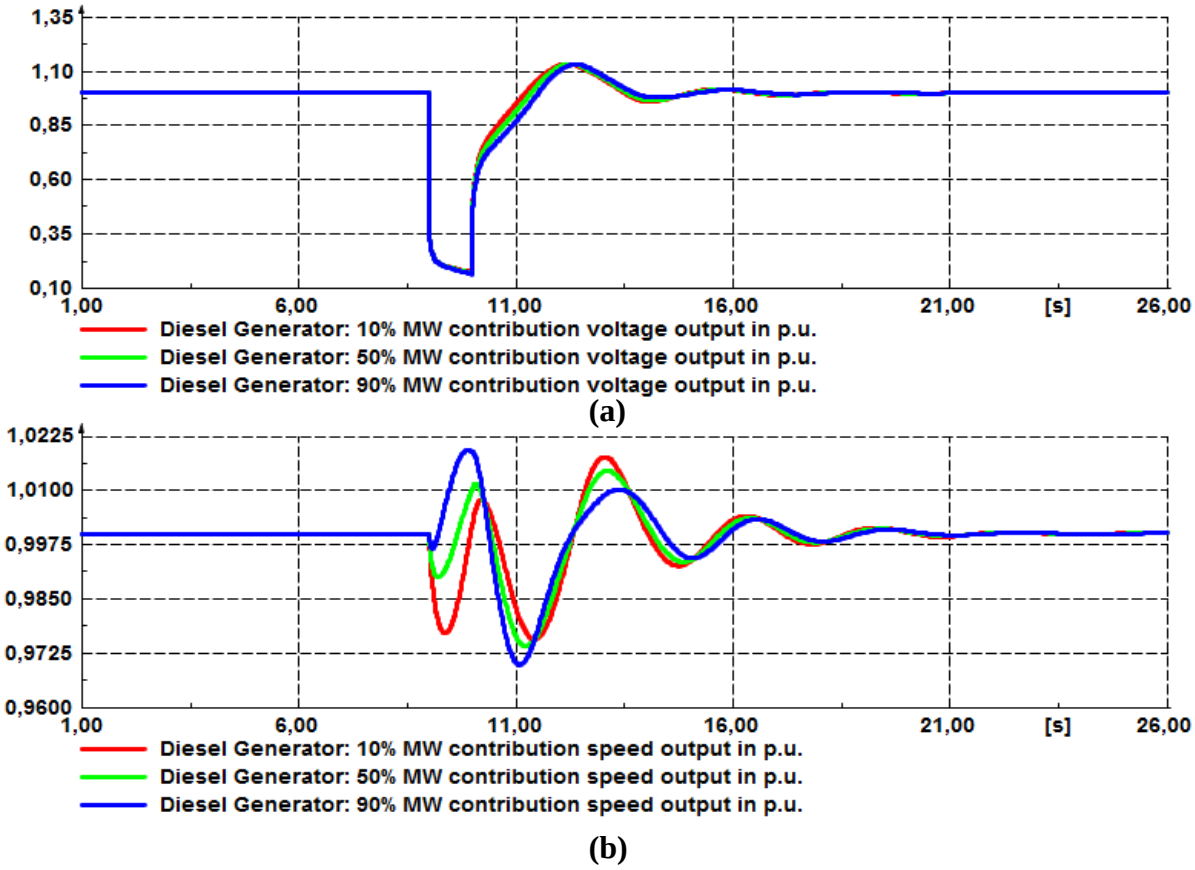


Figure 5.8: Series RL load (pf=0.9) (a) shows the RMS voltage of the SG prior to and during islanding due to an upstream three-phase short-circuit fault, (b) shows the speed of the diesel engine prior to and during islanding due to an upstream three-phase short-circuit fault.

5.1.3 **Induction motor**

The RMS voltage and speed/frequency behaviour of the SG as well the speed behaviour of the induction motor prior to and during islanding due to sectionalisation and upstream three-phase short-circuit fault were investigated. The induction motor in this section was modelled without the mechanical load.

This condition is used in a no-load test performed on induction motors.

A. Islanding due to sectionalisation

Figure 5.9 shows the RMS voltage and the speed of the diesel engine versus that of the induction motor prior to and during islanding due to sectionalisation. It is

observed that the RMS voltage and the speed of the induction motor follow that of the diesel engine prior to and during islanding due to sectionalisation.

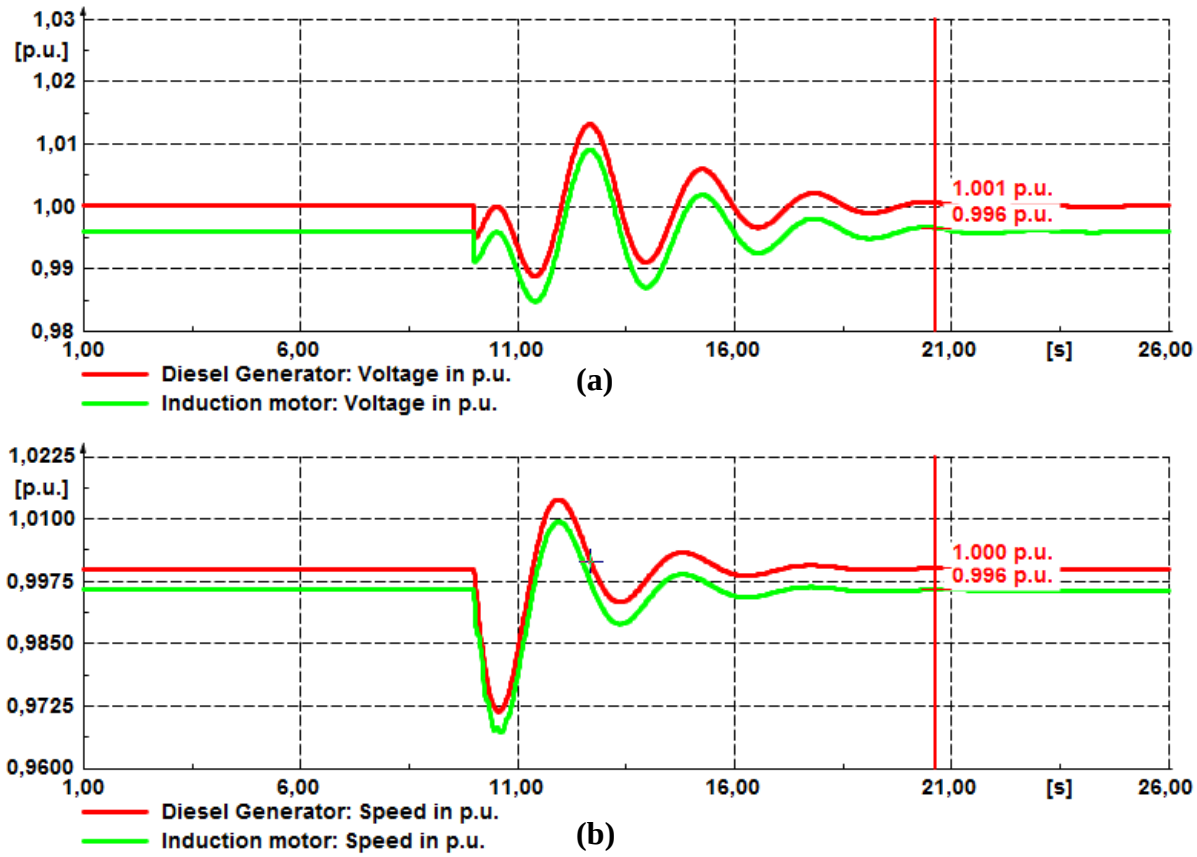
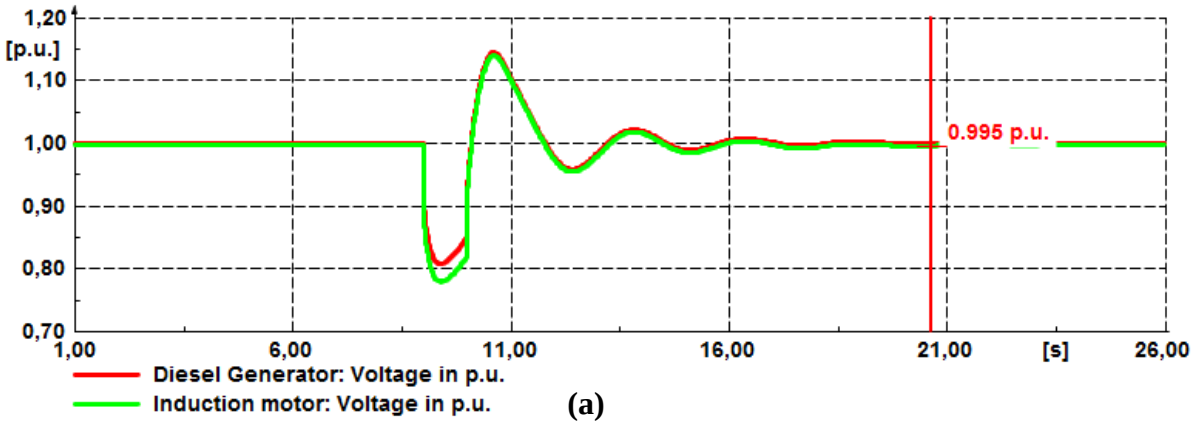


Figure 5.9: Unloaded induction motor (a) shows the RMS voltage at the SG and the RMS voltage at the induction motor prior to and during islanding due to sectionalisation, (b) shows the speed of the diesel engine and of the induction motor prior to and during islanding due to sectionalisation.

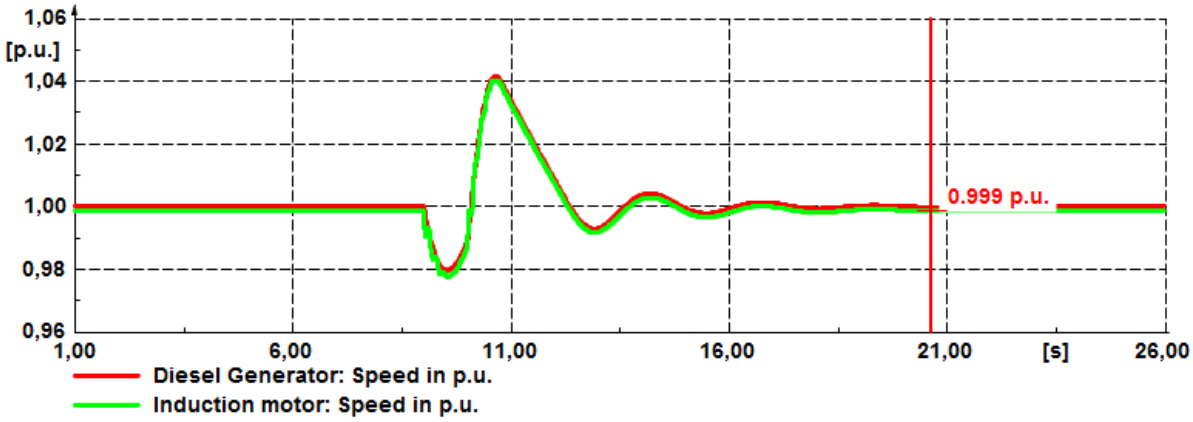
B. Islanding following an upstream three-phase short-circuit fault

The three-phase short-circuit fault was introduced at nine seconds and islanding introduced at ten seconds by opening the utility breaker.

Figure 5.10 shows the RMS voltage and speed/frequency of the SG versus the speed of the induction motor prior to and during islanding following an upstream three-phase short-circuit fault.



(a)



(b)

Figure 5.10:Unloaded induction motor (a) shows the RMS voltage at the SG and the voltage at the induction motor prior to and during islanding due to an upstream three-phase short-circuit fault, (b) shows the speed of the diesel engine and the speed of the induction motor prior to and during islanding following an upstream three-phase short-circuit fault.

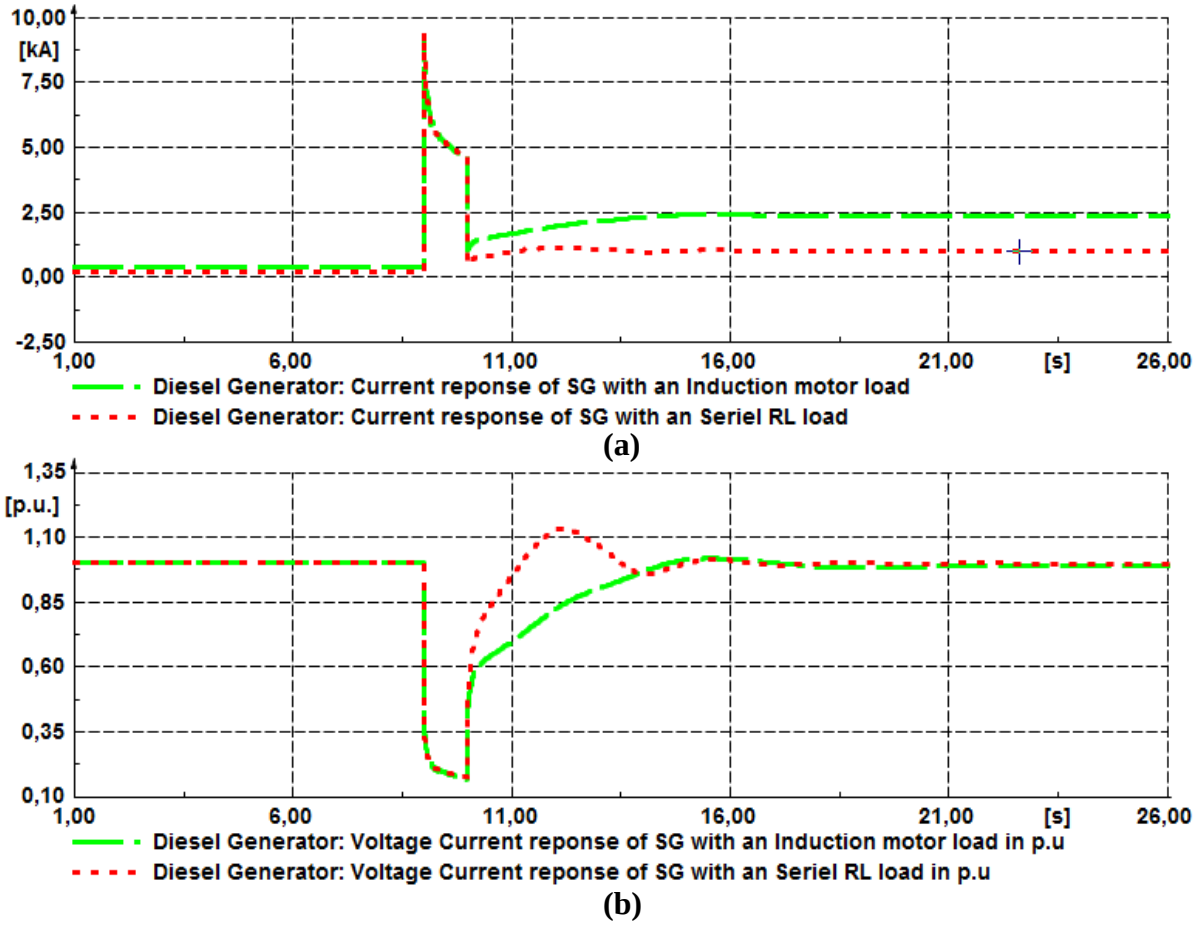


Figure 5.11:Unloaded induction motor versus series RL load (pf=0.9) (a) shows the RMS output current from the SG prior to and during islanding due to a three-phase short-circuit current fault, (b) shows the RMS voltage at the SG prior to and during islanding due to an upstream three-phase short-circuit fault.

Figure 5.11 illustrates the RMS output current and RMS voltage of the SG prior to and during islanding, in which the SG is supplying two different loads (series RL load and composite load with an induction motor). From Figure 5.11 (a) and (b), it is observed that when the three-phase short-circuit fault is introduced at nine seconds, there is an inrush current (approximately 30 times the network current prior to the fault) and a voltage collapse is experienced by the network. When the fault is cleared/isolated at ten seconds due to the protection settings of the utility breaker operating, the SG then tries to compensate for the load demand. The SG is able to meet the demand of the load and still be able to meet the voltage and frequency level of the network through the help of the governors and AVRs.

It is also observed that for a network with an induction motor, the voltage takes about 4.95 seconds to rise, whereas, for the network with just an RL load it takes about 1.2 seconds (4 times lesser) to stabilise. Hence, the network with an induction motor prior to islanding detection and termination, is exposed to poor power quality longer as opposed to a network without an induction motor.

5.1.4 Induction motor driving a pump

The RMS voltage and speed/frequency behaviour of the SG, as well as the speed and RMS current of the induction motor driving a centrifugal pump, was investigated during islanding due to sectionalisation and an upstream three-phase short-circuit fault. The mechanical load of the induction motor was assumed to be 0.1 MW (pf=0.9) and the RL load was 0.4 MW (pf=0.9).

A. Islanding due to sectionalisation

Figure 5.12 shows the RMS voltage and speed/frequency behaviour of the SG prior to and during islanding due to sectionalisation. It is observed that the speed/frequency and RMS voltage nadir of the SG during islanding is more favoured by a diesel generator supplying an induction load of a mechanical load driving a centrifugal pump.

The induction motor with a mechanical load of a centrifugal pump improves the RMS voltage and speed/frequency during islanding due to sectionalisation (no fault present). Since the induction motor is simulated with less demand as compared to the series RL load, it is expected to have an improved RMS voltage and speed/frequency behaviour as compared to the latter.

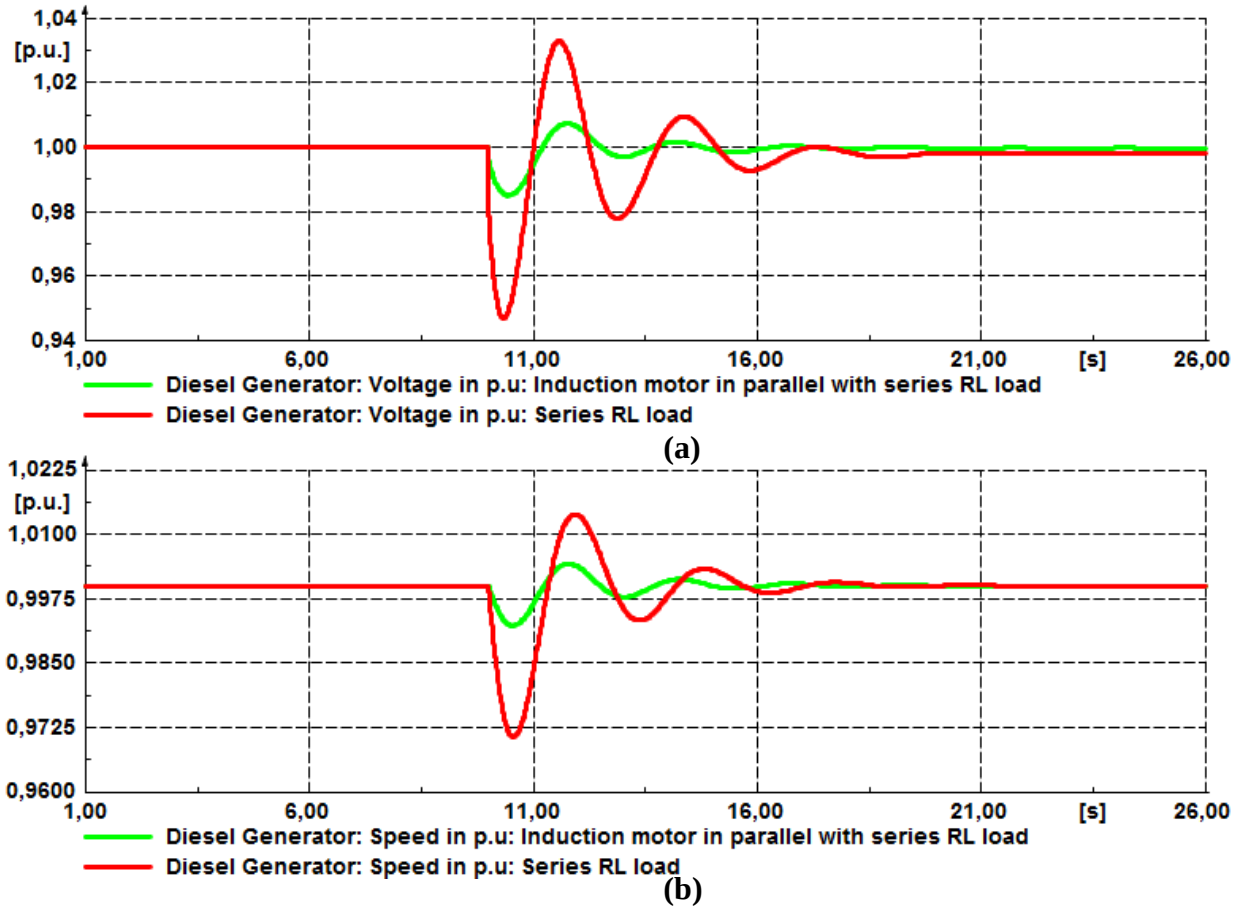
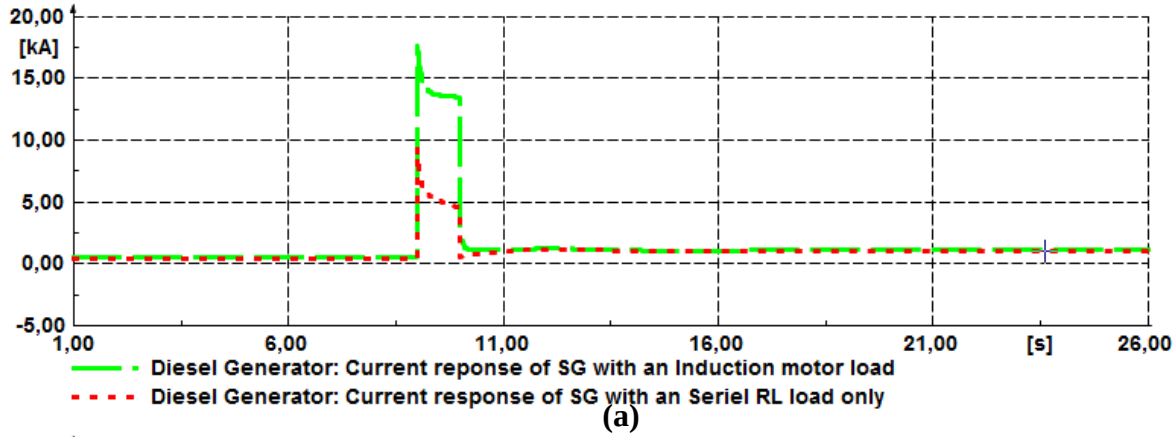


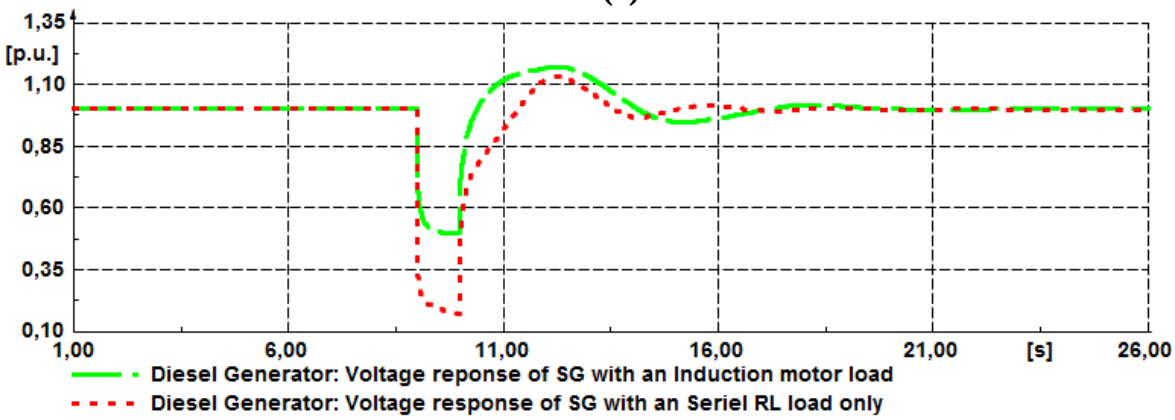
Figure 5.12: Induction motor driving a pump in parallel with a series RL load (pf=0.9) versus series RL load (pf=0.9) only (a) shows the RMS voltage behaviour of the SG prior to and during islanding due to sectionalisation. (b) shows the speed behaviour of the diesel engine prior to and during islanding due to sectionalisation.

B. Islanding due to a three-phase short-circuit fault

Figure 5.13 shows the RMS current and speed/frequency behaviour of the SG before and during islanding due to an upstream three-phase short-circuit fault. It is observed that the induction motor increases the maximum RMS three-phase short-circuit fault by about 50%. Synchronous motors are known to contribute about 4-6 times their full load current, as opposed to the previous induction motor.



(a)



(b)

Figure 5.13: Induction motor driving a pump in parallel with a series RL load (pf=0.9) versus series RL load (pf=0.9) only. (a) shows the RMS current behaviour of the SG prior to and during islanding due to an upstream three-phase short-circuit fault, (b) shows the RMS voltage behaviour of the SG prior to and during islanding due to an upstream three-phase short-circuit fault.

Figure 5.14 illustrates the speed of the induction motor during islanding due to sectionalisation versus the speed due to an upstream three-phase short-circuit fault.

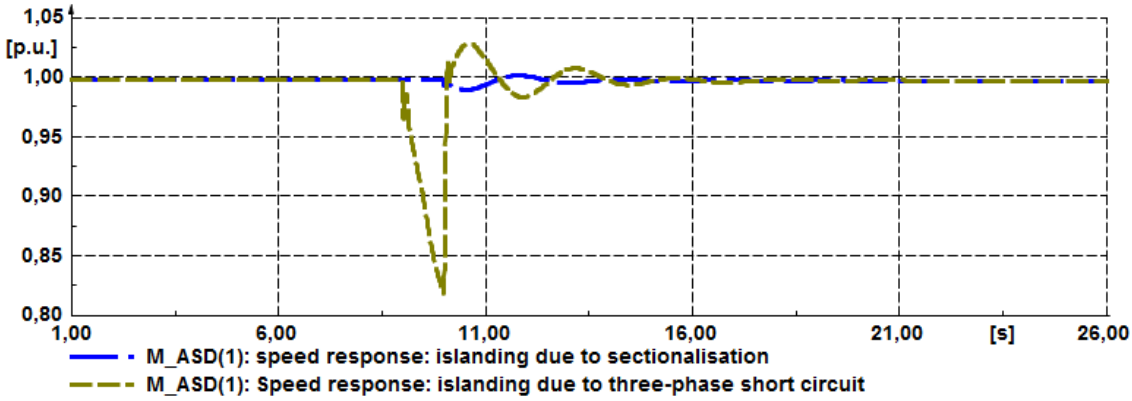


Figure 5.14: Induction motor driving a pump. Illustrates the speed behaviour of the SG prior to and during islanding due to an upstream three-phase short-circuit fault versus sectionalisation.

5.2 Solar PV Generation simulations results

The RMS voltage and frequency of the SPV prior to and during islanding supplying three different load conditions (purely resistive, series RL load (pf=0.9) and induction motor load) are studied.

5.2.1 Purely resistive load

The RMS voltage and frequency behaviour of a SPV supplying a purely resistive load during islanding due to sectionalisation and an upstream three-phase short-circuit fault were studied.

A. Islanding due to sectionalisation

At ten seconds, sectionalisation was initiated, which could be either intentional or un-intentional islanding. The SPV after ten seconds was forced to operate as a standalone supply (islanded mode) This implies the PowerFactory SPV model had grid-forming functionality after islanding. Figure 5.15 shows the RMS voltage and frequency behaviour of the SPV system supplying a purely resistive load, prior to and during islanding due to sectionalisation.

It is observed that the SPV tries to maintain the RMS voltage and frequency at their nominal values as expected for a GFW with VCC and FW controller, respectively.

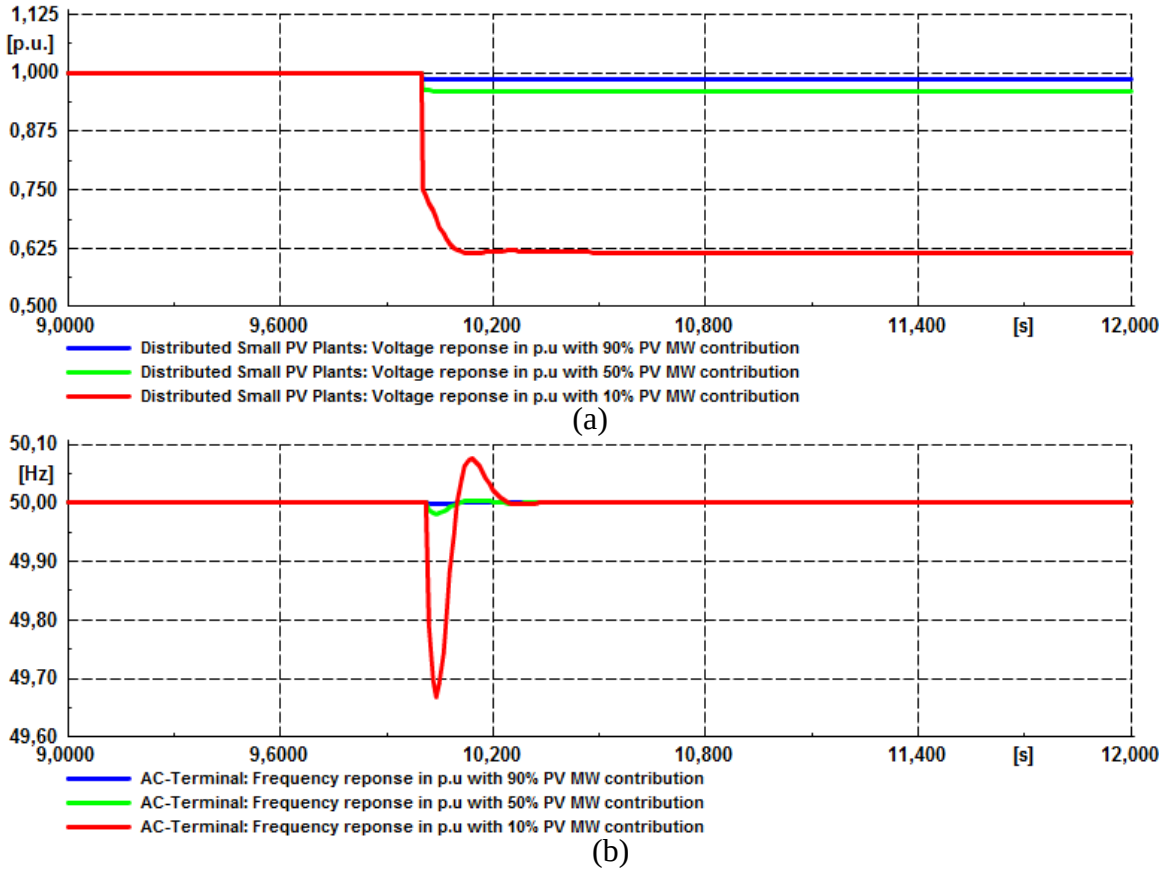


Figure 5.15: Purely resistive load (a) shows the RMS voltage of the SPV prior to and during islanding due to sectionalisation, (b) shows the frequency behaviour of the SPV prior to and during islanding due to sectionalisation.

The SPV is able to maintain the RMS voltage and frequency due to the SPV's ability to participate in the system inertia. That is, the SPV can self-sufficiently supply the load during the islanding for SPV initial percentage MW contributions of 90% and 50% (voltage slightly above 0.9 pu). Figure 5.16 shows the difference between when the SPV rated power can self-sufficiently supply the load ($PV_{MW_{rated}} \geq$ load MW) versus when it is not able to self-sufficiently supply the

load. It is observed that the power quality is greatly compromised when the SPV cannot self-sufficiently supply the load during islanding.

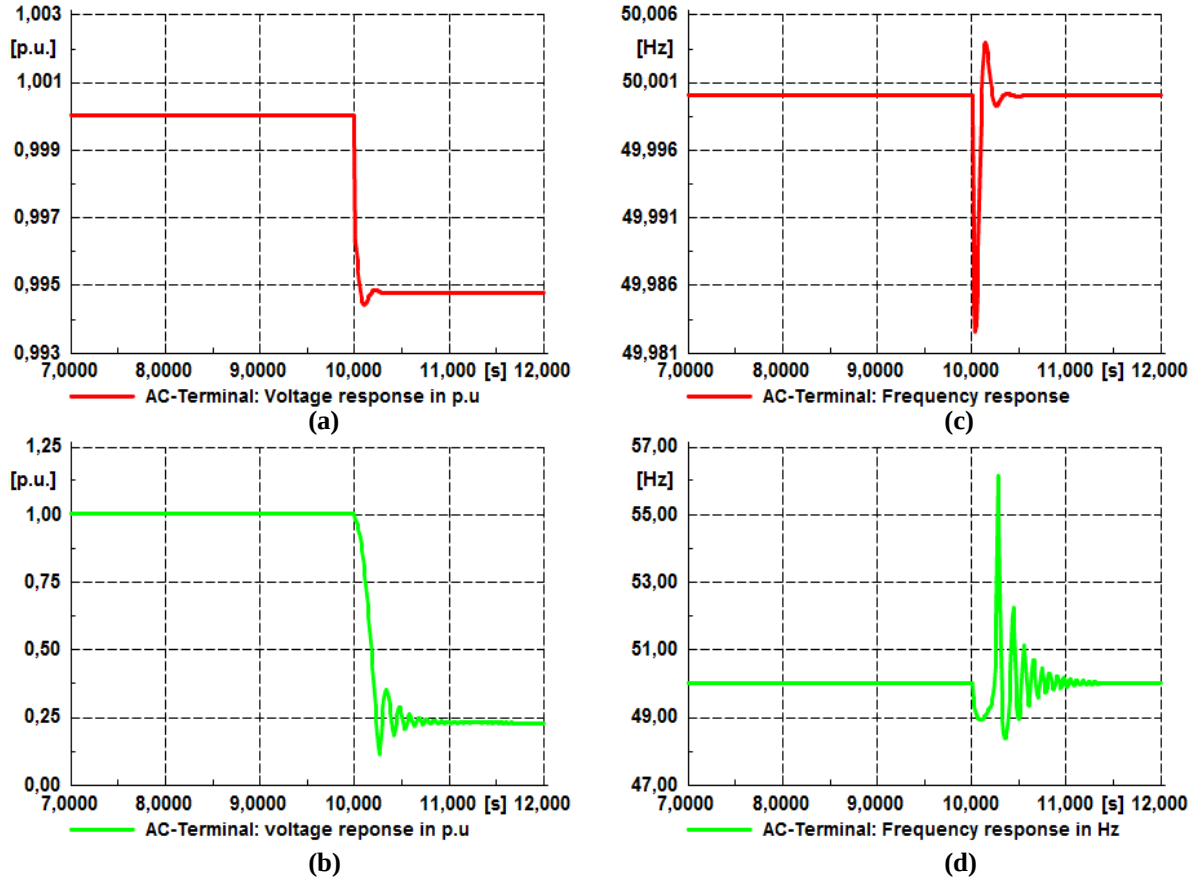


Figure 5.16: Purely resistive load (a) shows the RMS voltage behaviour of the SPV capable of supplying the load, (b) shows the frequency behaviour of the SPV capable of supplying the load, (c) shows the RMS voltage behaviour of the SPV not capable of supplying the load, (d) shows the frequency behaviour of the SPV not capable of supplying the load.

B. Islanding due to an upstream three-phase short-circuit fault

At nine seconds, an upstream three-phase short-circuit was initiated. The upstream breaker protection settings were set to operate at ten seconds. The SPV at ten seconds is forced to operate as a standalone supply. Figure 5.17 illustrates the RMS voltage and frequency behaviour of the SPV system supplying a purely resistive

load, prior to and during islanding due to an upstream three-phase short-circuit fault.

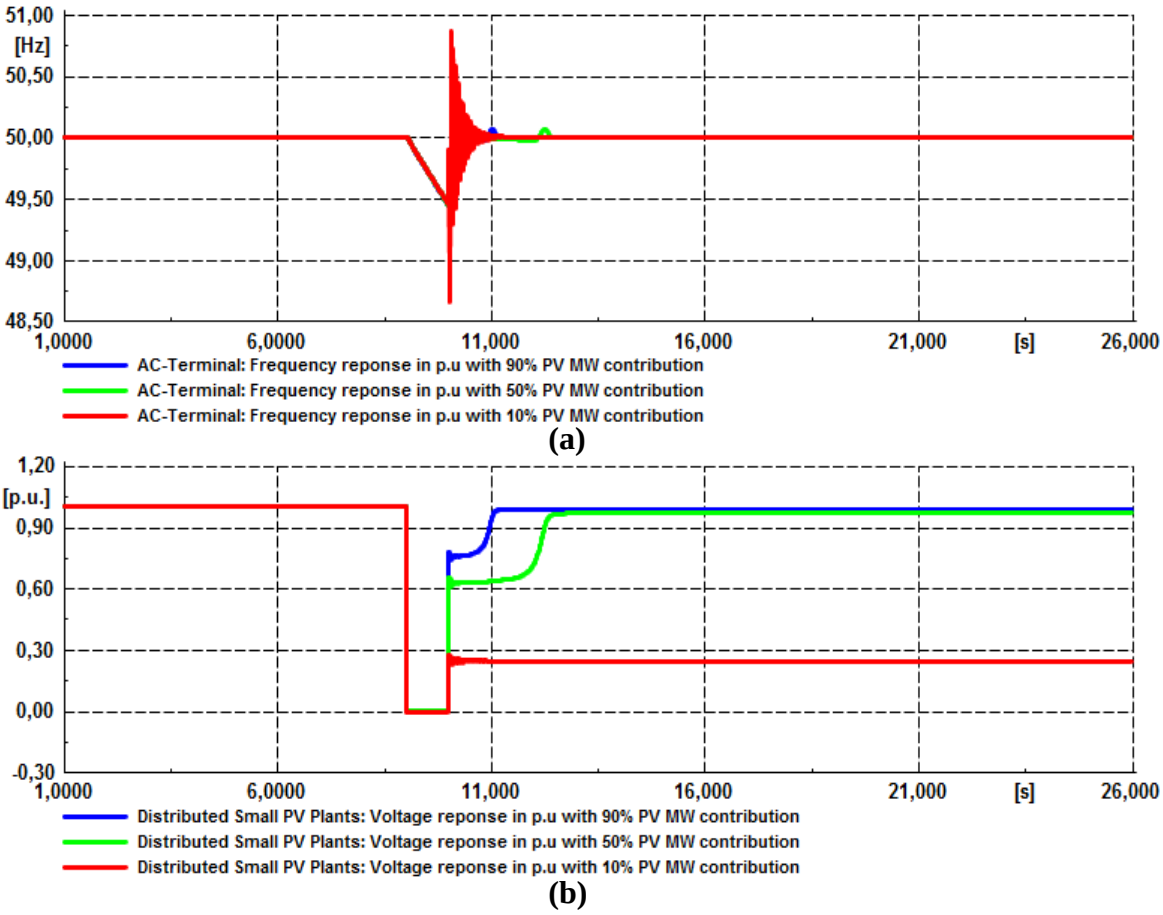
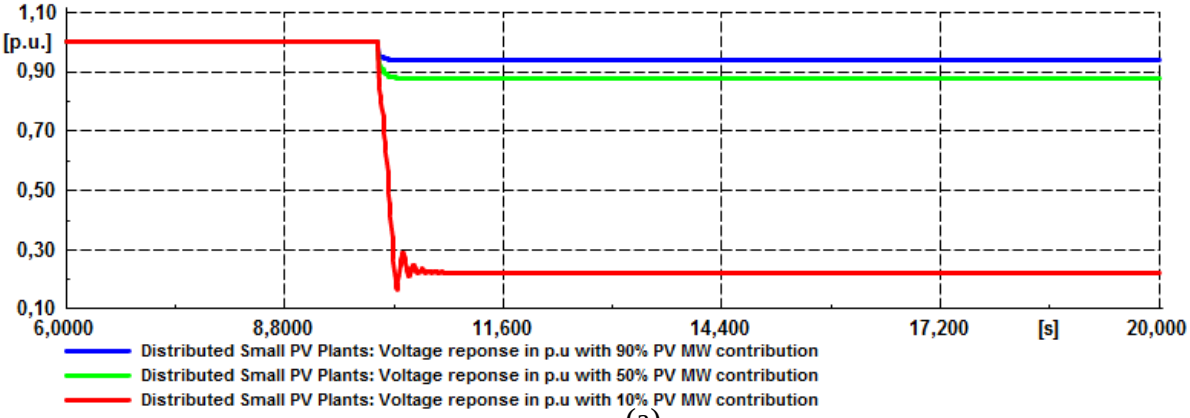


Figure 5.17: Purely resistive load (a) shows the frequency behaviour of the SPV prior to and during islanding due to an upstream three-phase short-circuit fault, (b) shows the voltage of the SPV prior to and during islanding due to an upstream three-phase short-circuit fault.

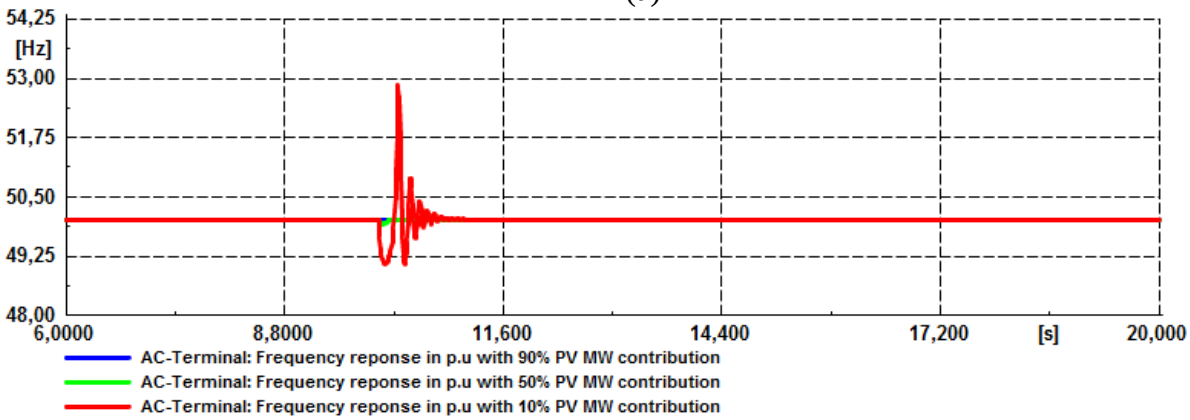
The PV can control and return the RMS voltage and the frequency of the network to values above 0 pu (depending on the SPV initial percentage MW contribution) due to the zero-fault ride-through capability. Without the ability to ride through, the RMS voltage and frequency of the network are expected to collapse, due to the inability of the SPV to stay connected during such faults.

5.2.2 **Series RL load**

Figure 5.18 shows the RMS voltage and frequency of the SPV supplying a series RL load prior to and during islanding due to sectionalisation.



(a)



(b)

Figure 5.18: Series RL load (pf=0.9) (a) shows the RMS voltage of the SPV prior to and during islanding due to sectionalisation, (b) shows the frequency behaviour of the SPV prior to and during islanding due to sectionalisation.

The volt-var control of the PVD1 model allows an inductive or capacitive output current based on the SPV terminal voltage. Between the dead band limits v1 and v0 (If v1=v0 there is no dead band), the inverter will effectively provide no reactive power and the voltage will remain constant. Outside the dead band, the PV exports or imports reactive power based upon the SPV terminal voltage. This is shown in Figure 5.19.

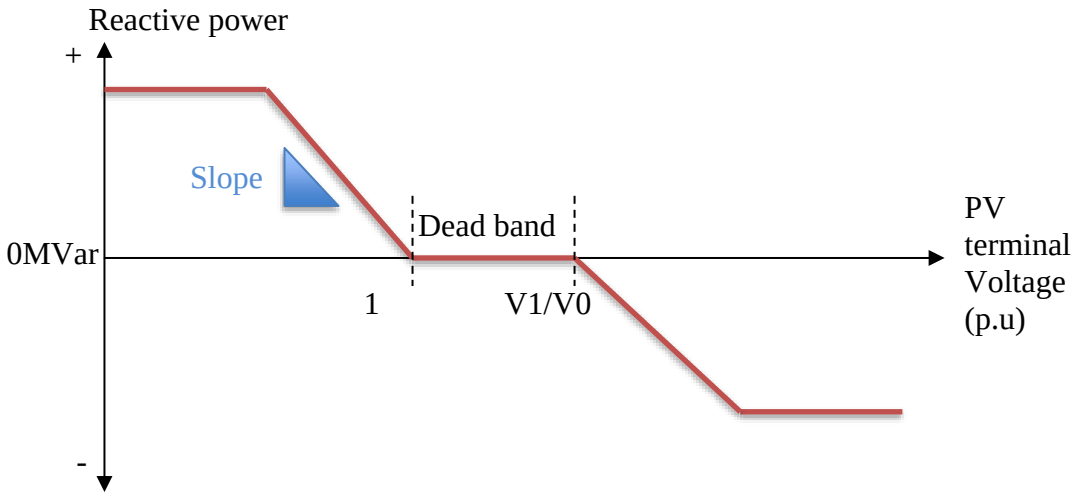


Figure 5.19: PVD1 volt-var control (VCC) curve

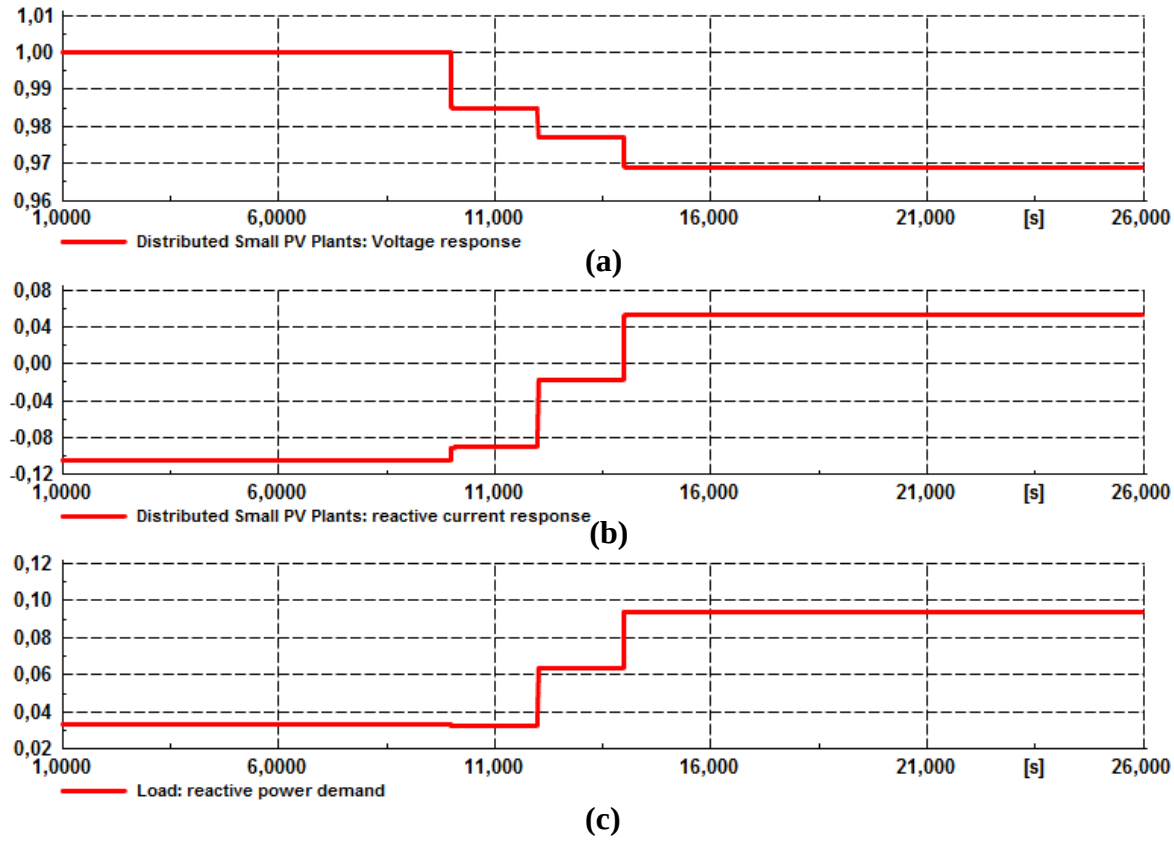
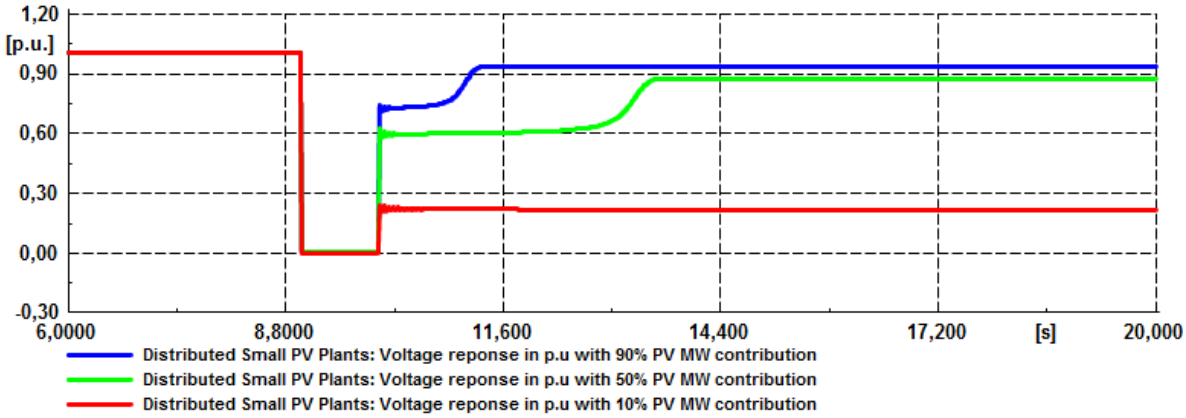
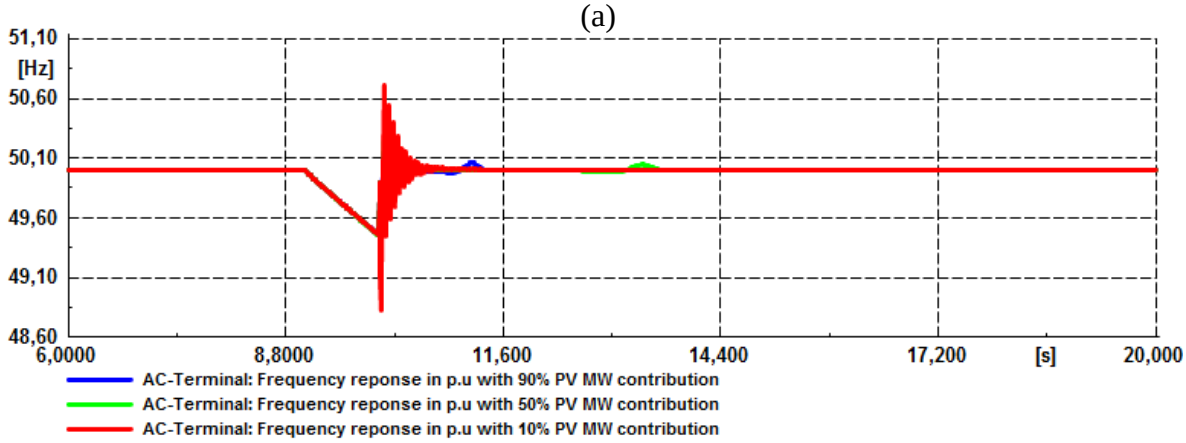


Figure 5.20: (a) shows the RMS voltage behaviour in pu of the SPV, (b) shows the RMS reactive current behaviour in pu of the SPV based on different reactive load demand, (c) shows the reactive load demand in pu.

Figure 5.20 shows how the VVC of the PVD1 model behaves. Initially, when grid-connected, the SPV is exporting only active power and the reactive load demand is supplied by the external grid. When islanding occurs at ten seconds, the SPV must meet the load demand (both active and reactive power). During islanding, the load is simulated as a step load, in which the reactive component of the load doubles up every two seconds (at 12 and 14 seconds). Every time the reactive load power is increased, this forces the SPV voltage to drop if the SPV is not able to supply the reactive power demanded (Figure 5.20).



(a)



(b)

Figure 5.21: Series RL load (pf=0.9) (a) shows the RMS voltage of the SPV prior to and during islanding due to an upstream three-phase short circuit fault, (b) shows the frequency behaviour of the SPV prior to and during islanding due to an upstream three-phase short circuit fault.

Figure 5.21 shows the RMS voltage and frequency behavior of the SPV during islanding due to an upstream three-phase short-circuit fault. It is observed that the voltage collapses during the three-phase short-circuit fault and the SPV tries to regain the voltage after islanding is initiated.

The frequency in the electrical system affects the reactive and capacitive reactance, therefore for a purely resistive load, the frequency will have little effect.

The frequency of the system decreases gradually due to loss of generation or overload. Smaller system inertia tends to cause a quicker frequency drop. It is observed from Figure 5.21, due to the fault-ride-through capability of the SPV, the system is able to pick up its frequency.

5.2.3 **Induction motor**

The RMS voltage and frequency behaviour of the SPV supplying a composite load (static and dynamic load), during islanding due to sectionalisation and an upstream three-phase short-circuit fault, is studied. The simulated network diagram is shown in Figure 5.22 and the simulated parameters are tabulated in Table 5.2.

Table 5.2: Simulated parameters

Parameter	**Value**
PV dispatched power	0.45 MW (10% curtailed)
RL load	0.4 MW (pf=0.9)
Induction motor	0.1 MW and 0.05 Mvar

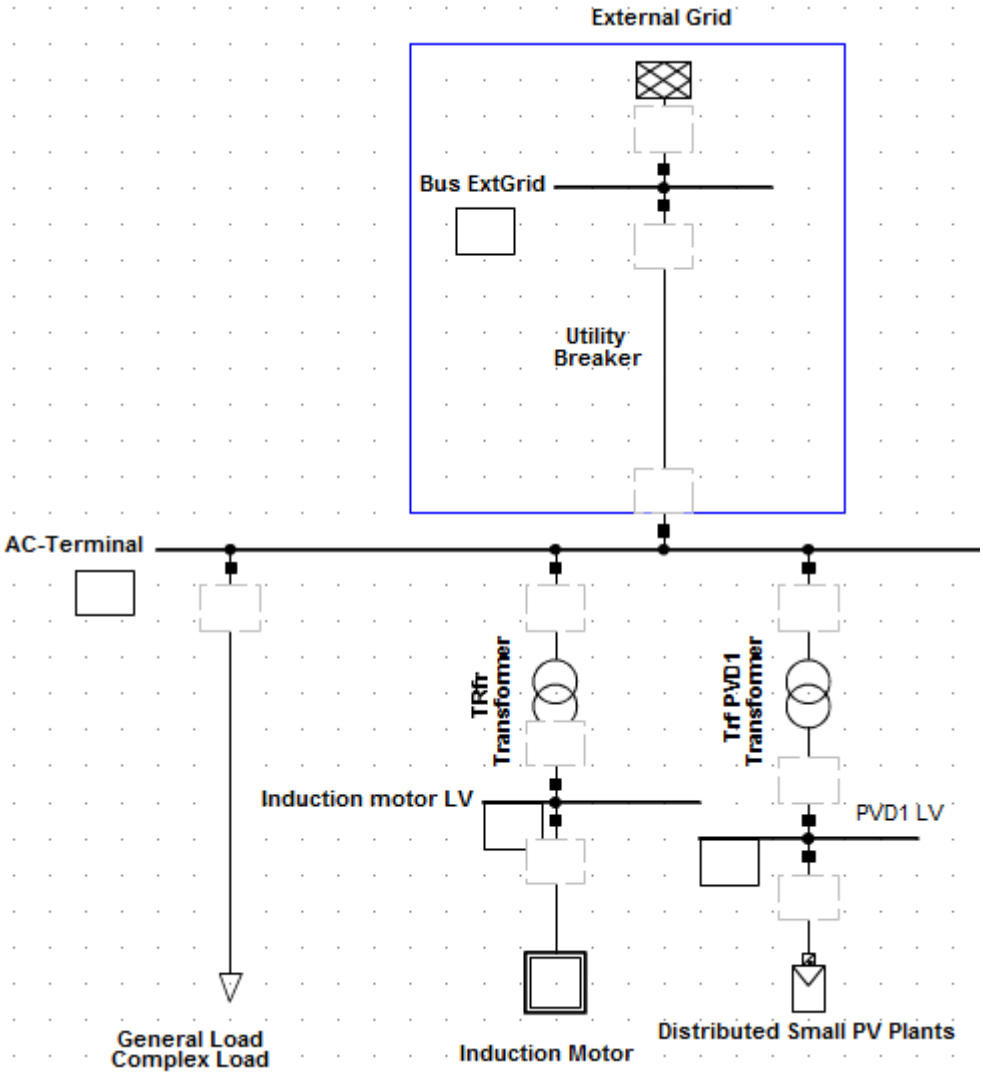


Figure 5.22: SPV supplying both series RL load and an induction motor

A. Islanding due to sectionalisation

Islanding was initiated at ten seconds by operating the utility breaker. Two scenarios were simulated:

- Scenario A: SPV simulated without an initial injection of reactive power into the network, and load shedding initiated at 11 seconds to allow the voltage of the SPV to be within the acceptable limits (according to IEEE 1159).

- Scenario B: SPV simulated with an initial additional reactive power (of 0.2 Mvar) that is able to supply the network (or capable of supplying) without load shedding.

Figure 5.23 (b) shows the RMS voltage behaviour of the SPV based on scenario A and Figure 5.24 (a) shows the RMS voltage behaviour of the SPV based on scenario B. It is observed that a network with SPV that initially exports the reactive power improves the network. Allowing the SPV to initially distribute reactive power is basically shifting the volt-var control up as indicated by Figure 5.25.

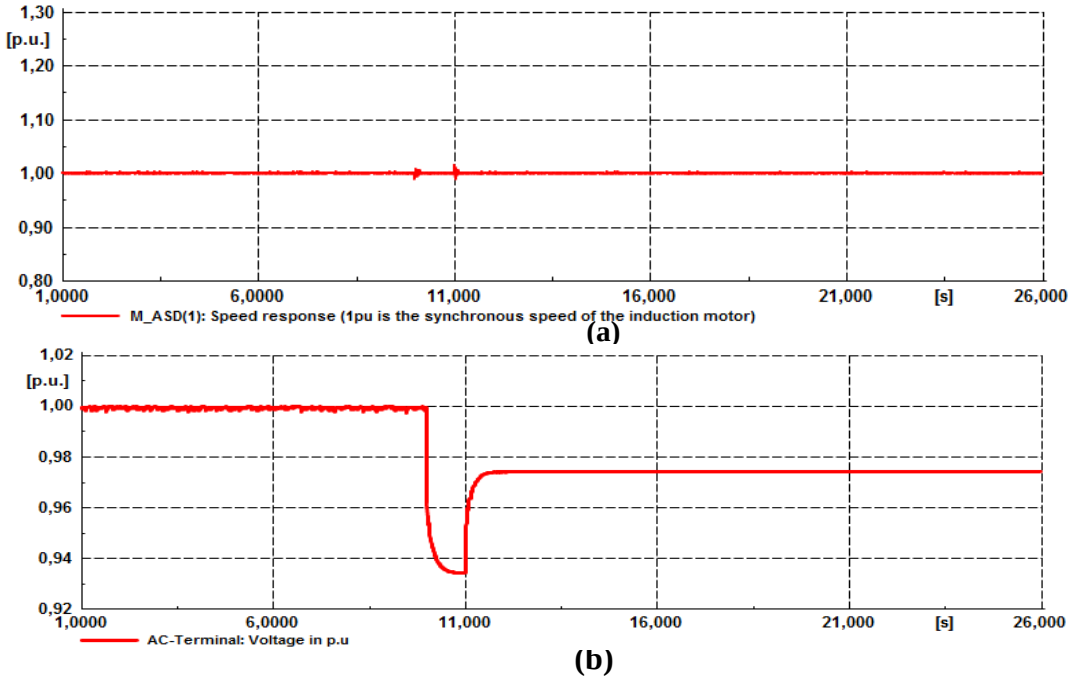


Figure 5.23: (a) shows the speed of the induction motor prior to and during islanding due to sectionalisation, (b) shows the RMS voltage behaviour prior to and during islanding due to sectionalisation.

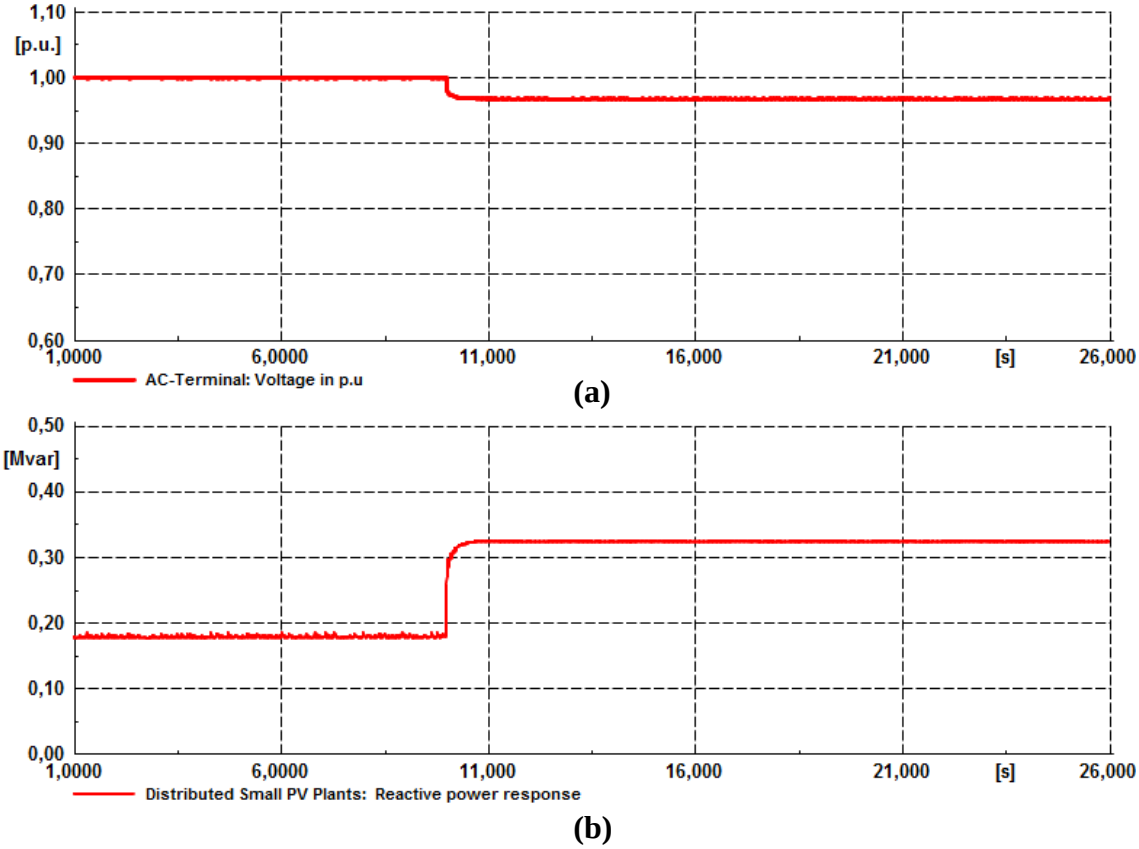


Figure 5.24: (a) shows the RMS voltage behaviour of the SPV prior to and during islanding due to sectionalisation, (b) shows the reactive current injected by the SPV prior to and during islanding due to sectionalisation.

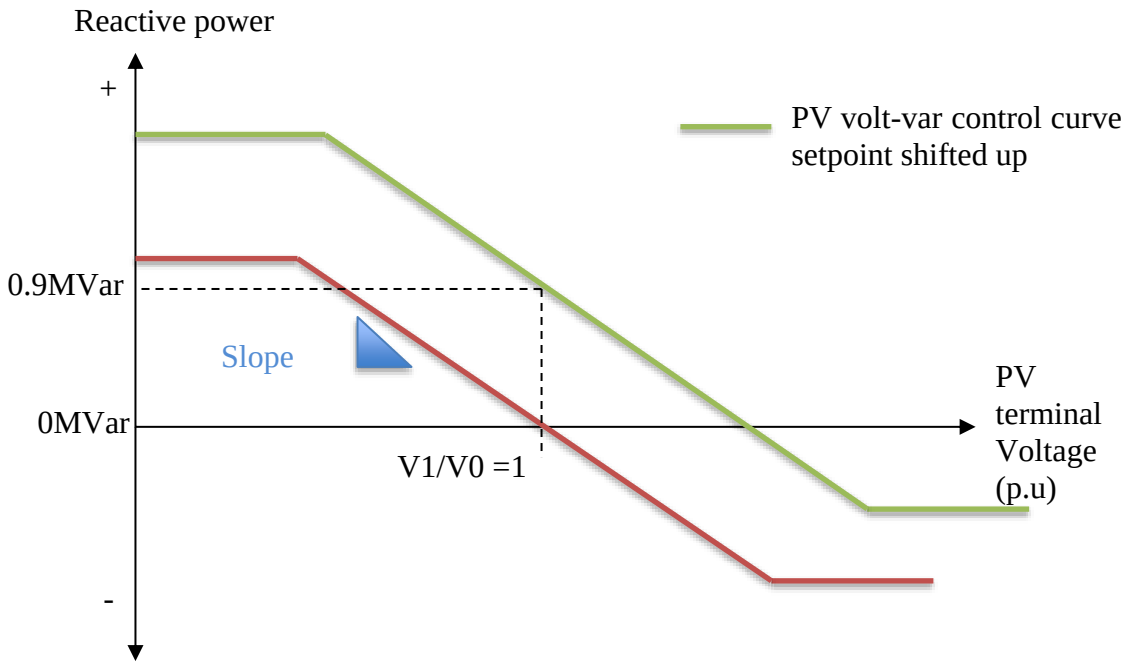


Figure 5.25: Modified volt-var controller for the PVD1 system

B. Islanding due to an upstream three-phase short-circuit fault

An upstream three-phase short-circuit fault is introduced at nine seconds and the islanding is initiated at ten seconds by opening the utility breaker to clear the fault. Figure 5.26 illustrates the induction motor speed and the RMS voltage behaviour prior to and during islanding due to an upstream three-phase short-circuit fault. It is observed that the speed of the induction motor decreases with the decrease of the RMS voltage. When the fault is cleared at ten seconds by opening the utility breaker, the SPV system then tries to control the RMS voltage back to its nominal value.

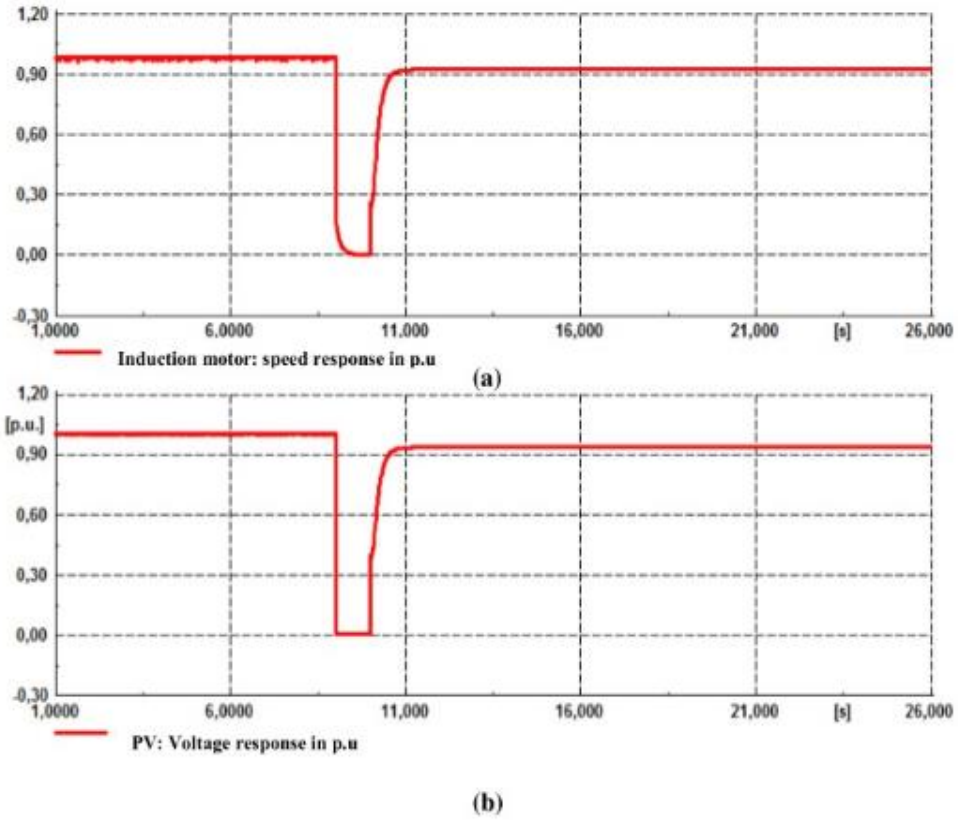


Figure 5.26: (a) shows the speed behaviour of the induction motor prior to and during islanding due to an upstream three-phase short-circuit fault, (b) shows the RMS voltage behaviour of the SPV prior to and during islanding due to an upstream three-phase short-circuit fault.

5.3 SG in parallel with SPV simulations

In this section, the SG is connected in parallel with the SPV. The frequency and the RMS voltage of the network at the Point of Connection (PC) are analysed. The simulation parameters are tabulated in Table 5.3.

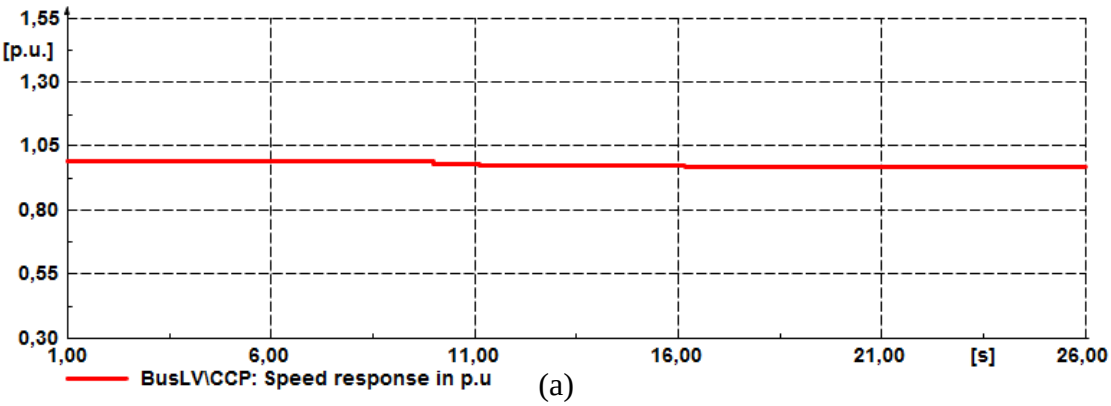
Table 5.3: Simulation parameters (SG and PV system in parallel)

Parameter	**Value**
PV dispatched power	0.5 MW
SG dispatched power	0.45 MW
RL load	0.5 MW (pf=0.9)
Purely resistive load	0.5 MW
Induction motor	0.1 MW and 0.2 Mvar

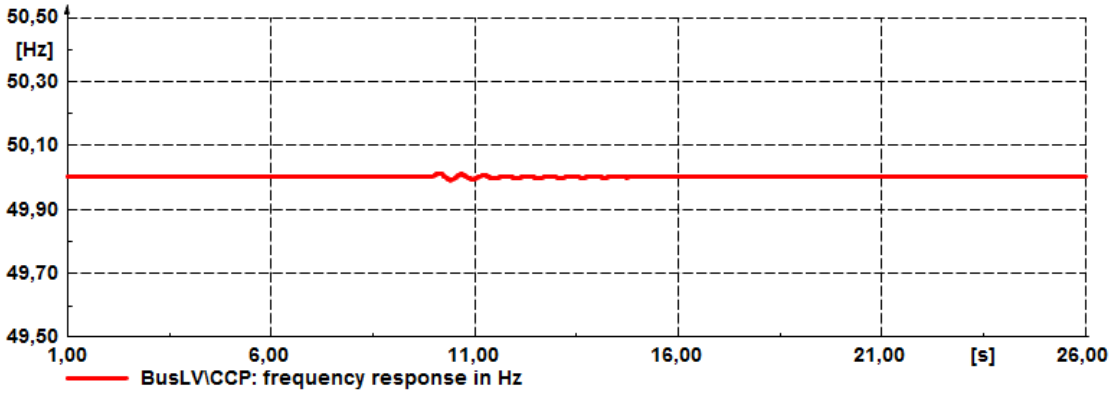
5.3.1 Islanding due to sectionalisation

Three different cases were studied: the network is supplying a purely resistive load, a series RL load, and a composite load that comprises a series RL load in parallel with the induction motor.

All the described cases showed similar frequency and RMS voltage behaviour at the CP, that is unity prior to and during the islanding due to sectionalisation. Figure 5.27 shows the RMS voltage and frequency behaviour of the network at the CP when the SG in parallel with the SPV system are supplying a series RL load in parallel with the induction motor.



(a)



(b)

Figure 5.27: Series RL in parallel with induction motor (a) shows the RMS voltage behaviour of the network at the PC prior to and during islanding. (b) Illustrates the frequency behaviour of the network at the CP prior to and during islanding.

5.3.2 **Islanding due to an upstream three-phase short-circuit fault**

The upstream three-phase short-circuit fault was introduced at nine seconds and islanding was initiated at ten seconds by opening the utility breaker in order to clear the fault. The simulated results of the RMS voltage and frequency behaviour of the network at the CP are shown in Figure 5.28. It is indicated that the voltage nadir of the network within two seconds of islanding is 0.4 pu. At normal operation of the network, that is, there is no fault in the network, the voltage drop in the network is affected by;

- The type of cable used and the length of the cable between the source and the load (impedance)
- The transformer loading between the source and the load

However, when there is a fault in the network, the voltage drop is also affected by the location of the fault. The short-circuit current decreases as you move further away from the location of the fault (this analogy is used commonly for fault location detection on radial networks, by performing a distance equation as a function of the fault) [34]. Figure 5.29 shows the difference between the network voltage behaviour when the fault has occurred close by or at some distance from the PV and SG in parallel.

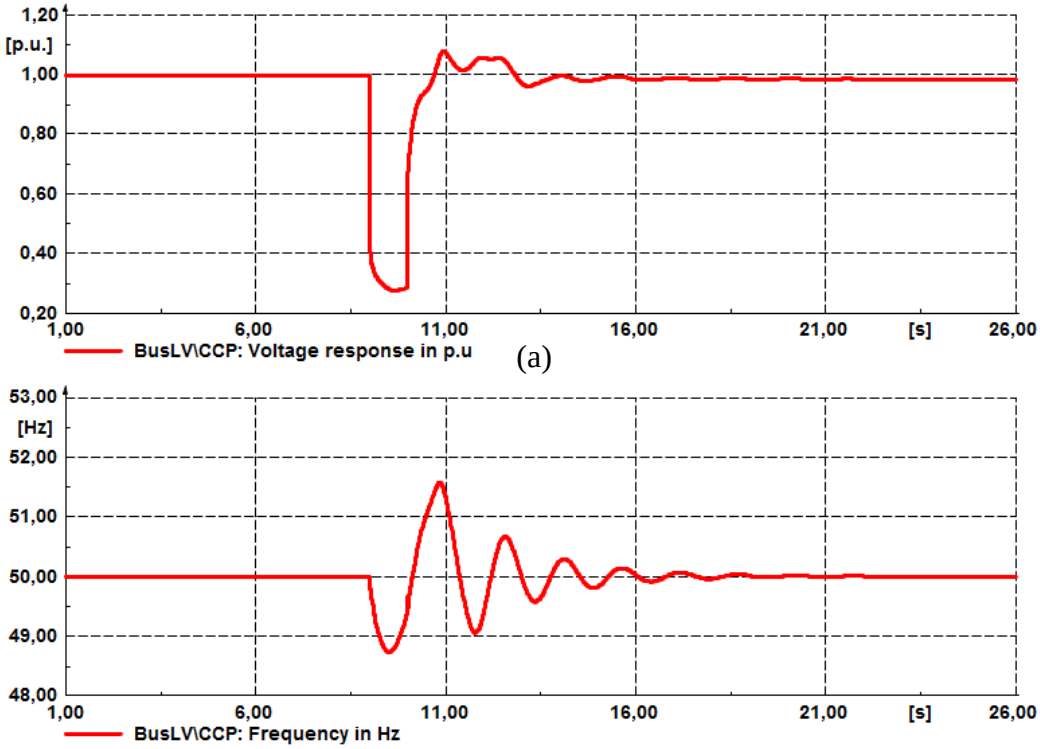


Figure 5.28: Series RL in parallel with induction motor (a) shows the RMS voltage behaviour of the network at the CP prior to and during islanding due to an upstream three-phase short-circuit fault, (b) shows the frequency behaviour of the network at the CP prior to and during islanding due an upstream three-phase short-circuit fault.

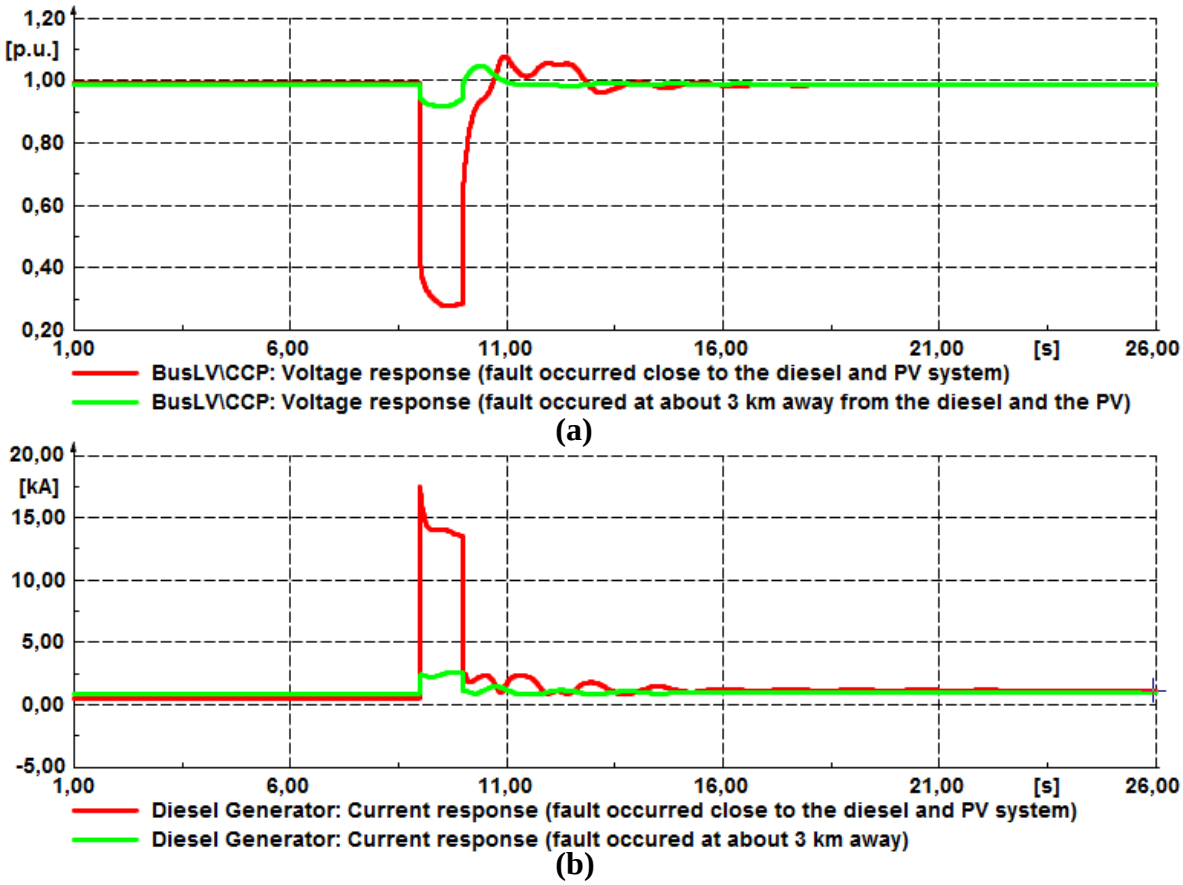


Figure 5.29: Series RL load in parallel with an induction motor (a) shows the RMS voltage behaviour of the network with the fault at different distances, (b) shows the RMS current behaviour of the SG with the fault at different distances.

Chapter 6 – Discussion

6.1 RMS voltage and frequency compatibility levels

There are national and international standards that bind network operators to acceptable values of RMS voltage and frequency during normal conditions and disturbances.

The compatibility levels for the RMS supply voltage shall be as specified in Table 6.1 unless otherwise agreed in a supply contract. In this study, assuming there is an absence of any agreement to the contrary, the supply voltage shall not deviate from the declared or agreed voltage by more than 10% for any period longer than 10 consecutive minutes.

Where the voltage supplied reduces to a value less than 0.9 pu of the standard or declared value for more than 3 seconds on one or more phases, the event shall be logged as an undervoltage event, otherwise the event shall be logged as a voltage dip [8], [35]. Undervoltage might occur when there is a disturbance (in this case: islanding due to sectionalisation or islanding due to an upstream three-phase short-circuit fault).

Table 6.1: Deviation from standard or declared voltage [8], [35]

Voltage level (V)	**Limit %**
<500	±10
≥500	±5

The nominal frequency in the country where the study is conducted, South Africa, is 50 Hz during normal operation [35]. The compatibility levels for the supply frequency shall be as specified in Table 6.2. The frequency shall not deviate from the declared or agreed frequency by more than 2% and 2.5% respectively during islanding for the grid and for the island.

Table 6.2: Deviation from nominal frequency [35]

Network type	**Limit %**
Grid	±2
Island	±2.5

6.2 SG discussion

The RMS voltage and frequency behaviour of the SG during islanding are analysed and discussed.

6.2.1 **RMS voltage and frequency behaviour analysis**

The primary operational droop of the diesel engine is summarised in Figure 6.1 (for speed/frequency versus load demand) and Figure 6.2 (for RMS voltage versus reactive power demand) [36]. When the load demands more active power, the frequency of the system will decrease [13]. Similarly, when the load demands more reactive power, the RMS voltage of the system will decrease [37].

For simulated results $P_{SG} < P_{load}$, therefore, there will always be an initial frequency decrease (below the nominal frequency value) before the degov takes corrective action. For an diesel engine without a governor, the speed/frequency will decrease below its nominal value and not recover. The summary of the frequency behaviour of an SG is illustrated in Figure 6.3 in correspondence to equation (6.1). According to reference [35] the supply frequency shall not deviate from the declared frequency to less than 0.975 pu. It is observed from Figure 6.3 that the supply frequency is violated for SG with initial contribution of 10% and 50% for all previously mentioned power factors (pf = 0.9, 0.95 and 0.996).

As per the simulation, the SG has the ability to supply reactive power. Depending on the SG reactive power export or import, there will be an increase or decrease of RMS voltage during islanding.

The RMS voltage was observed for times between the initiation of islanding and two seconds of islanding, and the RMS voltage nadir occurs at about 0.5 seconds.

Hence, the analysis only accounts for the RMS voltage and frequency after 0.5 seconds of islanding.

$$f_{system} = f_{nominal} - \frac{P_{load}}{S_g} \quad (6.1)$$

Where;

f_{system} = System frequency [Hz]

$f_{nominal}$ = System frequency when there is no load demand [Hz]

P_{load} = Load active power [MW]

S_g = droop slope (frequency bias) [MW/Hz]

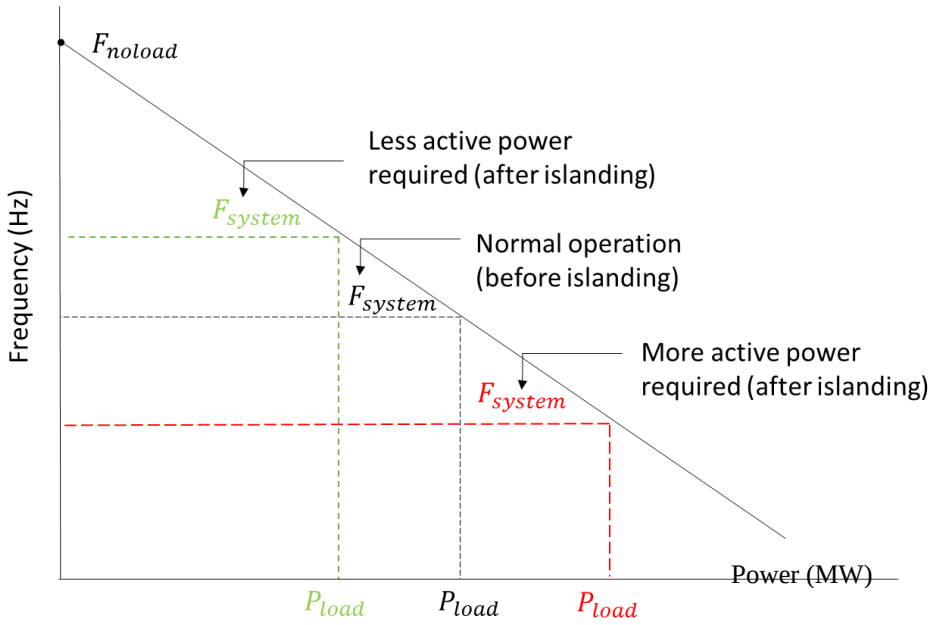


Figure 6.1: Frequency versus active power droop relationship

The network can experience both an increase or decrease of reactive power depending on the type of load (inductive or capacitive) and the percentage MW contribution of the diesel generator prior to islanding. For a series RL load there is a decrease in voltage as illustrated by Figure 6.4. According to reference [35] the

RMS supply voltage shall not drop to less than 0.9 pu of the declared voltage. It is observed from Figure 6.4 that the voltage limit is only reached during islanding due to an upstream three-phase short-circuit fault.

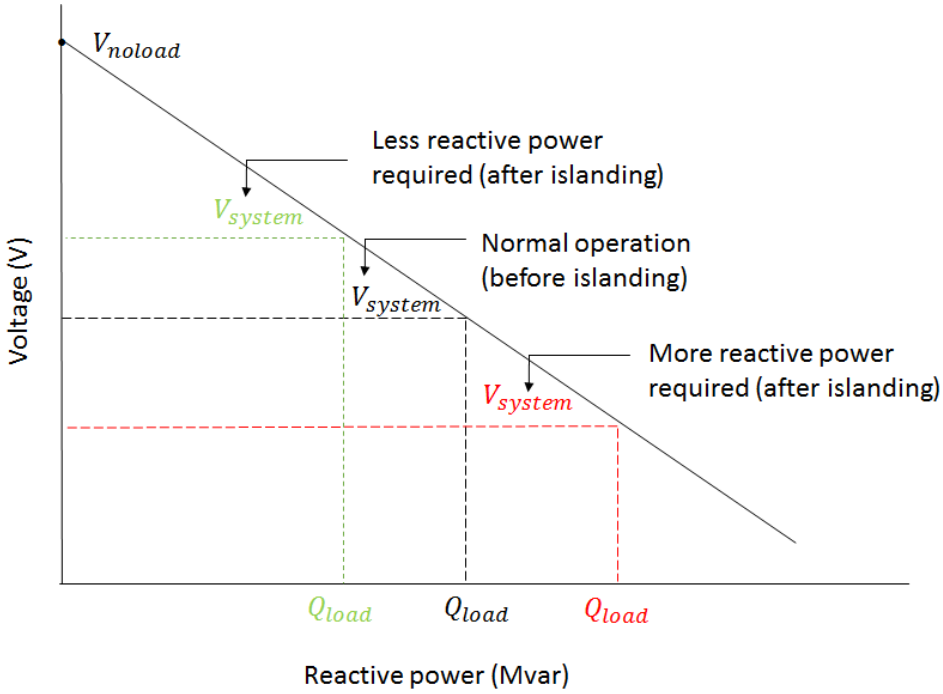


Figure 6.2: Reactive power versus voltage droop relationship

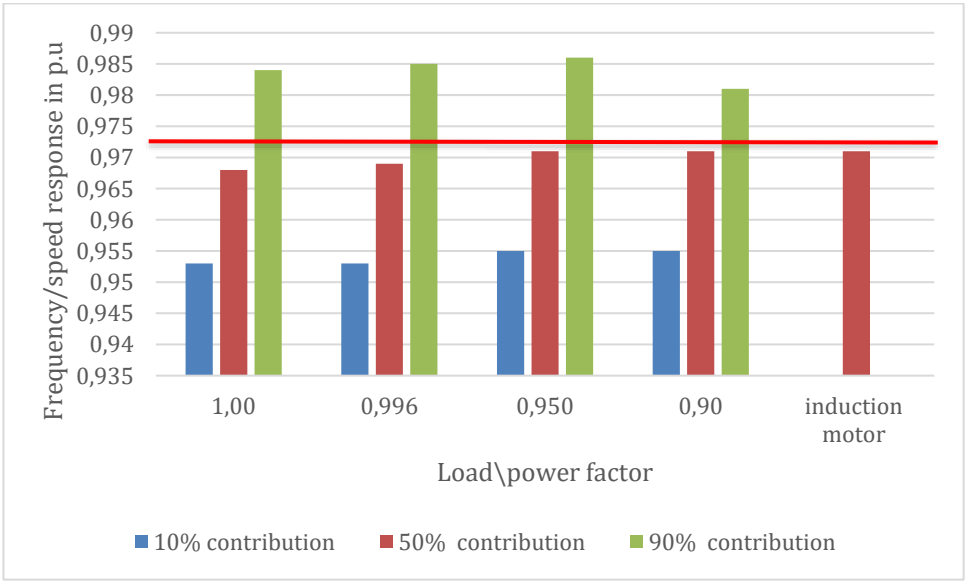


Figure 6.3: Frequency versus series RL load power factor, supplied by different SG initial percentage MW contributions (10%, 50%, and 90%), at 0.5 seconds after islanding

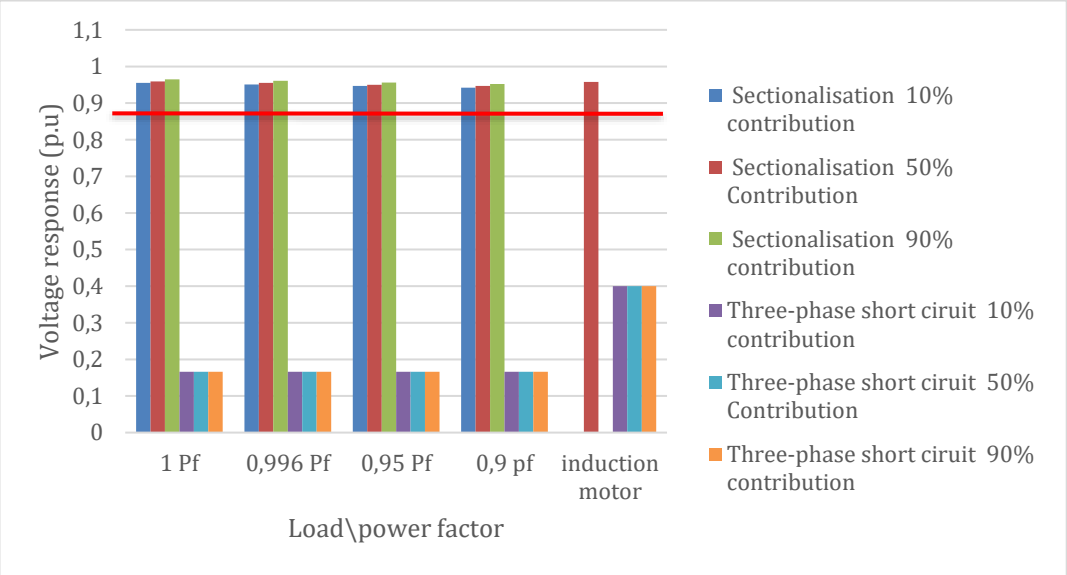


Figure 6.4: RMS voltage versus series RL load power factor on an islanded network, supplied by different SG initial percentage MW contributions (10%, 50%, and 90%) at 0.5 seconds after islanding

6.2.2 **RMS voltage and frequency percentage reduction (normal versus islanding)**

To determine and evaluate how critical it is to reduce the islanding time, a percentage reduction analysis with respect to the RMS voltage before islanding is used. The percentage reduction is used to represent a reduction value in relation to the initial value. Positive value represents an increase in percentage and a negative value represents a reduction in percentage in relation to the initial voltage value before islanding.

The percentage reduction equation is shown in equation (6.2). From the previous results, it is shown that the islanding due to a three-phase short-circuit fault is most probable to experience lower voltage levels at different SG initial percentage MW contributions. Similarly, islanding due to sectionalisation rarely experiences RMS

voltage issues (provided there is a governor and AVR implemented and the SG is able to ramp up to 100% of the load demand).

$$\Delta V_x(\%) = \frac{V_x - V_{initial}}{V_{initial}} * 100 \qquad (6.2)$$

$$= (V_x - 1) * 100$$

Where;

V_x = Voltage during islanding [pu]

x = 0.5 seconds islanding time

$V_{initial}$ = Voltage before islanding = 1 pu [pu]

$\Delta V_x(\%)$ = Voltage percentage reduction in relation to 1 pu [%]

The frequency percentage reduction is also analysed to determine how the frequency deviates from the nominal value (50 Hz) during islanding. The equation used to calculate the frequency percentage reduction is shown in equation (6.3)

$$\Delta f_x(\%) = \frac{f_x - f_{initial}}{f_{initial}} * 100 \qquad (6.3)$$

$$= \frac{f_x - 50}{50} * 100$$

Where;

f_x = Frequency during islanding [Hz]

x = 0.5 seconds islanding time

$V_{initial}$ = Frequency before islanding = 50 Hz

$\Delta f_x(\%)$ = Frequency percentage reduction in relation to 50 Hz [%]

6.2.2.1 Sectionalisation and upstream three-phase short-circuit fault

The RMS voltage and frequency percentage reduction of the SG supplying an RL load is illustrated in Figure 6.5 and 6.6, respectively. As previously mentioned, the negative value of $\Delta V_x(\%)$ and $\Delta f_x(\%)$ illustrates a reduction of the initial value of RMS voltage after the specified seconds of islanding.

As illustrated in Figure 6.5, the RMS voltage drops by about 5.8% during sectionalisation and by about 88.4% during an upstream three-phase short-circuit fault. Similarly, as illustrated in Figure 6.6, the frequency of the network drops by 4.5%, 2.9% and 1.9% for 10%, 50% and 90% SG initial percentage MW contributions respectively during sectionalization.

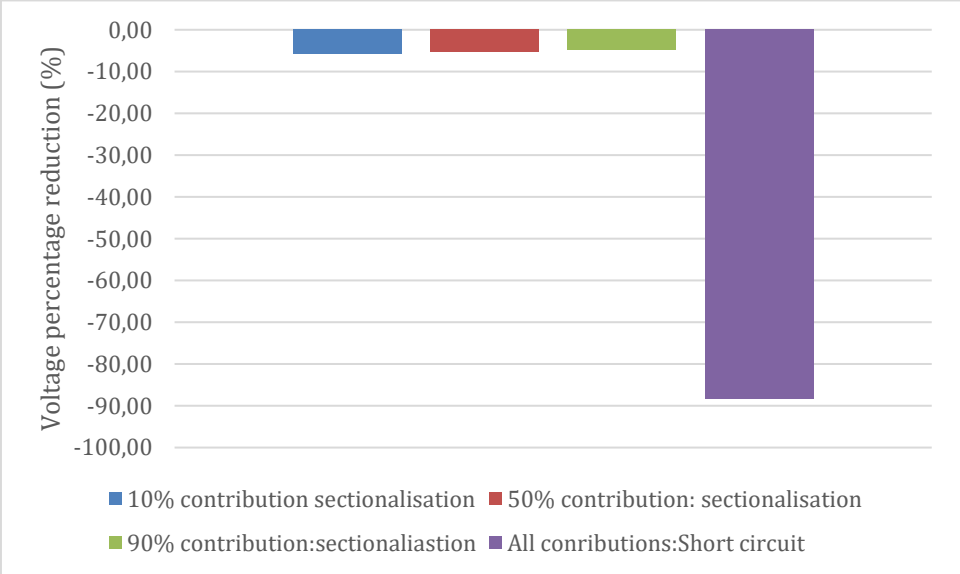


Figure 6.5: RMS voltage percentage reduction for different SG initial percentage MW contributions (10%, 50%, and 90%) for sectionalisation that leads to islanding for a series RL load (pf=0.9)

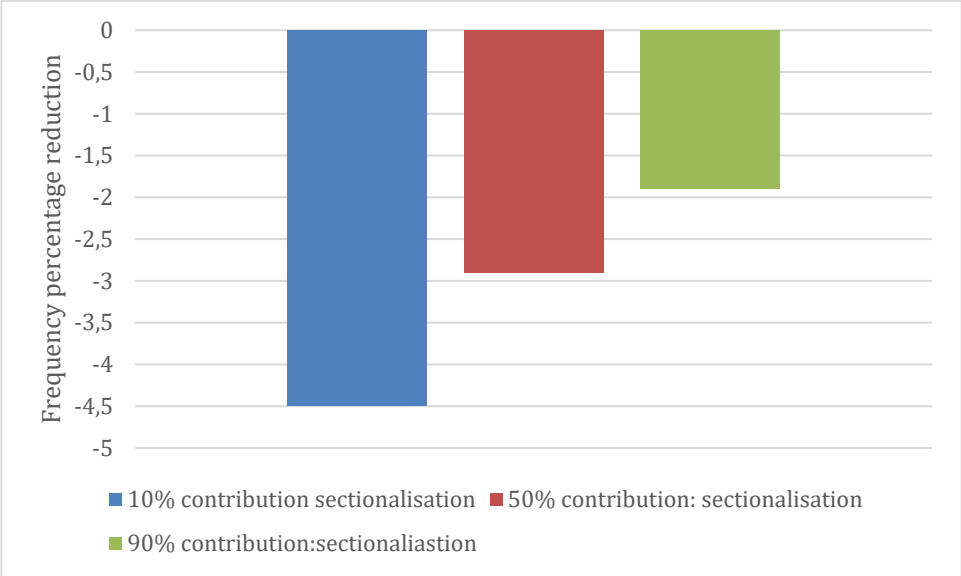


Figure 6.6: Frequency percentage reduction of different SG initial percentage MW contributions (10%, 50%, and 90%) for sectionalisation that leads to islanding for a series RL load (pf=0.9)

6.3 SPV discussion

The RMS voltage and frequency behaviour of the SPV during islanding are analysed and discussed.

6.3.1 RMS voltage and frequency behaviour analysis

SPV is normally made to work at its maximum power point so it can export maximum power into the network. SPV will always track the maximum power point and will give a fixed output if the ambient condition remains constant. SPV has no rotating parts and no mechanical inertia like synchronous generators and its output MW is solely dependent on the solar irradiance.

The SPV system is simulated with “synthetic” inertia control, to either decrease or increase the power export based on the change of nominal frequency of the primary source (external grid). The SPV, therefore, does have the capability to contribute to the inertia of the system. In such a situation, there is frequency control from the SPV and this is because there is power reserved for frequency control. The

maximum reserved power used during the simulation is 10% (SPV initially curtailed by 10%), as illustrated by Figure 6.7.

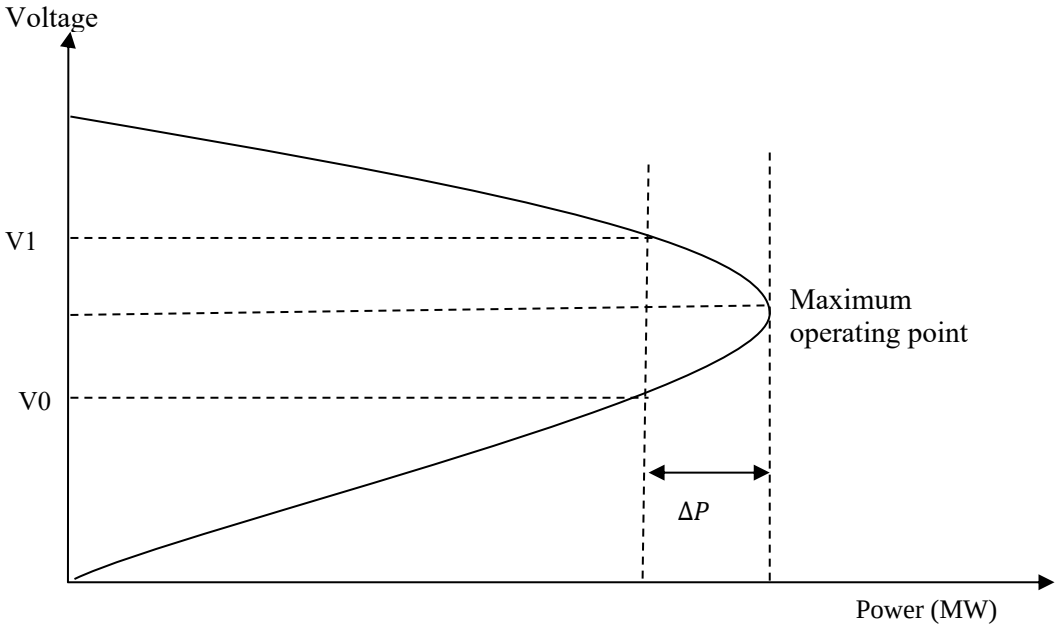


Figure 6.7: SPV power versus voltage curve

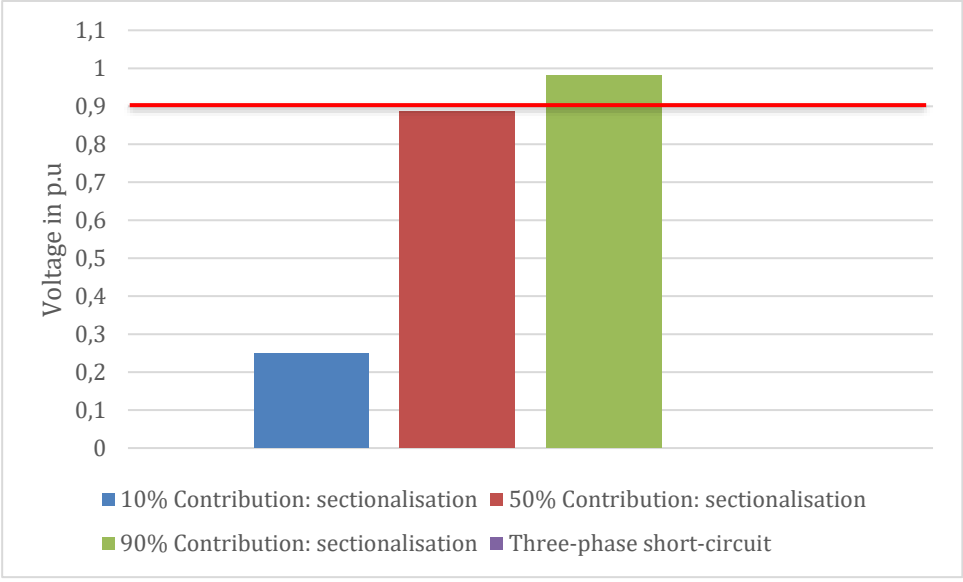


Figure 6.8: RMS voltage behaviour for a series RL load (pf=0.9), supplied by different PV initial percentage MW contributions (10%, 50%, and 90%) at 0.5 seconds after islanding due to sectionalisation or a three-phase short-circuit fault

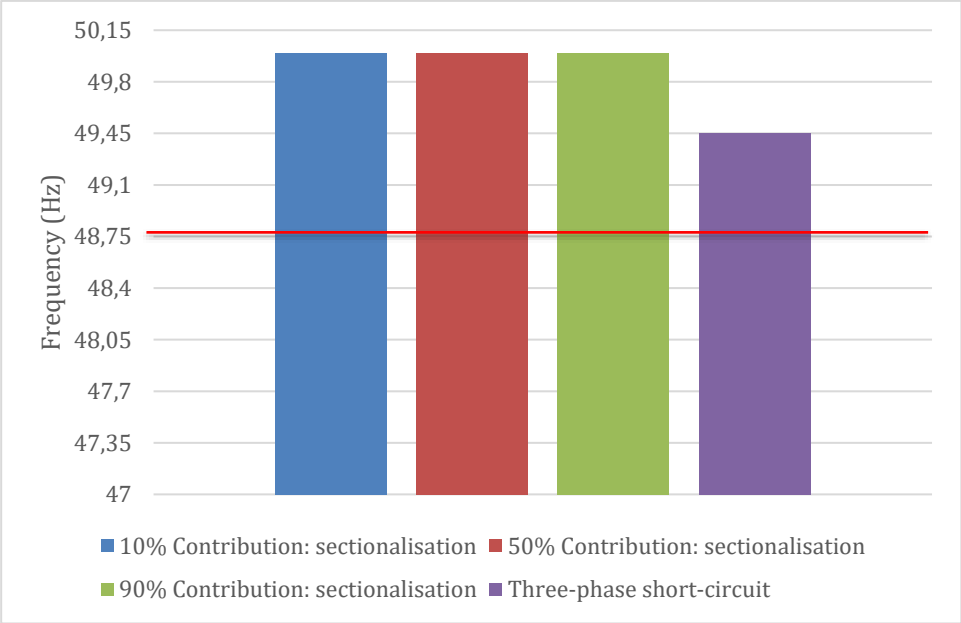


Figure 6.9: Frequency behaviour for a series RL load (pf=0.9), supplied by different solar PV initial percentage MW contributions (10%, 50%, and 90%) at 0.5 seconds after islanding due to either sectionalisation or a three-phase short-circuit fault

Figure 6.8 shows the RMS voltage behaviour of the SPV system of different initial percentage MW contributions (10%, 50%, and 90%) supplying a series RL load with a power factor of 0.9 at 0.5 seconds of islanding due to either sectionalisation or a three-phase short-circuit fault. It indicates the SPV system tries to maintain its voltage for islanding due to sectionalisation (with lower voltage behaviour for 10% initial percentage MW contribution) and the voltage collapses for islanding due to an upstream three-phase short-circuit fault.

Figure 6.9 shows the frequency behaviour of different SPV initial percentage MW contributions (10%, 50%, and 90%) supplying a series RL load of a power factor of 0.900 at 0.5 seconds after islanding. It is observed that the frequency of the network mostly remains close to the nominal value of 50 Hz for islanding due to sectionalisation and the frequency drops to a value of 49.45 Hz for islanding due to an upstream three-phase short-circuit fault.

6.3.2 RMS voltage and frequency percentage reduction (normal versus islanding)

To determine and evaluate how critical the RMS voltage behaviour of the SPV during islanding is, a percentage reduction analysis in comparison with the RMS voltage before islanding is used. The percentage reduction is used to represent a reduction value in relation to the initial value. A positive value represents an increase in percentage and a negative value represents a reduction in percentage in relation to the initial voltage value before islanding. The voltage percentage reduction formula used is shown in equation (6.4). The islanding time of focus is 0.5 seconds.

$$\Delta V_x(\%) = \frac{V_x - V_{initial}}{V_{initial}} * 100 \qquad (6.4)$$

$$= (V_x - 1) * 100$$

Where;

V_x = Voltage during islanding [pu]

x = 0.5 seconds islanding time

$V_{initial}$ = Voltage before islanding = 1 pu [pu]

$\Delta V_x(\%)$ = Voltage percentage reduction in relation to 1 pu [%]

The frequency percentage reduction is also analysed to determine how the frequency deviates from the nominal value (50 Hz) during islanding. The equation used to calculate the frequency percentage reduction is shown in equation (6.5).

$$\Delta f_x(\%) = \frac{f_x - f_{initial}}{f_{initial}} * 100 \qquad (6.5)$$

$$= \frac{f_x - 50}{50} * 100$$

Where;

f_x	=	Frequency during islanding [Hz]
x	=	0.5 seconds islanding time
$V_{initial}$	=	Frequency before islanding = 50 Hz [Hz]
$\Delta f_x(\%)$	=	Frequency percentage reduction in relation to 50 Hz [%]

6.2.2.1 Sectionalisation and three-phase short-circuit fault

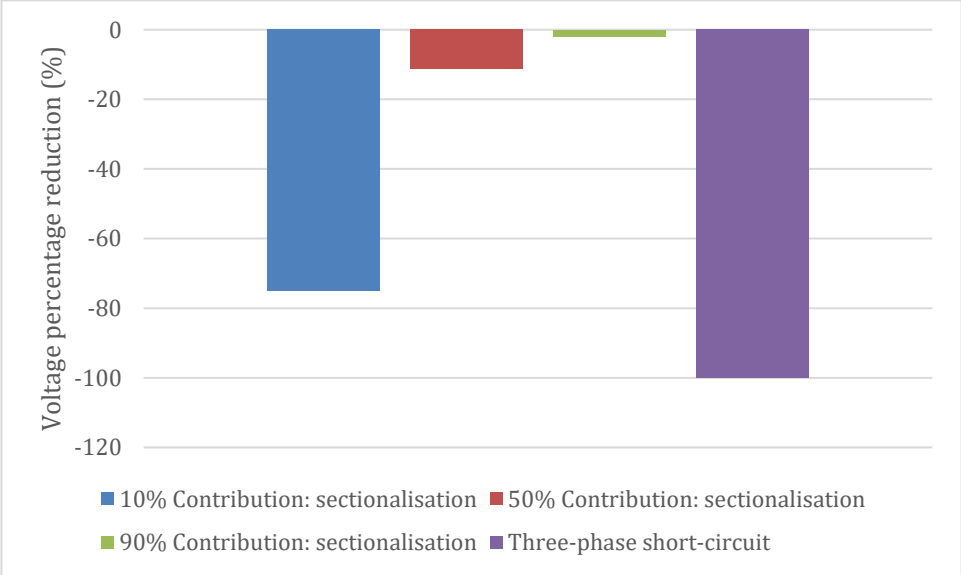


Figure 6.10: Percentage reduction of RMS voltage at 0.5 seconds after islanding of an RL load (pf=0.9) supplied by different PV initial percentage MW contributions.

The percentage RMS voltage reduction of a series RL load with 0.9 power factor, exposed to three different (10%, 50%, and 90%) PV initial percentage MW contributions, is shown in Figure 6.10. As previously mentioned, the negative value of $\Delta V_x(\%)$ illustrates a reduction of the initial value of voltage after the specified seconds of islanding.

From Figure 6.11, it can be observed that the voltage percentage reduction is 100% for islanding due to an upstream three-phase short-circuit fault. Due to the type of SPV system used it is shown that the voltage deviation of islanding due to sectionalisation is minimal for an initial percentage MW contribution of 90% and 50% and critical for an initial percentage MW contribution of 10%.

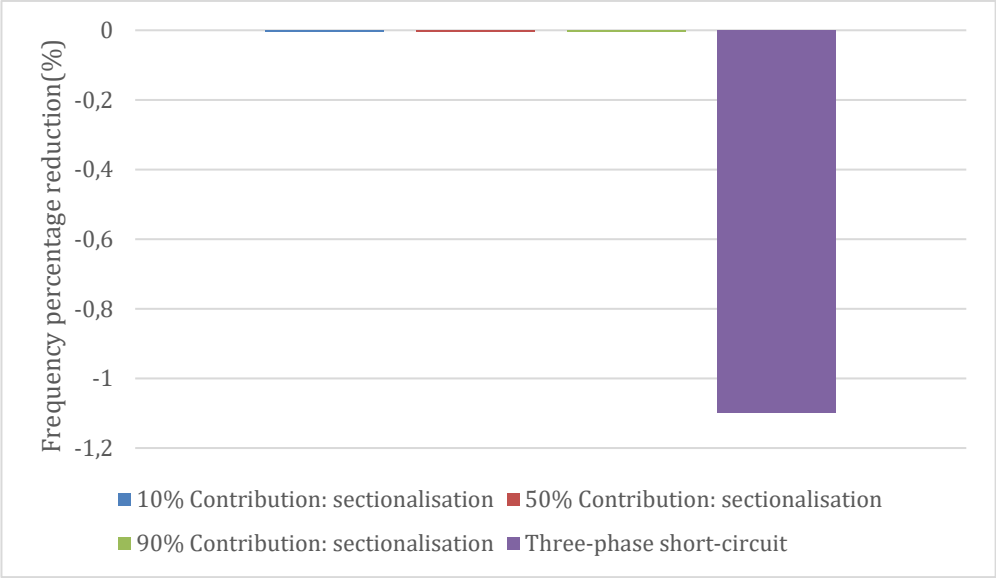


Figure 6.11: Percentage reduction of frequency at 0.5 seconds after islanding with RL load (pf=0.9) supplied by different SPV initial percentage MW contributions and following sectionalisation or a three-phase short circuit fault.

The percentage frequency reduction for a series RL load with 0.9 power factor, exposed to three different (10%, 50%, and 90%) SPV initial percentage MW contributions, is shown in Figure 6.11. As previously mentioned, the negative value of an $\Delta f_x(\%)$ shows a reduction of the initial value of voltage after the specified seconds of islanding. From Figure 6.11, it can be observed that the maximum frequency percentage reduction is 1.1% for islanding due to an upstream three-phase short-circuit fault.

Chapter 7 – Power quality versus IDM reliability

There is a trade-off of power quality versus reliability of the IDM used. In this chapter, the reliability of the islanding detection methods will be discussed. For the purpose of simplicity, only the Rate of Change of Frequency (ROCOF) type of IDM will be considered. A case study will be used to demonstrate the effect on the power quality during islanding versus the reliability of IDMs, in particular the ROCOF method.



Figure 7.1: Geographical area of Estancia/Estancia North 22 kV

A sample network was chosen called Estancia/Estancia north. It is an Eskom 22 kV network in Mpumalanga. For the study the load was chosen to be 0.6 MVA. The geographical view of the network is shown in Figure 7.1. For research purposes, the DGs will be installed at Estancia/Estancia north 92 T-off pole 7 (ETN 92/7),

shown in Figure 7.1. The RMS tool within PowerFactory DIgSILENT was be used to analyze the mid-term and long-term transients during balanced or unbalanced conditions. This function allows the voltage and frequency profile to be analyzed in the time domain.

The aim of the RMS analysis was to determine how the network behaves in terms of frequency and RMS voltage during islanding.

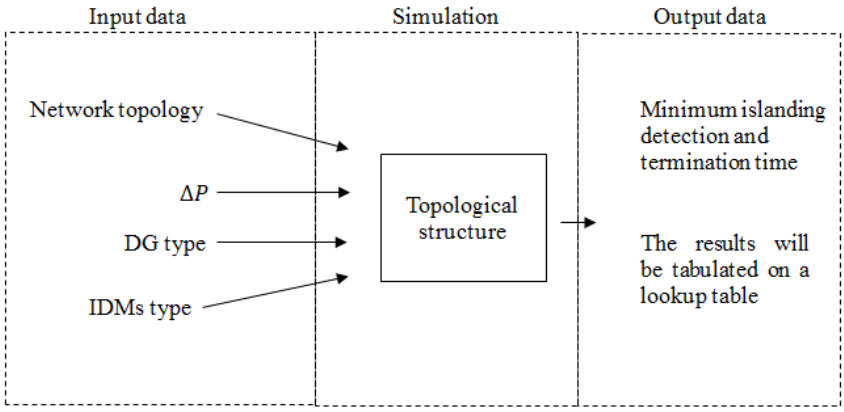


Figure 7.2: Research approach to simulated network

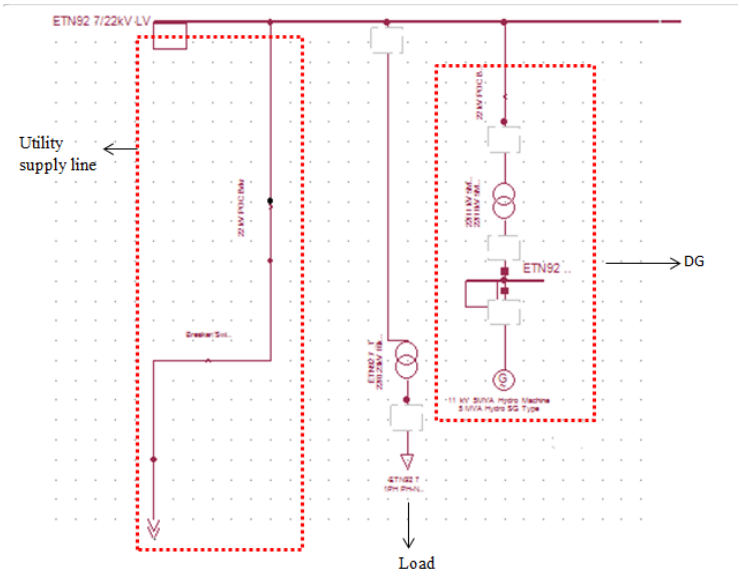


Figure 7.3: SG network diagram

The methodology of this chapter is illustrated in Figure 7.2 with the case study and the network diagram of interest shown in Figure 7.3, which consists of a SG (varied

parameter) and load in a radial network to determine the minimum islanding and detection time using a passive IDM. This is to demonstrate the impact of power mismatch between the load MW and SG MW while keeping other variables unchanged. The load was 0.6 MVA and the SG size was varied between 1 MVA, 2.25 MVA, 3.5 MVA and 5 MVA with a power factor of 0.8.

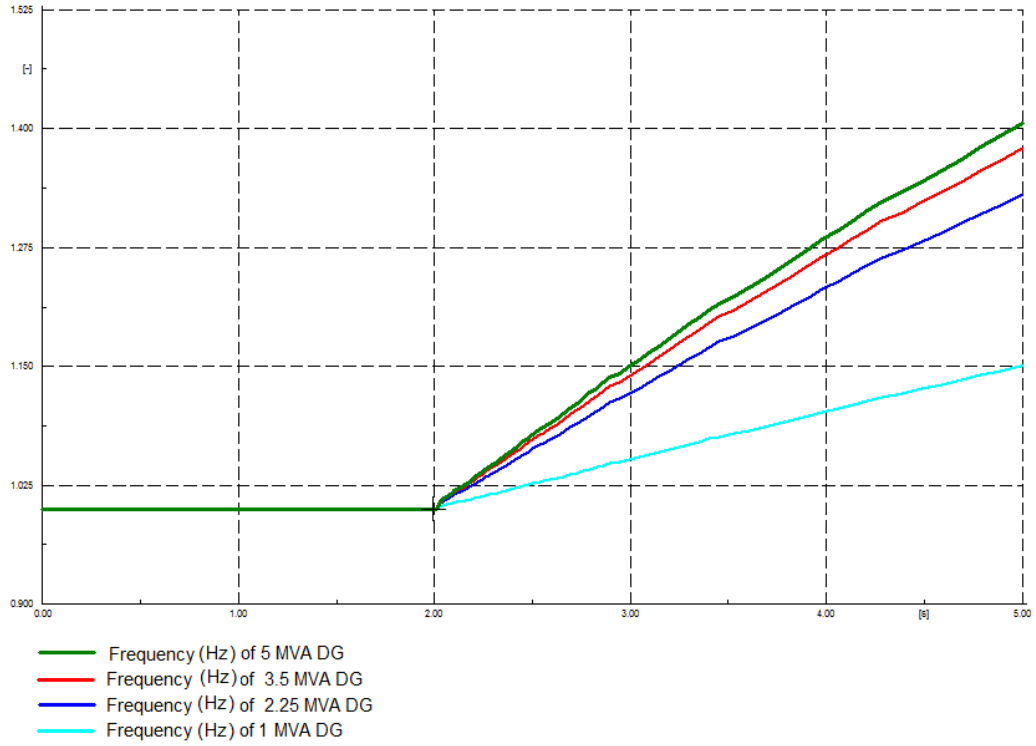


Figure 7.4: The frequency behaviour of the SG during islanding

Figure 7.4 shows the over-frequency behaviour of the simulated network. For all the three case scenarios of different SG size, the SG MW > the load MW. To determine if islanding can be detected on the specified network, a Rate of Change of Frequency (ROCOF) passive type IDM was used. The ROCOF method uses a frequency derivative threshold value determined by equation (7.1) to initiate a trip signal to terminate islanding. The frequency derivative threshold value was calculated to ensure that the ROCOF relay is triggered for islanding and not for load changes [38] . The minimum calculated frequency derivative threshold value is given by the minimum SG size simulated as tabulated in Table 7.1.

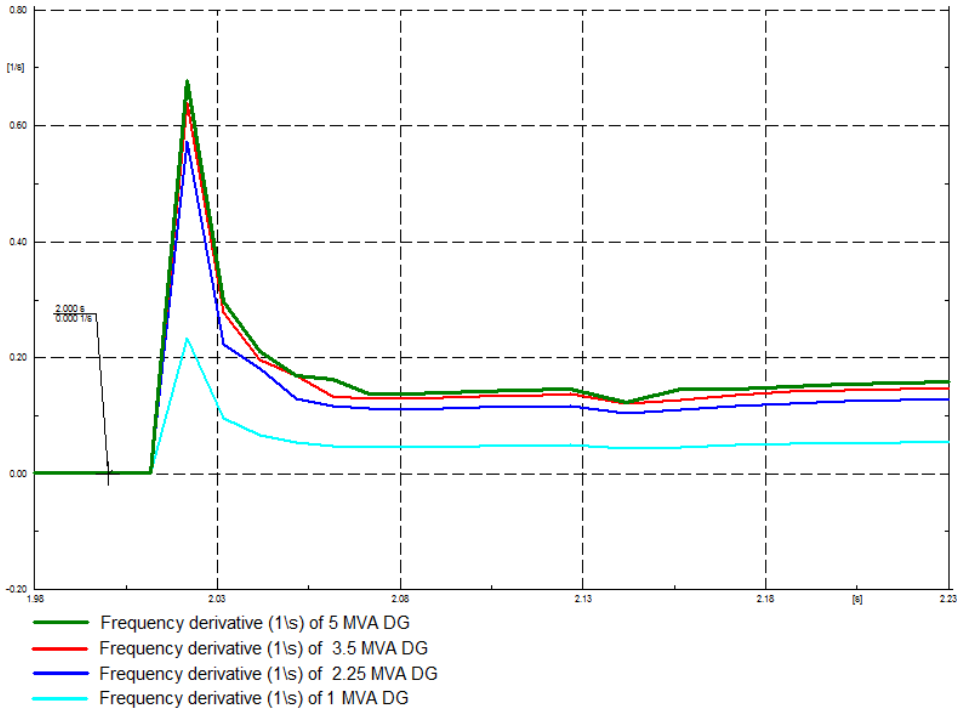


Figure 7.5: Frequency derivative behaviour

$$\text{ROCOF} = \frac{\Delta f}{\Delta t} = \frac{\Delta P * f}{2 * S_N * H} \qquad (7.1)$$

Where;

f	=	Rated frequency, Hz
ΔP	=	The difference between the SG output and the load power, MW
S_N	=	Distributed Generator apparent power, VA
H	=	Rotor inertia constant of the generator

Table 7.1: ROCOF value of a load of 0.6 MVA, nominal frequency of 50 Hz and rotor inertia constant of 5

DG rating (MW)	ΔP (MW)	ROCOF (1/s) theoretical threshold value	ROCOF (1/s) simulated value
1	0.013	0.065	0.046
2.25	0.021	0.047	0.112
3.5	0.024	0.034	0.129
5	0.026	0.026	0.145

At normal operation (when both SG and utility are supplying the load), the frequency derivative is expected to be zero as shown in Figure 7.5. The system disturbance was initiated at two seconds. It is observed in Figure 7.5 that there is a rapid change of frequency for 0.052 seconds as the SG and load try to find a balance condition on a different rate of change of frequency. For the 2.25 MVA rated SG, it is also illustrated that the minimum measured frequency derivative after the rapid change is 0.112 1/s at 0.062 seconds after initiated islanding. Hence the minimum anti-islanding time of 0.062 seconds can be achieved with the specified network topology, SG type, ΔP and IDM.

For the 5 MVA rated SG, it is also shown that the minimum measured frequency derivative after the rapid change is 0.145 1/s at 0.072 seconds after the initiation of islanding. Hence the minimum anti-islanding detection time of 0.072 seconds can be achieved with the specified network topology, SG type, ΔP and IDM.

It is also observed that for a 1 MVA SG, the measured frequency derivative (0.046 1/s) is smaller than the calculated ROCOF (0.065 1/s). Hence this will result in continued islanding due to a smaller power mismatch ΔP.

Islanding is a crucial condition within the network, posing a risk to the utility workers, customer and utility equipment. Reference [11] stipulates that islanding must be terminated within a maximum time of two seconds. Reducing the maximum islanding time below two seconds with respect to network topology, type

of SG, type of IDM and the power mismatch between the load MW and the SG MW are considered. It is shown that the power mismatch does have an impact on the islanding detection time and continued islanding. The smaller the power mismatch, the smaller the frequency and RMS voltage percentage fluctuations. For smaller frequency fluctuations, continued islanding becomes a possibility. Therefore, if power quality of islanded network has to be considered, the type of IDM to be used must also be considered to avoid continued islanding.

Chapter 8 – Conclusion

The RMS voltage and frequency behaviour of a 400 V microgrid of different initial percentage MW contributions (10%, 50% and 90%) connected to a 22 kV rural network supplying three different load types: purely resistive load, series RL load (pf=0.9, 0.95 and 0.996), and composite load (static load in parallel with a dynamic), prior to and during islanding were investigated. Islanding can be due to sectionalisation or due to an upstream three-phase short-circuit fault that is cleared by the utility breaker.

The purely resistive load and the series RL load show similar linear trends of voltage behaviour. That is, as the load demand increases or as the power factor decreases, there is also a decrease in voltage during islanding. If the DG is capable of self-sufficiently (with the help of voltage and frequency controllers) supplying the load during islanding, then poor power quality issues can be eliminated.

The voltage and frequency behaviour of a SPV of different initial percentage MW contributions during grid-tied operation supplying three load types were also investigated. Similarly, the three different load types of interest are purely resistive, series RL, and composite load (introduction of an induction motor). There is a moderate change in SPV frequency behaviour during islanding for all cases. Similarly, power quality issues are mostly observed for a SPV with a lower initial percentage contribution and in general islanding due to an upstream three-phase short-circuit fault.

The type of SPV system used in a network also plays a significant role in the power quality prior to and during islanding. The type of SPV system used for this study (PVD1) has the capability to monitor and control the voltage and frequency behaviour based on the reactive and active power demand, respectively. It is also observed that SPV operating without the help of reactive power compensation can compromise the SPV RMS voltage during islanding.

It is also observed that the RMS voltage behaviour of the network is also affected by the location of the three-phase short-circuit fault. The greater the fault distance from the microgrid, the smaller the probability of the islanded network being exposed to power quality issues. A lot of factors need to be taken into consideration for a network exposed to a three-phase short-circuit fault prior to and during islanding. Such factors are, where the fault is and the network withstand capability to supply the load.

Chapter 9 – Recommendations

There are several ways to improve the RMS voltage and frequency fluctuation of the network during islanding. This includes making sure that the DG MW is self-sufficient to supply the load, through the DG inertia or external source. The other way is to make sure that islanding is detected and terminated at minimal time to avoid RMS voltage and frequency dips and/or swells.

The advantage of an SG is its inertia, to allow it to contribute to the frequency behaviour of the network. The disadvantage of SPV is that SPV has no rotating parts and no mechanical inertia, as the SPV MW is solely dependent on the solar irradiance. Hence, they cannot contribute to the inertia of the system unless they have reserved power.

For a network that comprises SPV, careful network design must be in place, such as having reactive power compensators and reserved active power to avoid poor power quality issues during islanding. A network with only SPV is more prone to poor power quality as opposed to SG networks.

PV inverters are capable of injecting reactive power to support voltage sags in the network. PV inverters are also capable of absorbing reactive power to counteract voltage rise at the point of connection.

Most PV inverters are only set up to operate at unity power factor, meaning they only supply active power. However, PV inverters have been designed for deployment in the distribution system, where applicable interconnection standards (IEEE 1547-2003) do not currently allow for voltage regulation. Inverters for that application are designed to operate at unity power factor and are sold with a kilowatt (kW) rating, as opposed to a kilovolt-ampere (kVA) rating.

If there is an inadequate or no dynamic reactive capability available from the SPV, it may be necessary to supplement the SPV with dynamic reactive power controllers.

Different types of dynamic reactive power controllers are namely:

- Synchronous condenser
- Static var compensators
- Static synchronous compensator

There reason for reactive management is that if the reactive power is not managed the following will results

- Too much reactive power can lead to an inefficient power flow
- Too little reactive power can create an instability in the network

Running on diesel at normal condition or during islanding can be expensive; hence consideration of having both SG and PV in parallel can eliminate both cost and poor power quality issues. A network diagram with both SG and PV in parallel was investigated in section 5.3 It is observed that there is power quality improvement when a PV is connected in parallel with the SG.

9.1 Reducing the RMS voltage and frequency fluctuations after islanding

The dynamic behaviour of the primary and secondary controller influences the RMS voltage and frequency behaviour of the network during islanding. Determining which level of controller for a different application to be implemented is critical to avoid unnecessary poor-quality issues within the network.

There are different levels of controller hierarchy, namely primary, secondary and tertiary, as illustrated in Figure 3.1 from section 3.1. The interest of this research was in the primary level.

References

[1] K. M. Jagtap and K. D. K, "Impact of different types of distributed generation on radial distribution networ," *2014 International Conference on Reliability, Optimization and Information Technology -ICROI,* pp. 1-4, 2014.

[2] N. Panigrahy, T.Ilamparithi, M. Kashinath and R. Prakash, "Comparison and review of Islanding Detection Techniques for Power Distribution Studies," *International Journal of Advanced Research in Electrical, Electronic and Instrumental Engineering,* vol. 5, no. 7, pp. 1-8, 2016.

[3] "IEEE Standard 1547 for Interconnection and Interoperability of Distributed Energy Resources with Associated Electric Power Systems Interfaces," *IEEE Standards Coordinating Committee 21,* vol. II, pp. 1-138, 2018.

[4] M. Kari, K. Anna, R. Sami and J. Pertti, "Problems related to islanding protection of distributed generation in Distributed Networks.," *IEEE Lausanne Power Tech,* pp. 346-472, 2007.

[5] I. K. Hobbs, "Evaluation and Implementation of Anti-islanding Methods for Converter-Fed Distributed Generator,"page no. 1-175, 2009.

[6] M. Xu, K. Mauch and S. Martel, "An assessment of distributed generation islanding detection methods and issues for Canada," *Canmet Energy Technology centre-Vereness,* pp. 1-67, 2004.

[7] C. P. Allessing , H. Kruger and J. Van Coller , "Simulation-based analysis of the anti-islanding requirement specified within the grid connection code for renewable power plant (gccrpp)," *2019 Southern African*

Universities Power Engineering Conference/Robotics and Mechatronics/Pattern Recognition Association of South Africa (SAUPEC/RobMech/PRASA), pp. 406-411, Jan 2019.

[8] "IEEE-1159 Recommended Practice for Monitoring Electric Power Quality," *IEEE Power and Energy Society,* p. 91, 2009.

[9] W. Bower and M. Ropp, "Evaluation of Islanding Detection Methods for Utility-Interactive Inveters in Photovoltaic Systems," *Sandia Report,* pp. 1-60, 2002.

[10] D. Wilston and D.F., "Consequences of out-of phase reclosing on feeders with distributed generators", Semantics schola pp. 1-6, 2012.

[11] "Grid Connection Code for Renewable Power plants (RPPs) connected to the electricity transmission system (TS) of the distribution system (DS) in South Africa," vol. 2.8, pp. 1-62, 2014.

[12] V. Terzija, "Synchronous and asynchronous generator frequency and harmonic behavior after suddent load rejection," *IEEE Transactions on power systems,* vol. 18, no. 2, pp. 730-736, 2003.

[13] P. Mahat, Z. Chen and B. Bak-Jensen, "Review on islanding operation of distribution system with distributed generation," *2011 IEEE Power and Energy Society General Meeting,* pp. 1-8, 2011.

[14] A. Bidram, "Hierarchical Structure of Microgrids Control System," *IEEE TRANSACTIONS ON SMART GRID,* vol. 3, no. V, pp. 1963-1976, 2012.

[15] F. Gao, R. Kand, J. CAO and T. Yang, "Primary and secondary control in DC microgrids: a review," *Springer,* pp. 227-242, 2019.

[16] P. Kundur, Power System Stability and Control, McGraw-Hill, 1994.

[17] S.-H. Lee, J.-S. Yim, J.-H. Lee and S.-K. Sul, “Design of Speed Control Loop of A Variable Speed Diesel Engine Generator by Electric Governor,” pp. 1-5.

[18] M. Htay and K. S. Win, “Design and Construction of Automatic Voltage Regulator for Diesel Engine Type Stand-alone Synchronous Generator,” *World Academy of Science, Engineering and Technology* , pp. 1-7, 2008.

[19] IEEEstd 421.5 IEEE Recommended Practice for Excitation System Model for Power System Stability Studies, 2016.

[20] A. Anmar, W. Zhaoyu, W. Jianhui, M. Barry, B. Hugo and Z. Dongbo, “Load Modeling-review,” *IEEE Transactions on Smart Grid,* vol. 9, no. 6, pp. 5986-5999, 2017.

[21] F. S. Chassin, E. T. Mayhorn, M. A. Elizondo and S. Lu, “Load modeling and calibration techniques for power system studies,” *2011 North American Power Symposium,* pp. 1-7, 2011.

[22] Edited by Leornard, L.G, Power Stability and Control, Taylor and Francis, 2012.

[23] “Load representation for Dynamic performance simulation (of power system),” *IEEE Trans Power system,* vol. 10, no. 1, pp. 472-482, 1993.

[24] “Integrated Governor Control for a Diesel-Generating Set,” *McGowan, David J; Morrow, D. John,* vol. 21, no. 2, pp. 476-483, 2006.

[25] R. Lee, P. P and R. Harley, “D, Q reference Frames for the Simulation of Induction Motors,” *Electric Power System Research* , pp. 15-26, 1985.

[26] S. Benhamed, H. Ibrahim, H. Belmokhtar, A. Ilinca, D. Rousse, A. Chandra and D. Ramdenee, Dynamic Modeling of Diesel Generator Based on

Electrical and Mecanical Aspects, IEEE Electrical Power and Energy Conference (EPEC), 2016.

[27] D. Pattabiraman, R. Lasseter and T. Jahns, “Comparison of Grid Following and Grid Forming Control for a High Inverter Penetration Power System,” *2018 IEEE Power & Energy Society General Meeting (PESGM,* pp. 1-5, 2018.

[28] J. C. Boemer, E. Vittal, M. Rylander and B. Mather, “Derivation of WECC Distributed PV System Model Parameters from Quasi-Static Time Series Distribution System Simulations,” *2017 IEEE Power & Energy Society General Meeting,* pp. 1-5, 2017.

[29] W. Suampuna, “Voltage Stability Analysis of Grid-Connected Photovoltaic Power Systems Using CPFLOW,” *2016 International Electrical Engineering Congress, iEECON2016, 2-4 March 2016, Chiang Mai,,* pp. 301-304, 2016.

[30] D. Pattabiraman, J. Tan, V. Gevorgian, A. Hoke, C. Antonio and D. Arakawa, “Impact of Frequency-Watt Control on the Dynamics of a High DER Penetration Power System,” *2018 IEEE Power & Energy Society General Meeting (PESGM), Portland,* pp. 1-5, 2018.

[31] P. Jahangiri and C. A. Dionysios, “Distributed Volt/VAr Control by PV Inverters,” *IEEE transactions on power systems* , vol. 28, no. 3, pp. 3429-3440, 2013.

[32] R. Elliot, A. Ellis, P. Pourbeik, J. Sanchez-Gasca, J. Senthil and J. Weber, “Generic photovoltaic system models for WECC - A status report,” *2015 IEEE Power & Energy Society General Meeting,* pp. 1-5, 2015.

[33] H. Zimmer, W. M. Asmah and J. Hanson, “Influences of Excitation Systems on the Dynamic Voltage Behavior of Power Systems,” *International Conference on Power Systems (IPST2015),* pp. 1-8, 2015.

[34] F. Han, X. Yu, M. Al-Dabbagh and Y. Wang, “Locating Phase-to-Ground Short-Circuit Faults on Radial Distribution Lines,” *IEEE Transactions on Industrial Electronics,* vol. 54, no. 3, pp. 1581-1590, 2007.

[35] “ NRS 048-2: Electricity supply - Quality of Supply, part 2: voltage characteristics, compatibility levels, limits and assessement methods,” 2008.

[36] S. Chapman, Electric Machinery Fundamentals 4th Edition, 2005.

[37] T. S. Tran, D. T. Nguyen and F. Goro, “The analysis of technical trend in Islanding Operation, Harmonic Distortion, Stabilizing Frequency and voltiage of islanded Entities,” *Resources,* pp. 1-28, 2019.

[38] K. Prasartsuwan and P. Jirapong, “Analysis of Islanding Detection Methods for Grid-Connected Distributed Generation in Provincial Electricity Authority Distribution System,” *2012 9th International Conference on Electrical Engineering/Electronics, Computer, Telecommunications and Information Technology*, Phetchaburi, 2012, pp. 1-4

[39] N. Panigrahy, T. Ilamparithi, M. Kasinath and R. Praksh, “Comparison and revie of islanding detection technique for power distribution studies,” *International Journal of Advanced Research in Electrical, Electronic and Instrumentation Engineering,* vol. 5, no. 7, pp. 1-8, 2016.

[40] D. M. Mark McGranaghan, “Effects of Voltage Sags In Industry systems,” *Conference Record. Industrial and Commercial Power Systems Technical Conference 1991,* Memphis, TN, USA, 1991, pp. 18-24, doi: 10.1109/ICPS.1991.153061.

[41] S. Saksena and S. G. Karady, "Effects of Voltage Sags on Household loads," *IEEE Power Engineering Society General Meeting, 2005*, San Francisco, CA, 2005, pp. 2456-2461 Vol. 3.

[42] M. Z. Kreishan, G. P. Fotis, V. Vita and L. Ekonomou, "Distributed Generation Islanding Effect on Distribution Networks and End User Loads Using the Load Sharing Islanding Method," *Energies,* pp. 1-24, 2016.

[43] D. Lam and H.Yee, "A study of frequency responses of generator electrical torques for power system stability," *IEEE Transactions on Power systems,* vol. 13, no. 3, pp. 1136-1142, 1997.

[44] "IEC 60034-1 Rotating machines International standard," *IEC,* vol. 12, pp. 1-19, 2010.

[45] N. Jacob, R. Sarah and M. H. J. Bollen, "An an analysis of frequncy variations and its implications on connected equipment for nano-grid during islanding conditions," *Enegies,* pp. 1-13, 2018.

[46] N. K. Lal and S. E. Mubeen, "Voltage dependent load in powerflow analysis,"Electrical and Electronics Engineering," *An InternationalJournal (ELELIJ),* vol. 4, no. II, pp. 65-77, 2015.

[47] P. Sen, Principle of Electric Machines and Power Electronics, 2nd Edition, John Wiley and Sons, 1997.

[48] H. Renmu, M. Jin and D. J. Hill, "Composite load modeling via measurement approach," *IEEE Transactions on Power Systems,* vol. 21, no. 2, pp. 663-672, 2006.